

Energimyndighetens titel på projektet – svenska Energilagring för integritet kring smarta elmätare - STOMP	
Energimyndighetens titel på projektet – engelska Energy STorage for smart Meter Privacy - STOMP	
Universitet/högskola/företag Kungliga Tekniska högskolan	Avdelning/institution Elektroteknisk teori och konstruktion
Adress Teknikringen 33, 114 28 Stockholm	
Namn på projektledare Daniel Månson	
Namn på ev övriga projektdeltagare Cong-Toan Pham, Tobias Oechtering	
Nyckelord: 5-7 st Energilagring, smarta elmätare, integritet	

Förord

Projektet har i huvudsak genomförts som ett postdoktor projekt på KTH, under perioden 2019-2021, av avdelningen för elektroteknisk teori och konstruktion tillsammans med avdelningen för teknisk informationsvetenskap. Projektet har finansierat av energimyndigheten tillsammans med KTH. Det har för projektet funnits ett parallellt samarbete med ett annat, internt finansierat, doktorandprojekt.

Innehållsförteckning

Sammanfattning	2
Summary	2
Inledning/Bakgrund	3
Genomförande	5
Resultat	7
Diskussion.....	10
Publikationslista.....	11
Referenser, källor.....	13
Bilagor	15

Sammanfattning

Ett "smart elnät", som effektiviserar energianvändningen, lyfts ofta fram som ett viktigt verktyg för att motverka klimatförändringarna samt skapa en modern och pålitlig infrastruktur. Ett sådant elnät bygger bl.a. på distribuerad förnybarenergi, energilager och smarta tjänster. "Smarta elmätare" är här viktiga så att användarens förbrukning rapporteras noggrant och frekvent.

Emellertid är detta problematiskt eftersom en sådan beskrivning kan ge detaljer om beteende och levnadssätt. På flera håll i världen finns oro för att elleverantörer, eller tredje part, ska göra sådana integritetsbrott och risken finns att lanseringen av nästa generations smarta elmätare försenas.

I projektet här studeras ett fysiskt sätt att åtgärda detta genom att låta ett energilager hos användaren laddas och urladdas så att ett förutbestämt förbrukningsmönster rapporteras (dvs. köps) istället för det verkliga. Det finns kommersiella system som uppfyller kraven och om flera användare samsas om ett större energilager minskar bördan. Det fanns att degraderingen av litium-jon batterier, för applikation, är som förväntad. Intervjuer med människor visade på låg kännedom om risken med smarta elmätare men att integritetsbrottet upplevdes som allvarlig. Intervjuer med olika typer av aktörer på marknaden visade på att smarta elmätare inte anses vara ett integritetsproblem men att diskussionen har generellt ökat pga. GDPR.

Summary

A "smart grid", which streamlines energy use, is an important tool for counteracting climate change and create a modern and reliable infrastructure. It is based on distributed renewable energy, energy storage and smart services. "Smart meters" are important for accurately and frequently report the user consumption. However, such a description is problematic as it can provide details about behavior and lifestyle. There are concerns that power suppliers, or third parties, will commit such privacy breaches. There is a risk that the launch of the next generation of smart meters will be delayed. In the project here is a physical method to mitigate this studied. An energy storage at the user is charged /discharged so that a predetermined consumption pattern is reported (i.e. purchased) instead of the actual one. Commercial systems that meet the requirements exist and if several users share a larger storage, the burden is reduced. For the application, the degradation of lithium-ion batteries is as expected. Interviews with users showed low awareness about the risks, but that the privacy breach was perceived as serious. Interviews with different market entities showed that smart meters are not considered a privacy problem but the discussion has increased due to GDPR.

Inledning/Bakgrund

Ett "smart elnät", som effektiviserar energianvändningen, lyfts ofta fram som ett viktigt verktyg för att motverka klimatförändringarna. Ett sådant elnät bygger bl.a. på distribuerad förnybarenergi, energilager och smarta tjänster. Ett uttryck av detta är att konsumenter/slutanvändare/elkunder själva kan producera, lagra och hantera sin effekt (de blir då s.k. "prosumenter"). För dessa slutanvändaren, förlitar sig detta dock på att informationsteknologi, här "smarta elmätare" [1], ska rapportera användarens producerade och förbrukade effekt. Det finns idag, i vissa EU länder, Nordamerika och andra delar av världen, en viss folklig opinion mot smarta elmätare. En bred och allmän implementering riskerar stoppas pga. oroa för att elleverantören och/eller annan tredje part använder dessa data (genom s.k. "Non-Intrusive Load Monitoring" NILM [2]) för att ur användarens konsumtionsmönster identifiera beteende, leverne, politisk eller religiös åskådning etc [3-5]. T.ex., har man kunna utröna vilken Tv-kanal en användare tittar på ur data för elanvändningen [6] vilket skulle kunna användas för att rikta t.ex. reklam till användaren [7]. Eftersom frågan om personlig integritet är viktig inom EU finns det sedan 25/5 2018 GDPR direktivet ("EU General Data Protection Regulation") som också kan komma att påverka hur sådana data får insamlas och användas i medlemsländerna. Frågan om integritetsbrott mot slutanvändare, pga. smarta elmätare, ses som ett stort problem av vissa grupper som i värsta fall kan hejda en bred introduktion av smarta elmätare och därmed förnyelsebar energiproduktion. I Sverige skulle det kunna leda till att nästa generations smarta elmätare inte accepteras [8] trots att Sverige mellan 2006 och 2009 var det första landet att i princip ha 100% smarta elmätare [9]. Detta skulle i så fall vara ogynnsamt för både klimatarbetet men även för vissa satsningar inom energisektorn.

Åtgärderna som har undersökts detta projekt, är att förbättra integriteten för slutanvändaren genom att använda ett energilager som installerats innanför användarens smarta elmätare. Energilagret kommer att, i varje ögonblick, laddas och urladdas efter en vald algoritm så att förbrukningsmönstret som rapporteras av den smarta elmätaren följer ett förutbestämt mönster (t.ex., helt konstant eller sinus format). Därmed rapporteras inte användarens verkliga förbrukningsmönster utan det som skapas av energilagret. Denna "fysiska" metod att säkra användarens integritet anses här vara bättre jämfört med att tillämpa metoder som bygger på mjukvaruhantering av datan över förbrukningen [10].

Dock så finns det ett aber och det är slutanvändarens villighet till att betala delar eller ev. hela kostnaden för energilagringen. Det grundar sig i hur användaren upplever integritetsbrottet. Ett incitament är att energilagringen skulle kunna användas för att underlätta för egen förnybarenergiproduktion genom t.ex. vindkraft eller solceller. Frågan är hur slutanvändaren upplever att elleverantören, eller tredjepart, kan utröna somliga övergripande beteendemönster (såsom när man är hemma) och då bara betala för ett mindre och/eller långsammare energilagringssystem eller om enbart total integritet är ett krav.

Att installera olika former av energilagring hos prosumenter kan därmed potentiellt kraftigt minska förmågan att utläsa konsumtionsmönstren och därmed bevara slutanvändarens integritet. Energilagring banar samtidigt potentiellt väg för förnyelsebar energiproduktion och nya s.k. smarta tjänster, då dessa i mångt och mycket kräver energilagring för att utnyttjas fullt ut. En invändning skulle därmed kunna vara att man tar bort nätägarens möjlighet till att övervaka slutanvändarna för att t.ex. kunna planera och implementera nya tjänster (såsom lastflyttning) men det stämmer inte. Effekten som rapporteras av den smarta elmätare, dvs. som energilagret hanterar, är inte integritetsbrytande och kan rapporteras i förväg så att nätägaren kan planera. Till viss grad kan denna effekt vara samma från dag till dag (dock beroende på årstid, helger etc.) och därmed möjliggöra långsiktig planering. I kort, så kan existensen av energilagring hos slutanvändaren ge ett flexiblare och stabilare elnät, något som i längden ger en lägre kostnad för reparationer och översyn samtidigt som slutanvändarens integritet bevaras.

Genomförande

Projektet har i huvudsak genomförts som ett postdoktor projekt med några mindre sidospår som gjorts av seniorforskare eller som examensarbete. Som postdoktor har Cong-Toan Pham anstälts i början av 2019 och det är han som är huvudförfattare till de två journalartiklarna.

Första steget i projektet var att bedöma de teoretiska värdena för lagringskapaciteten [kWh] och effekthanteringsförmågan [kW] som skulle krävas för att maskera förbrukningsmönstret för en genomsnittlig användare i Sverige [I]. Detta gjordes genom att använda tillgängliga förbrukningsdata för genomsnittliga användare i Sverige tillsammans med både genererade dygnsförbrukningsprofiler och tillsammans med en databas [11,12] över uppmätta sådana profiler. Ur dessa analyserades kraven på ett energilager för att kunna ändra den effekt som rapporteras av den smarta elmätaren. Det studeras även hur dessa krav skulle ändras om flera användare delade på ett större energilager som de gemensamt laddade och urladdade istället för att varje användare hade ett enskilt energilager.

Undersökningen ovan ger bara en första hänvisning till kraven och därför användes en verifierad [13-16] ekvivalent kretsmodell för att undersöka [II] hur lämpliga några olika realistiska energilagringssystem skulle vara för integritetsskyddande ändamål för de i [12] uppmätta förbrukningsprofilerna. Här tas parametrar såsom försluter och responstider i åtanke och undersöktes gjordes lagringskapacitet [kWh] och den erforderliga totala kostnaden [€] som funktion av olika valda grader av integritet (en faktor definierad mellan [0:1]).

I arbetet [IV] undersöktes hur integriteten ev. bevaras om användaren har solceller eller om användaren har solceller tillsammans med ett energilager. Med mer hushåll/användare som ökar sin grad av självförsörjande kommer potentiellt konsekvenserna av integritetsbrott att sjunka eftersom mindre effekt köps utifrån. Detta kan potentiellt minska tillfällena då användarens förbrukningsmönster synliggörs. Därtill, studerades kapacitetskraven med en kontrollalgoritm där man tillät ett visst återflöde tillbaka till nätet om batteriet nådde SoC = 0.8 (eng. SoC, "State-of-Charge").

Det finns en tekno-socio-ekonomisk aspekt i problemet som uppstår med slutanvändaren. Möjligheten är stor att människor faktiskt inte upplever att det är något integritetsbrott att t.ex. elbolagen har deras förbrukningsmönster. Om nu så är fallet, till vilken grad gör de det och vad är de villiga att i så fall betala för att mildra problemet? I [IV] studerades, genom att intervjua privatpersoner, åsikterna kring smarta elmätare och upplevelsen av integriteten kring dessa samt graden av teknikacceptansen när det gäller energilager i hemmet. Intervjuer gjordes även med talespersoner från Ellevio AB (elnätsbolag), E.On (elbolag), Power2U (energilösningar), OneNordic (leverantör av smarta elmätare) samt f.d. Datainspektionen (nu Integritetsskyddsmyndigheten) för att skapa en bättre bild som inkluderar företag och myndigheter.

Ett vanligt sätt att bedöma hur lämpliga olika energilager är för olika användningsområden eller tjänster är att undersöka hur de åldras för dessa (s.k.

”dynamiskåldring”) och jämför med andra applikationer eller om de bara ”lämnas på hyllan” (s.k. ”kalanderåldring”). Eftersom batteriers användning, för den integritetsbevarandeapplikationen som diskuteras här, är relativt ny finns det mycket lite information om hur de presterar i verkligheten. Med avstamp i att ett batterilager måste kontinuerligt laddas/urladdas för att dölja användarens förbrukningsmönster finns det en möjlighet att batteriernas prestanda försämras snabbare än förväntat och att detta kommer starkt påverka möjligheten att bevara användarens integritet. Därför genomfördes experimentella åldringstester [III] över lång tid för att kunna utvärdera hur batterier påverkas av att kontinuerligt försöka maskera en användares förbrukningsmönster. Vid regelbundna intervaller testades batterierna för att utröna hur deras egenskaper (och kretsparametrar) hade förändrats. Dessa användes sen i modellen för att bedömma graden av informationsläckage som sker vid olika hälsotillstånd.

Resultat

Hur energilagrets laddas och urladdas kan kontrolleras olika vilket gör att den från nätet köpta, och av den smarta elmätaren, rapporterade effekten ser olika ut. De mönster som testades var konstant effekt (över hela dygnet, dvs. en total lastutjämning), sinusformad (med olika våglängder), triangelformad (med olika antal pulser/periodtider) samt fyrkantsvågor (med olika antalet pulser/periodtider). Det sågs att alla dessa senare fall krävde mycket mer, ofta 2-3 ggr, av energilagret än det första fallet där en konstant effekt rapporteras av den smarta elmätaren.

Ett tidigt steg i projektet var att bedöma de teoretiska värdena för lagringskapaciteten [kWh] och effekthanteringsförmågan [kW] som skulle krävas för att maskera förbrukningsmönstret för en genomsnittlig användare i Sverige [I]. Ur de genererade och uppmätta förbrukningsprofilerna sågs att det skulle krävas, i genomsnitt, ca. 6-10 kWh för att kunna hantera effektsvängningarna så att förbrukningen för genomsnittlig svensk användare döljs. Detta är inom ramen för existerande småskaliga kommersiella batterilager. Det sågs även att kapacitetskraven, per person, skulle minska till ca. 70% om flera än ca. 6 användare delade på ett större energilagret som de gemensamt laddade och urladdade. Detta bekräftades även i [II].

Eftersom verkliga energilagringssystem har icke-perfekta egenskaper (t.ex. responstider, effektiviteter vid laddning/urladdning, självurladdning etc.) studerades i [II] lämpligheten av några realistiska energilager. Det visade sig att litium-jon och bly-syra batterier skulle vara mest lämpliga, svänghjul sågs vara mindre lämpliga och superkondensatorer ännu mindre (delvis pga. den höga kostnaden och graden av självurladdning). Den erforderliga kapaciteten som krävs är linje med vad som sågs i [I] för de uppmätta förbrukningsprofilerna och fanns vara 10-15 kWh. I studien [II] definierades ett integritetsmått som:

$$C_f = 1 - \frac{\int_0^T |P_{\Delta}(t) - P_{st}(t)| dt}{\int_0^T P_{\Delta}(t) dt} = [0: 1]$$

Om energilagret, $P_{st}(t)$, inte kan leverera den erforderliga effekten, $P_{\Delta}(t)$, för att den smarta elmätaren ska rapportera valt mönster (t.ex. här en konstant förbrukning) över vald period, $t=0:T$, kommer C_f avvika från 1 (dvs. perfekt täckning). Det sågs, här, att med superkondensatorerna resulterade det som bäst i ett integritetsmått på 0.8 pga. de olika förlusterna (jämfört med batterierna och svänghjulen som alla kunde prestera ca. 0.99). Studien visar på ett tekno-socio-ekonomisk huvudbry kring kostnad per kWh, villighet samt effektivitet och förluster. Om användaren är beredd att acceptera en viss lägre nivå av integritet, dvs att information läcker och $C_f \neq 1$, faller storleken (och därmed kostnaden). på energilagret som krävs (dock mest i början). Kapacitetskravet på ett batteri blir bara ungefär 60% av det som krävs för $C_f = 1$ om man istället accepterar $C_f = 0.9$.

I [IV] sågs att enbart solceller (2.88 respektive 5.28 kW) tyvärr inte ger något vidare integritetsskydd för användaren eftersom den momentana matchningen

mellan produktion och förbrukning, för hela dygnet, inte är pålitlig. Effekt kommer, i realiteten, att hela tiden behöva exporteras eller importeras och detta avslöjar, tillsammans med t.ex. väderdata, förbrukningens karakteristik. Tillsammans med ett batterilager är situationen mer gynnsam och man får ett inflöde som nu beror på solcellsproduktionen och energinivån i batteriet istället för användarens förbrukningsmönster direkt. Här sågs att för given förbrukning hos användaren, och att den smarta elmätare ska rapportera en konstant effekt, kommer kapacitetkravet på ett energilager att minska något med ökad solcellsproduktion (dock ökar kapacitetskravet snabbare med ökad förbrukning). Notera att kravet aldrig överstiger ca. 50% av användarens förbrukning. Om man däremot tillåter ett konstant effektflöde tillbaka till nätet då batteriets SoC = 0.8, tills det når SoC = 0.2, kommer situationen att förändras något. Man får ett stegvist konstant effektflöde och det sågs att kapacitetskraven på batteriet istället ökade vid ökad solcellsproduktion. Här kommer kraven att överstiga 50% av användarens förbrukning och speciellt om solcellsproduktionen kraftigt överstiger förbrukningen kan den nå 90-110%.

Ur intervjuerna med privatpersoner [IV] framkom några intressanta saker. Fast de flesta hyrde sin bostad (70%) var majoriteten (62%) överlag intresserade av förnyelsebar energi (här solceller). Därtill, 41% skulle direkt vara intresserade av att investera i sådana och ytterligare 49% beroende på kostnaden. Som förväntat, kände inte en stor andel (89%) till integritetsproblemen kring smarta elmätare men 75% ansåg sedan att det är ett allvarligt problem att elbolag, eller tredje part, kan använda data från smarta elmätare för att utröna information om användaren. Vidare så var 79% (62% + 18%) villiga att antingen betala en engångssumma eller en månadskostnad för en teknisk lösning. Dock skulle bara ca 6% (av de 62%) vara villiga att betala mer än engångssumma 10.000 kr men 70% (av de 18%) skulle vara villiga att betala mer än 100 – 250 kr/månad. Det verkar finnas ett genuint samhällsintresse för ny grön teknik (t.ex. solceller, energilager, smarta elmätare etc.) men privatpersoner ser också potentiella problem med vissa aspekter av användningen. Det är däremot osäkert om det skulle vara ekonomiskt gångbart att använda batterier enbart för att upprätthålla integriteten och det skulle kräva en djupare analys av marknadskrafter samt andra nuvarande incitament. Detta låg dock utanför projekts ramar.

Intervjuerna med Ellevio AB, E.On, Power2U, OneNordic samt Datainspektionen visade på att smarta elmätare inte anses vara ett integritetsproblem, bla. pga. avsaknaden av tillbud och anmälningar, men att diskussionen har generellt ökat i och med GDPR samt vikten av att korrekt bevara användarens integritet [IV]. De visade också på att smarta tjänster, där data från smarta elmätare används, fortfarande är ett relativt nytt koncept (men att potential finns) och att nyttan över andra lösningar inte alltid är lätt att se. Det poängterades också att det krävs användares skriftliga tillåtelse för att tredje part ska få tillgång till användarens data, vilket i realiteten inte är ett så starkt skydd.

Åldringstesterna som utfördes på batterierna när de användes i den integritetsbevarandeapplikationen visade på att de ungefär åldrades likvärdigt som om batteriet använts till andra applikationer med motsvarande krav [III]. Efter ca.

800 dagar (motsvarande ca. 980 cykler) kommer lagringskapaciteten att sjunka till 80% (SoC = 0.8), vilket ofta används som "end-of-life" punkten. Detta är i linje med andra studier över användningsområden, såsom för solceller eller Plug-in hybrid elbilar, där livslängden, under olika kontrollstrategier och situationer, anges vara 2-6 år. De extraherade värdena för kretsparametrarna visade att när batteriets hälsnivå (eng. SoH, "State-of-Health") sjönk minskade, som förväntats, både lagringskapaciteten men även effektförmågan. Hur mycket av informationen som då läcker beror på kraven (dvs. effektnivåerna i användarens förbrukningsmönster) i relation till hur batterierna dimensioneras. När effektförmågan faller med tiden kommer ett batteri som dimensionerats sparsamt att fortare nå sin begränsning och det förutbestämde mönstret kommer inte kunna upprätthållas jämfört med om batteriet har mer kapacitet. Därtill, ett sparsamt dimensionerat batteri kommer att åldras snabbare då kraven som ställs på det mest troligen ligger närmare dess förmåga. I experimentet här så visade det sig att vid SoH = 0 (dvs. 80% lagringskapacitet kvar) skulle förbrukningsmönstret läcka igenom vid flera tillfällen under dygnet.

Diskussion

Teknik utvecklas hela tiden och samhället med den. Nya tjänster tillkommer och människors acceptans till tekniken förändras när de synliga fördelarna framträder. Samtidigt så finns det en baksida där användarnas information kan användas för andra syften än det som annonserats. Detta gäller framför allt sociala media-plattformar men allteftersom även energinätverken förändras kommer detta även att ske här. Det kommer ständigt ny teknik för att hantera, mäta och analysera användarens förbrukning, ofta med budskapet att användaren ska ta makten över sin förbrukning. Nya aktörer är på ingång till energisektorn; prosumenter (användare som även agerar producenter), energigemenskaper (där flera användare kan samsas kring t.ex. en källa till förnybar energi och/eller ett batterilager), energiaggregatorer som kontrollerar ett, eller flera, energilagrar för att leverera tjänster till nätet o.s.v. När möjligheten till smarta tjänster breder ut sig och blir vanligare kommer värdet av användares förbrukningsmönster att stiga i värde och det måste klargöras vem som äger datan. Det är inte orimligt att tänka sig en utveckling där aktörer får betala användarna för att få använda deras förbrukningsdata. Detta skulle, i värsta fall, kunna vara en faktor som dämpar utvecklingen av smarta tjänster för användare och i förlängningen av smarta elnät. I projektet här har vi sett att med ett energilager är det tekniskt mycket möjligt att fysisk dölja konsumenters/slutanvändares/elkundens förbrukningsmönster men samhället får svara på om det är önskvärt.

Publikationslista

- I. D. Månsson, "**Sizing Energy Storage Systems used to Improve Privacy from Smart Meter Readings for Users in Sweden**" i Proceedings - 2018 IEEE PES Innovative Smart Grid Technologies Conference Europe, ISGT-Europe 2018, 2018.

[The smart power grid of the future will be heavily dependent on accurate information from the users via smart meter readings. However, from the information on the users power profile much knowledge about the behavior can be acquired, resulting in a breach of privacy. To mask the power profile an energy storage system can be used that obfuscates the smart meter readings. In this paper, we investigate the storage capacity needed if the smart meter is required to report a constant power usage for the user, electricity as well as distributed heating, to the utility. Both single and multiple users per energy storage system are investigated using both derived as well as measured power profiles.]

- II. C.-T. Pham och D. Månsson, "**A Study on Realistic Energy Storage Systems for the Privacy of Smart Meter Readings of Residential Users**" IEEE Access, vol. 7, s. 150262-150270, 2019.

[The introduction of smart meters sparked concerns about privacy breach through real-time monitoring of electric power consumption. Valuable private information about occupancy, behaviour, health, religion and wealth can be extracted from the user's power profile which urges measurements to protect the integrity of the user. One physical mitigation technique to assure privacy is explored using energy storage systems. Real energy storage technologies are limited in their energy capacities and power capabilities, which have to be appropriately sized to fulfil their role. This paper analyses and compares different energy storage technologies (li-ion, lead-acid, electric double layer capacitor and flywheel) for the protection of residential users by estimating the minimal required capacities and costs for both single and multiple user cases. The analysis is based on actual measured user data from the REDD data set. The results show that the integrity can be protected with reasonable capacities and investments ranging in the margin of market available products.]

- III. C.-T. Pham och D. Månsson, "**Effects of smart meter privacy protection management on the lifetime performance of 18,650 lithium-ion batteries**" IET Smart Grids, Oct 2021, <https://doi.org/10.1049/stg2.12055>.

[Concerns over privacy leaks through real-time monitoring in smart meters (SMs) raise questions about how to effectively protect the user power consumption data. As one potential solution, energy storage systems have been suggested to physically manipulate SM readings to hide the true load pattern. Lithium-ion batteries (LiBs) are commonly utilised

in the residential area in various applications such as solar and home batteries. Its use in a privacy-focussed operation has shown potential with reasonable system sizes in the range of commercially available products. However, batteries are subjected to ageing and the deterioration of performance over the course of time, which can limit the feasibility in such application. Hence, this work aims to investigate the ageing influence on LIBs' performance to deduce the life expectancy and how well privacy is protected over time. The study includes ageing tests with a specifically designed cycle life test procedure for the privacy protection scheme to extract relevant model parameters for the equivalent circuit battery model.]

- IV. S. Bindu, “**Energy storage systems for smart meter privacy: a study of public perceptions**”, Masters Officials - Máster universitari en Enginyeria de l'Energia (Pla 2013), KTH/UPC collaboration.

[Smart meters are a vital step for transitioning to a smart grid architecture. Studies have shown that it is possible to extract appliance usage information through non-intrusive load monitoring methods. This data can be used by third-parties for unwanted activities like targeted marketing, home invasion, etc. It is postulated that the data leakage will be minimum when the power flow from/to the grid is piecewise linear. To achieve linearity, the use of energy storage systems is investigated. Energy storage systems (ESS) are being increasingly used by customers having solar energy production. In this project, an algorithm for the energy management unit (EMU) to control the ESS is proposed which maintains piecewise linearity. Two types of users are considered for the study: 1. user who injects excess energy to the grid 2. user who does not (or is not allowed by law) to inject power to the grid. The effect of the algorithm on both users is studied. The minimum capacity of ESS for data leakage prevention is analysed for both cases. Data from four different households is used in different combinations to obtain the mean capacity required. Using this data, an equation is formulated for the minimum capacity of ESS required to maintain linearity in power flows. The second part of the study is to understand how people perceive smart meter privacy issues and how much they are willing to spend for mitigating privacy breaches. The survey is done in Sweden. Sweden was the first European country to have 100% smart meter roll-out. In 2020, the smart meters installed during the first roll-out will reach their economic lifespan. Hence, the country is preparing for a second-generation mass roll-out of smart meters. The perception of people regarding smart meters is identified from two perspectives. First, the consumers are directly surveyed for estimating their awareness of smart meter privacy problems and their willingness to invest in technologies that prevent such issues. Second, different stakeholders in smart metering are surveyed regarding their experience during first and second roll-out. The methods currently employed to safeguard consumer data is also explored during the second survey]

Referenser, källor

- [1] ERGEG, “*Smart Metering with a Focus on Electricity Regulation*”, E07-Rmf-04-03, no. October, 2007
- [2] G.W. Hart, “*Nonintrusive appliance load monitoring*”. Proceedings of the IEEE. 80 (12): 1870–1891. doi:10.1109/5.192069, 1992
- [3] M. A. Lisovich, D. K. Mulligan, and S. B. Wicker, “*Exploiting In-Home Data*”, no. February, pp. 1540–7993, 2010.
- [4] P. McDaniel and S. McLaughlin, “*Security and Privacy Challenges in the Smart Grid*”, pp. 75–77, 2009.
- [5] E. McKenna, I. Richardson, and M. Thomson, “*Smart meter data: Balancing consumer privacy concerns with legitimate applications*”, Energy Policy, vol. 41, pp. 807–814, 2012.
- [6] U. Greveler, P. Glösekötter, B. Justus, and D. Loehr, “*Multimedia Content Identification Through Smart Meter Power Usage Profiles*”, Proc. Int. Conf. Inf. Knowl. Eng. (IKE), 2012
- [7] F. Brian, M. Anthony, D. Argenio, G. Brook, and H. Donald, “*Methods and Systems for Presenting an Advertisement Associated with an Ambient Action of a User*”, US Pat. Trademark Off. Pat. Appl. Full Text Image Database, 2012.
- [8] L. Jaakonanti, “*Översättning , en sammanfattning av Ei : s rapport om funktionskrav på elmätare - Summary of the report from Ei about smart meters (Ei R2017 : 08)*”, vol. 1, no. 3, pp. 1–3, 2018.
- [9] S. Zhou and M. A. Brown, “*Smart meter deployment in Europe: A comparative case study on the impacts of national policy schemes*”, J. Clean. Prod., vol. 144, no. 2017, pp. 22–32, 2017.
- [10] Asghar, M. R., Miorandi, D., Dán, G., Chlamtac, I.: “*Smart meter data privacy: A survey*”, IEEE Communications Surveys Tutorials, 19, (4), pp. 2820-2835, 2017
- [11] Z. Kolter and M. J. Johnson, “*REDD: A public data set for energy disaggregation research*”, proceedings of the SustKDD workshop on Data Mining Applications in Sustainability, 2011.
- [12] <http://redd.csail.mit.edu/>
- [13] C.-T. Pham and D. Månsson, “*On the physical system modelling of energy storages as equivalent circuits with parameter description for variable load demand (Part I)*”, Journal of Energy Storage, vol. 13, s. 73-84, 2017.
- [14] C.-T. Pham and D. Månsson, “*Optimal energy storage sizing using equivalent circuit modelling for prosumer applications (Part II)*”, Journal of Energy Storage, vol. 18, s. 1-15, 2018.

- [15] C.-T. Pham and D. Månsson, "Experimental validation of a general energy storage modelling approach (Part III)", *Journal of Energy Storage*, vol. 20, s. 542-550, 2018.
- [16] C.-T. Pham and D. Månsson, "Assessment of energy storage systems for power system applications via suitability index approach (Part IV)", *Journal of Energy Storage*, vol. 24, 2019.

Bilagor

Bilagor följer här efter i ordning.

- Administrativ bilaga
- D. Månsson, "Sizing Energy Storage Systems used to Improve Privacy from Smart Meter Readings for Users in Sweden" i Proceedings - 2018 IEEE PES Innovative Smart Grid Technologies Conference Europe, ISGT-Europe 2018, 2018.
- C.-T. Pham och D. Månsson, "A Study on Realistic Energy Storage Systems for the Privacy of Smart Meter Readings of Residential Users" IEEE Access, vol. 7, s. 150262-150270, 2019.
- C.-T. Pham och D. Månsson, "Effects of smart meter privacy protection management on the lifetime performance of 18,650 lithium-ion batteries" IET Smart Grids, Oct 2021, <https://doi.org/10.1049/stg2.12055>.

Sizing Energy Storage Systems used to Improve Privacy from Smart Meter Readings for Users in Sweden.

Daniel Månsson

Department of Electromagnetic Engineering
School of Electrical Engineering and Computer Science
Royal Institute of Technology KTH
Stockholm, Sweden
Email: manssond@kth.se

Abstract—The smart power grid of the future will be heavily dependent on accurate information from the users via smart meter readings. However, from the information on the users power profile much knowledge about the behavior can be acquired, resulting in a breach of privacy. To mask the power profile an energy storage system can be used that obfuscates the smart meter readings. In this paper, we investigate the storage capacity needed if the smart meter is required to report a constant power usage for the user, electricity as well as distributed heating, to the utility. Both single and multiple users per energy storage system are investigated using both derived as well as measured power profiles.

I. INTRODUCTION

The modern smart power grid infrastructure brings new user services and possibilities for financial plans, as well as facilitates the implementation of renewable power production. The feature relies heavily on ICT to connect, gather and analyze generated data from different types of sensors at various levels of the grid. At the user the sensor is most often a "smart meter" (SM) that records and transmits the current power usage or energy usage during some interval. The SM is a crucial instrument that has evolved from being used for simple billing purposes to an advanced ICT needed for the utility provider to be able to plan for future power production or track renewable power produced by the user.

Thus, the SM keeps an eye on the power profile of the user and concerns have been raised about this [1]. Using non-intrusive load monitoring [2] much information about the user can be deduced by looking at the gathered data¹. Trends on, e.g., when the residence is empty or not is easy to see from the power profile [3] but even the actual TV program being watched has also been reported [4]. A quick search online reveals many groupings and campaigns in different countries concerned over the possible privacy breaches by smart meters. In addition, in the light of the EU General Data Protection Regulation (GDPR), the users have more right to control the

¹Some smart meters work by wireless protocols which creates an even greater threat from third parties gaining access to the data.

generated personal data, e.g., the right to erasure of such (Article 17). However, it is of course an obstacle if the utility can not plan for the future, e.g., load scheduling.

Assuming that the primary goal is to simply obscure the actual power profile of the user this can be done by manipulating either the data transmitted to the utility or the data gathered from the user. In both cases "noise" is added either directly to the data stream or by physically altering the power profile of the user. For the later case we can use an energy storage system (ESS) and this is what the work presented here investigates.

In this paper, available data on power consumption is used to judge the ES capacity needed for Swedish households to mask their power profile. As available and usable data with high resolution is often hard to find the numbers presented here indicates the range and approximate behavior. With more high resolution data more studies on, e.g., the synergy with power quality capabilities of the ESS could be made.

The paper is organized as follows; after the introduction in Section I the basis and importance of energy storage (ES) in this context is stated (II.A). Then the description of the general user profiles used is described in Section II.B. In Section III the capacity requirements are investigated, first for a single user per ESS (III.A) and then for multiple users (III.B and III.C). In Section IV.A and IV.B we compared the findings from the preceding sections with two different data sets and after conclusions some points for discussion are added.

II. ENERGY STORAGE FOR PRIVACY

A. Introduction

The need for ES in the grid has increased due to the inherent stochastic nature of renewable power sources (e.g., wind power) and ESSs are needed to implement these into the grid. This is done by, at times of low consumption, storing the surplus of power produced until needed at peaks of demand or low production. In addition, an ESS has many other uses such as frequency stabilization, voltage regulation, backup power, load shedding, shifting of peak consumption for economic gain etc.

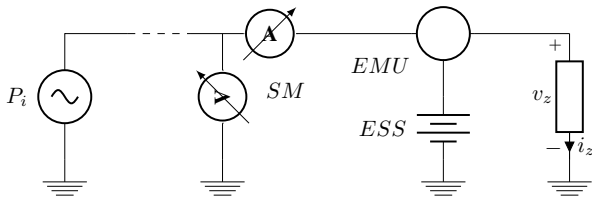


Fig. 1. Schematics of utility (left) and user (right) with an ESS (here depicted as battery). Notice how the SM is positioned before the ESS and if the conditions are met the user is supplied in full, or in part, by the ESS instead. The control (i.e., power flow) is handled by the energy management unit (EMU) that monitors the load and ESS.

This energy transfer can also be used to improve the privacy of the user by implementing the mitigation at the physical layer as opposed to manipulating the data stream. As ESSs are essential for the modern power grid the already many existing applications is an incitement and possibility for ease of implementation of also this use.

As seen above, depending on the underlying principle (economic gain, usage of renewable power, privacy etc.) there are many possible methods and control algorithms for how the ESS should operate to alter the power profile of the user (and reported by the SM). However, for privacy preserving, the simplest, but here not acceptable method, would be to add a random amount of load at random times, thus, creating noise and no need for an ESS. Instead, similar to the approach discussed in [5], we here use the following postulate as the basis for our investigation:

postulate: *A reported constant flat power profile gives the minimum information about the user.*

Of course, we would like to have this flat power profile constant over the entire year but due to weekly and seasonal variations in the power demand this is not possible without considerable overcapacity in the ESS which hinders a realistic implementation. Early investigations, e.g., [6] initially assumed an infinite capacity but later, as we will see here, this has been refined and the work described in this paper is a continuation using real data. Also, it has to be stated that the utility will benefit if they can plan ahead using the knowledge that the users will only request a constant power across the day.

B. User power profiles

We define the instantaneous power usage of the user/load as $P_o(t)$ and assume, barring more detailed fluctuations in time, that $P_o(t)$ approximately follows one out of the three general types given in Fig. 2. This generalization arises from experience with collected data sets and literature surveys. A detailed measurement on the power consumption can show highly transient phenomena and, thus, the profiles here should be viewed as a constructed average envelope that approximate the consumption. The activities of the user can be focused to either night or day or to two peaks during the day, where in all cases the actual length of the time periods and amount of power used can be varied to allow for user variations. For the

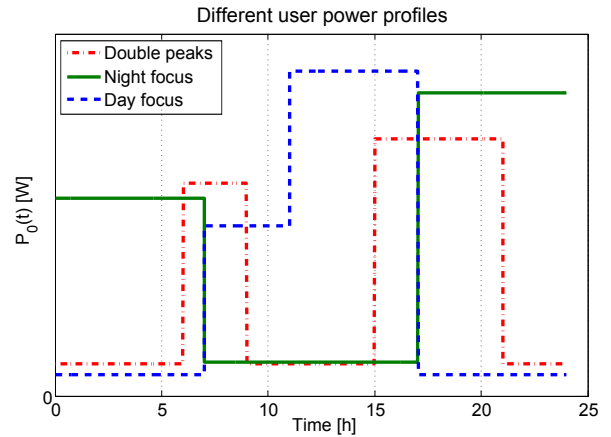


Fig. 2. Approximately, the user power profile follows one out of three general types, that, with detailed measurements and knowledge, reveals much about the user behavior.

three types the given hours for start and stop of activity can here vary with $\pm 2h$ but the average total usage has, in all three cases, been set to $9h$ so that the average energy usage is equal. The period of activity has been chosen to be:

- Double peaks: $06:00 \pm 2h \rightarrow 09:00 \pm 2h$; $15:00 \pm 2h \rightarrow 21:00 \pm 2h$
- Night focus: $00:00 \rightarrow 05:00 \pm 2h$; $20:00 \pm 2h \rightarrow 00:00$
- Day focus: $08:00 \pm 2h \rightarrow 12:00$; $12:00 \rightarrow 17:00 \pm 2h$

The actual time stamps are drawn, within the given intervals, from a continuous uniform distribution. Notice how the ‘Night focus’ is equivalent to a time shifted ‘Day focus’. Due to the privacy infringement the utility, or a third party, can undertake with detailed knowledge of $P_o(t)$, we want, as stated above, the user to request (and SM to report) a constant power, i.e., $P_i(t) = k$, from the utility, throughout the time period². By enforcing this in the investigation we don’t, as opposed to, e.g., [5], look at the effect on the privacy if the SM report a piecewise constant profile. This could come to pass if, e.g., the capacity of the ESS is not enough (e.g., if self-discharge losses are substantial) and $P_i = k$ can’t be delivered across the entire time period. Then partial privacy is reached and there are several privacy metrics (e.g. the relative entropy a.k.a Kullback-Leibler distance [7]) conveying the information leakage. Thus, the results here should be viewed in the light of investigating a best case scenario for privacy concerns.

From this, we define that the momentaneous power required to be handle by the ESS as³ $P_\Delta(t) = P_i(t) - P_o(t) = k - P_o(t)$, i.e.:

$$P_\Delta(t) = k - (P_0\Pi_{01} + P_1\Pi_{12} + P_0\Pi_{23} + P_2\Pi_{34} + P_0\Pi_{45}) \quad (1)$$

where $\Pi_{ij} = H(t - t_i) - H(t - t_j)$ (i.e., a boxcar function between t_i and t_j) and $H(t - t_i)$ is the Heaviside step function

²The ESS is controlled by the EMU which determines if the ESS charges or discharges at any given time.

³This definition follows the passive sign convention that the power utilized by the storage is negative when it is discharging and positive when it is charging.

at time $t = t_i$. Thus, if the ESS can deliver $P_{\Delta}(t)$ across the selected time period the SM would report $P_i = k$ and privacy would be ensured. The variables for $P_o(t)$ are here derived from available information on residential electricity usage and will, as stated above, vary with type of user (e.g., apartment or villa), habits, type of connected equipment, geographic location and time of year and will, naturally, influence the specific details of the outcome. Without detailed measurements it is difficult to assign specific values to the variables in (1) but we can make realistic assumptions that will hold true for an average⁴ Swedish household. Note that, in section III we assume that the SM only reports on residential electricity usage which is assumed for the numeric values below and, thus, not power usage connected to, e.g., distributed heating or gas (see section IV.A.2.)

According to *Gapminder* [8] (and the World energy outlook) the residential electricity use per person in Sweden was 4310 kWh⁵ in 2008 and the average number of persons per household⁶ was 2.1. Thus, an average household in Sweden consumes 9051 kWh per year (i.e., ≈ 25 kWh/day) in energy for electricity. Our user profiles have to reproduce this to be realistic. As stated above, the user power profile is very dynamic and it is difficult to find reliable and, here, usable data (exception to some degree being the data used in section IV and, e.g., [10]).

From this, using *Matlab* [11], we generate random users that are based on the type of profiles given in Fig. 2. The variables for the momentaneous power usage in (1) are random variables drawn from a uniform distribution. The ranges are $P_0 = [175 - 580]$ W, $P_1 = [1.25 - 2.75]$ kW and $P_2 = [1.25 - 2.75]$ kW (giving ≈ 23.8 kWh/day). Then, to simulate many different users (or days) several profiles are generated using this.

III. CAPACITY REQUIREMENTS

A. Capacity requirement for single user per ESS and smart meter

As stated above, the goal is to mitigate a breach of privacy by reporting a constant power usage from the utility, i.e., $P_i(t) = k$, and the ESS has to be able to handle the discrepancy between $P_i(t)$ and $P_o(t)$. The amount of energy in the ESS is, at any given time, given by;

$$W(t') = \int_0^{t'} P_{\Delta}(t) dt = \int_0^{t'} (k - P_o(t)) dt. \quad (2)$$

and we demanded here that $W(t) \geq 0 \forall t$ as a state of negative energy in the ESS has, here, no real physical meaning⁷. The capacity needed is found from $\max(W(t))$ when increasing k

⁴Average in the sense of the mean of the behavior of the users, not the most common behavior.

⁵The total electricity consumption in Sweden is more or less stable since about 1985 [9].

⁶Although this number varies with age group, type of household etc.

⁷However, $W(t') < 0$ for some time $t = t'$ could be defined to mean that energy has been scheduled to be delivered although it doesn't yet exist in the ESS at t' .

TABLE I
CAPACITY REQUIREMENTS FOR SINGLE USER PER ESS.

Profile	μ kWh	σ kWh	% of load energy usage
Double peaks	6.2	2.1	26%
Day focus	7.0	1.6	30 %
Night focus	~	~	~

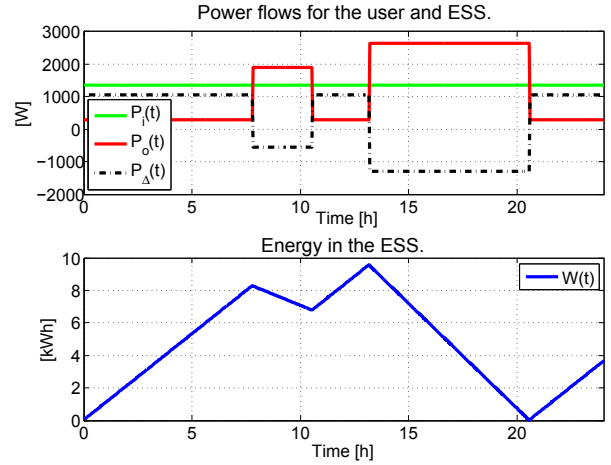


Fig. 3. For this example of a random user, following a "Double peaks" profile, the capacity of the ESS needs to be at least 9.6 kWh when the minimum amount of power is bought from the utility to fulfill $W(t) \geq 0 \forall t$. As also can be seen there is approximately 4 kWh at the end of the day left in the storage.

until $W(t) \geq 0$ is met $\forall t$. We look at a single 24h period (as if often done) and assume $W(0) = 0$, i.e., no initial energy in the ESS. Repeating the procedure with more random users (here 10000) drawn from the "Double peaks" profile gives that, on average, an ESS with ≈ 6.2 kWh capacity (standard deviation of $\sigma \approx 2.1$ kWh) will be sufficient to have the SM report a constant flat power consumption profile. Also, this is $\approx 26\%$ of the energy demand of the user. As can be found [12], this capacity and peak power demand is feasible with existing products on the market where, e.g., peak power and capacity capabilities of 8.5 kW and 19.4 kWh, respectively, has been reported [13]. The modularity of the ESS will also affect these numbers if units are clustered. In Table I the average, μ , and the standard deviation, σ , of the required capacity is given for the three profile types in Fig. 2. As the 'Night focus' and 'Day focus' are equal after a time shift, the results are similar.

B. Capacity requirement for multiple users per ESS and smart meter

Instead of having each user requiring a dedicated ESS we now look at the situation where several users share a larger storage. We assume that this ESS is a collection of smaller units where each user has a connection to the whole via the EMU that at any given time handles the power flow. However, we still consider a single SM reporting the profile for the collection of users. Thus, this is similar to a hotel, some type of apartment housings (e.g., dormitory) or any other situation

where the load that the utility sees (and sells power to, i.e., $P_i(t) = k_M$) is actually a collection of smaller loads sharing the same SM. The same approach as above is used with the exception that, at any given time, the user profile to mask is:

$$P_{oM}(t) = \sum_{j=1}^N P_{o,j}(t) \quad (3)$$

where N is the number of individual users that share the ESS and SM. Editing (2) then gives:

$$W_M(N, t') = \int_0^{t'} \left(k_M - \sum_{j=1}^N P_{o,j}(t) \right) dt \quad (4)$$

Again, for each profile⁸ given in Fig. 2 we generate 10000 groups of N random users which is repeated for $N = [1:10]$. It was seen, as could be expected, that due to the stochasticity in time $P_{oM}(t)$ becomes increasingly triangular when N increases (see Fig. 4) and also that the required capacity per user as a function of N converges towards a minimum (see Fig. 5) which is smaller compared to the sum of the capacity needed for each individual separately. Thus, coordinating the use of a larger ESS is better than each individual user having their own small ESS. In addition, the average capacity per user at the end of the day decreases to about 46% and 84%, respectively, compared to the single user case, hinting also at a more effective use of the ESS (see Fig. 6). (Overcapacity is often a problem as is also found in [14] where it was found that the information leakage decreases when the wasted energy increases). Finally, we calculate the empirical CDF using the data for $\max(W_M(N, t))$ to see how likely it is that different capacities manages to mask the profile (see Fig. 7 and compare the 0.5 point with the data for $\mu_{DP}(N)$ in Fig. (5)). Note that even one extra user sharing a larger ESS improves the situation substantially.

C. Capacity requirement for multiple users per ESS with dedicated smart meters

Finally, we investigate the situation where several users share a larger storage system (as above) but all with their own dedicated SM that reports their individual consumption (i.e., k_j) to the utility. This is similar to the situation of most apartments. At any given time we now enforce on the storage:

$$P_{\Delta}(t) = \sum_{j=1}^N (k_j - P_{o,j}(t)) \quad (5)$$

where we in the investigation add the exception that each individual user never have to buy more energy than to fulfill their individual need (i.e., for user j , k_j is not increased beyond fulfilling $W_j(t) \geq 0 \forall t$). However in the analysis it was found that this produced the same results as for (4) which is due to $\sum_{j=1}^N (k_j - P_{o,j}(t)) = \sum_{j=1}^N k_j - \sum_{j=1}^N P_{o,j}(t) \approx k_M - P_{oM}(t)$. The statement that $\sum_{i=1}^N k_i \approx k_M$ is validated

⁸“Night focus” again being similar to “Day focus” and, thus, not shown for clarity.

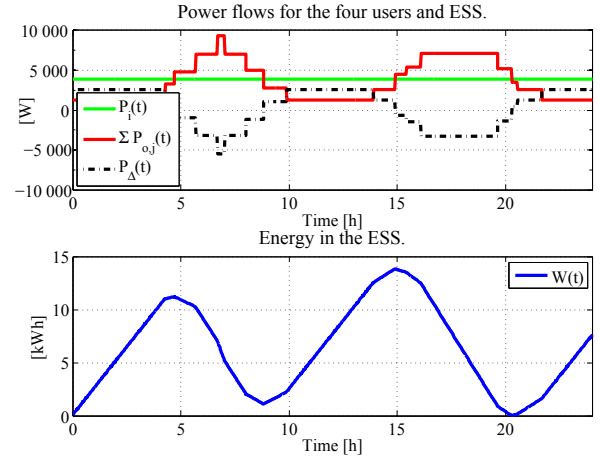


Fig. 4. When four random users share one ESS more total capacity is needed to hide the profiles (notice that the separate user profiles are more or less still distinguishable in $\sum P_{o,j}(t)$). For this example, the capacity of the ESS needs to be at least 13.8 kWh and there is approximately 7.6 kWh at the end of the day left in the storage.

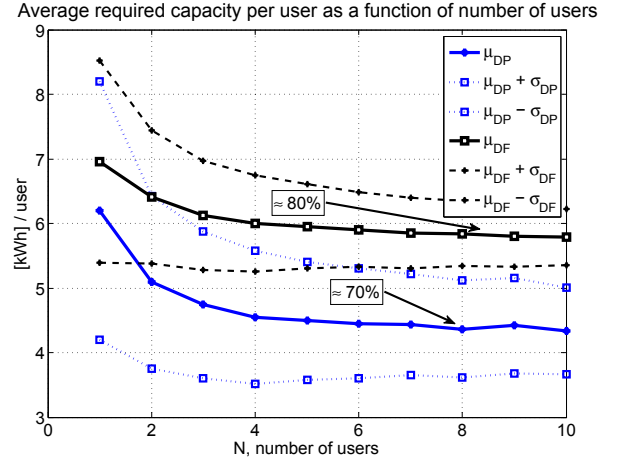


Fig. 5. For the profiles “Double peaks” and “Day focus” it is here shown that the average needed capacity per user (i.e., μ_{DP} and μ_{DF} with standard deviation σ_{DP} and σ_{DF}) decreases when the number of users sharing the ESS increases. If W_1 is the average capacity required to ensure privacy for one single user (of that profile), then instead of requiring a capacity of NW_1 for N users only about $0.7NW_1$ and $0.8NW_1$, respectively, is needed when, here, $N \gtrsim 7$.

in Fig. 8 which shows the average value of $P_i(t)$ (i.e., $\sum_{j=1}^N k_j$ and k_M) required (here) to be requested from the utility to mask the power profile of the user (only the “Double peaks” profile is used here for clarity). As can be seen in Fig. 8 the difference is negligible.

IV. COMPARISON WITH MEASURED DATA SETS

A. Comparison with single-family detached house

Available was also a data set with the energy consumption, in kWh, every hour, for both electricity as well as distributed heating, for a single-family house in Sweden during the winter period 2017-11-28 – 2018-02-20. With this we can compare the capacity requirements if privacy breaches due to patterns

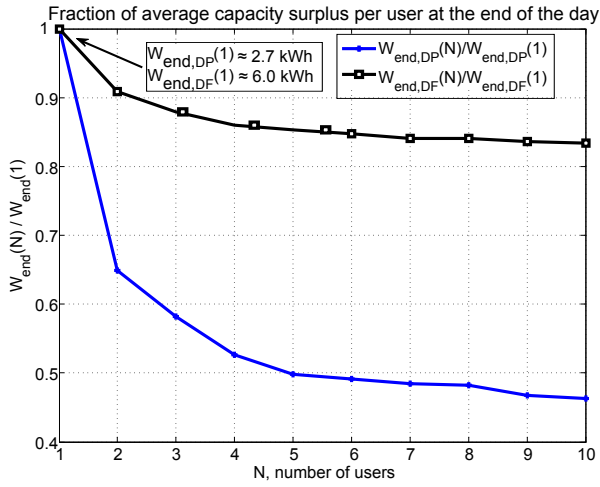


Fig. 6. At the end of the 24h period, compared to the case with only one user per ESS, the amount of energy per user left in the storage, and as a function of the number of users connected to the ESS, decreases. Also, there is more energy per user left when the users have "Day focused" profiles.

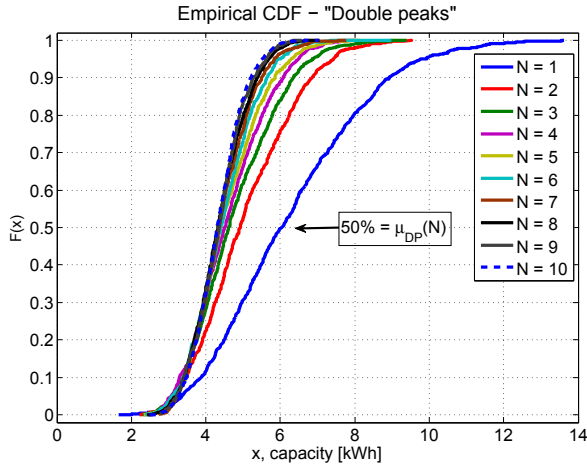


Fig. 7. Different ESS with different capacity have different likelihood to be able to mask the power profile of a user. A 10 kWh ESS will in most cases here be enough.

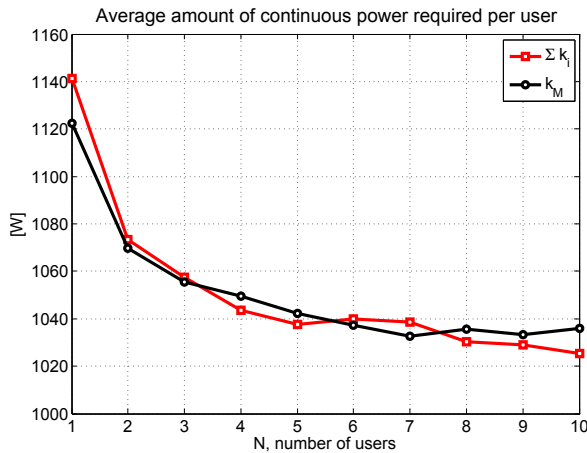


Fig. 8. The power requested (i.e., reported needed) per user from several individual users or a group of users together is approximately the same.

in heating also should be mitigated. However, the data for distributed heating was given with a kWh discretization, which is quite rough, but trends are still visible, see Fig. 10. As we will see, there are differences in the details but it still leads to a good agreement with the capacity requirement found above. Note that, as opposed to before, the usage during the period includes a mix of normal work days, weekends and Christmas holidays, thus, giving a more realistic situation for a (Swedish) household.

1) *Electricity usage:* During the period, data for 84 days was usable and looking at this data we can find variations of the three profiles used above, (see Fig. 9 for examples of the "Double peaks" and "Day focused" profiles). From this data the average ES capacity needed was $\mu \approx 3.0$ kWh (with $\sigma \approx 1.1$ kWh and maximum of ≈ 5.8 kWh). This is somewhat less than the requirements given above but as the electricity energy usage is also less (on average ≈ 16.6 kWh/day compared to ≈ 23.8 kWh/day above). Thus, the capacity requirements compared to the energy usage is about the same percentage ($\approx 18\%$ compared to $\approx 26\%$ above) validating the analysis above.

2) *Distributed heating:* During the period, data for 79 days was usable and looking at this data we saw that the usage profiles, day to day, are quite similar. This is due to the discretization of the data (see Fig. 10) but the mean of the data shows the trend that more energy is used for heating in the evenings. From this data we found that the average ES capacity needed was $\mu \approx 8.1$ kWh (with $\sigma \approx 5.8$ kWh and maximum of ≈ 28.0 kWh). The energy usage for heating was on average ≈ 78.3 kWh/day, thus, the capacity requirements compared to the energy usage is about 10% (which is believed to be low due to the more or less constant usage of heat, see Fig. 10). Thus, if both the usage profiles should be masked the capacity of the ESS should on average not be less than ≈ 11 kWh which is here about four times as much as if only the electricity should be masked (i.e., not including heating).

B. Comparison with the REDD data set

The Reference Energy Disaggregation Data Set [10] is a set of publicly available measurements on the power usage of six different households used here for validation of the results. However, one problem with directly using the REDD is that although it covers almost three weeks and six households, there is in fact only two complete 24 h periods in the whole data set (i.e., $24 \cdot 60 \cdot 60 = 86400$ subsequent data points). For these we get the required capacity to be 6.9 kWh and 1.1 kWh. To get more data we disregard any interruption in the power measurements that last less than 60 seconds (which give us 27 24 h periods to analyze) and assume for the time gap a constant power from the last available data point and perform the numerical integration with this gap length. The findings can be seen in Fig. 11 and the results are, more or less, of the same order as presented above.

V. CONCLUSION

Using data from Gapminder and the World energy outlook for Swedish residential electricity power usage it was seen

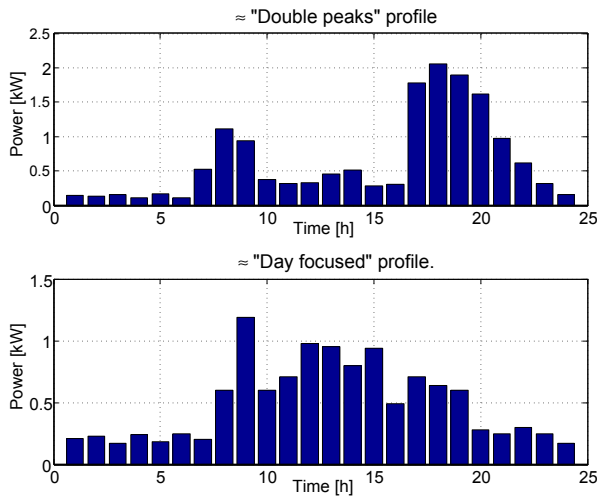


Fig. 9. Variations of the "Double peaks" and "Day focused" profiles could be found in the collected data for residential electricity usage.

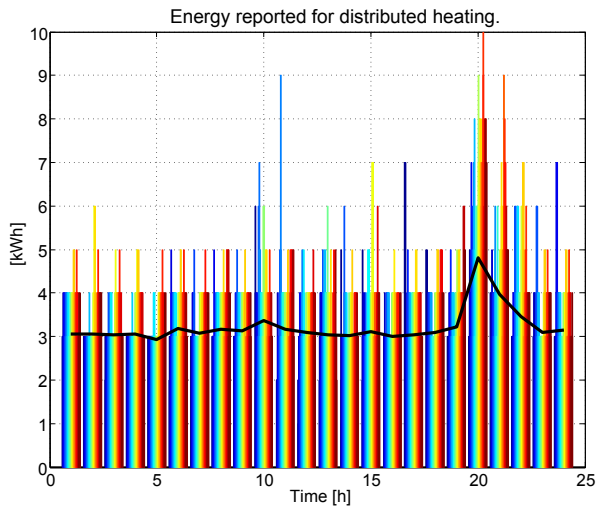


Fig. 10. Energy usage each hour as a function of time for 79 days (each color bar represents one day). As the mean shows (black line) more heat is used during a short time period in the evenings.

that it is relatively easy, with commercially available products, to mask the power profile completely from SM readings. In addition, if several users share a larger ESS the capacity required per user decrease with the number of users. Further, comparison with two available sets of data gives that the capacity requirements are in the same range, if not the user profile for heating should also be masked in which case the requirements increase. All in all, we conclude that a capacity of 6 – 10 kWh will most probably be enough for the SM to be able to report a constant flat power profile.

ACKNOWLEDGMENT

The author would like to thank the Swedish Energy Agency for funding the project *Energy STORAGE for smart Meter Privacy - STOMP* under the SamspeL program as well as the

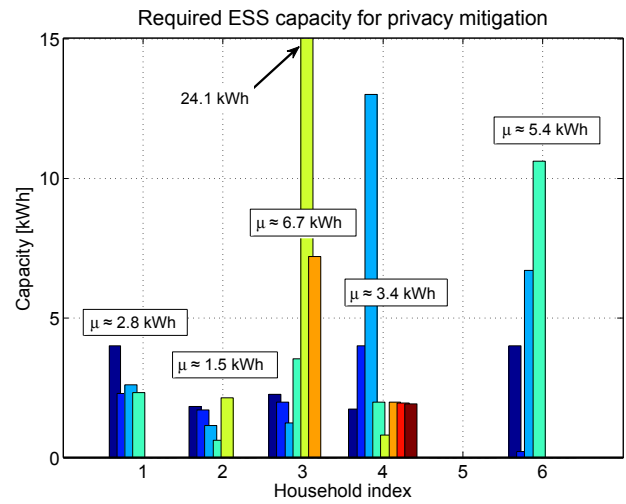


Fig. 11. The required capacity extracted from the REDD for the different households. Notice that, here, no usable data for number 5 existed.

StandUp for Energy project via the Swedish Research Council that makes this work possible.

REFERENCES

- [1] P. McDaniel and S. McLaughlin, Security and privacy challenges in the smart grid, *IEEE Security & Privacy*, vol. 7, no. 3, 2009.
- [2] G.W. Hart, Nonintrusive appliance load monitoring, *Proceedings of the IEEE*, vol. 80, no. 12, pp. 1870-1891, 1992.
- [3] G. Kalogridis and S. Z. Denic, "Data Mining and Privacy of Personal Behaviour Types in Smart Grid", *2011 IEEE 11th International Conference on Data Mining Workshops*, Dec. 2011, pp.636-642
- [4] U. Greveler, B. Justus, and D. Loehr "Multimedia Content Identification Through Smart Meter Power Usage Profiles" *In proceedings of the Computers, Privacy and Data Protection, CPDP*, January 2012, Brussels, Belgium
- [5] O. Tan, J. Gmez-Vilardeb and D. Gndz, "Privacy-Cost Trade-offs in Demand-Side Management With Storage", *IEEE Trans. Inf. Forens. Security*, vol. 12, no. 6, pp. 1458-1469, June 2017.
- [6] <http://copes.gforge.inria.fr/>
- [7] G. Kalogridis, C. Efthymiou, T. Lewis, S. Denic, and R. Cepeda, Privacy for Smart Meters: Towards Undetectable Appliance Load Signatures, *IEEE SmartGridComm10*.
- [8] Gapminder: Ranking of residential electricity user, per person. <https://www.gapminder.org/tools/>
- [9] SCB Statistics Sweden, "Electricity supply, district heating and supply of natural and gasworks gas 2016", *EN11 - Electricity energy supply, district heating and supply of natural and gasworks gas*, ISSN 1654-3661
- [10] Z. Kolter and M. J. Johnson, "REDD: A public data set for energy disaggregation research", *In proceedings of the SustKDD workshop on Data Mining Applications in Sustainability*, 2011. <http://redd.csail.mit.edu/>
- [11] MATLAB version 7.11.0, Massachusetts: The MathWorks Inc., 2010.
- [12] G. Giaconi, D. Gündüz and H. V. Poor, "Smart Meter Privacy With Renewable Energy and an Energy Storage Device", *IEEE Trans. Inf. Forens. Security*, vol. 13, no. 1, pp. 129-142, January 2018.
- [13] The Sunverge Solar Integration System <http://www.sunverge.com>
- [14] G. Giaconi, D. Gündüz and H. V. Poor, "Increasing Smart Meter Privacy Through Energy Harvesting and Storage Devices", *IEEE Journal on Selected Areas in Communications*, July 2013, Vol.31(7), pp.1331-1341

Received August 30, 2019, accepted September 20, 2019, date of publication October 7, 2019, date of current version October 28, 2019.

Digital Object Identifier 10.1109/ACCESS.2019.2946027

A Study on Realistic Energy Storage Systems for the Privacy of Smart Meter Readings of Residential Users

CONG-TOAN PHAM¹ AND DANIEL MÅNSSON

School of Electrical Engineering and Computer Science, KTH Royal Institute of Technology, 114 28 Stockholm, Sweden

Corresponding author: Cong-Toan Pham (ctpham@kth.se)

This work was supported by the Swedish Energy Agency through the project Energy STorage for smart Meter Privacy - STOMP.

ABSTRACT The introduction of smart meters sparked concerns about privacy breach through real-time monitoring of electric power consumption. Valuable private information about occupancy, behaviour, health, religion and wealth can be extracted from the user's power profile which urges measurements to protect the integrity of the user. One physical mitigation technique to assure privacy is explored using energy storage systems. Real energy storage technologies are limited in their energy capacities and power capabilities, which have to be appropriately sized to fulfil their role. This paper analyses and compares different energy storage technologies (li-ion, lead-acid, electric double layer capacitor and flywheel) for the protection of residential users by estimating the minimal required capacities and costs for both single and multiple user cases. The analysis is based on actual measured user data from the *REDD* data set. The results show that the integrity can be protected with reasonable capacities and investments ranging in the margin of market available products.

INDEX TERMS Energy storage system, privacy, smart meters, residential user.

I. INTRODUCTION

Smart meters (SMs) are the next generation of electricity meters enabling near real-time monitoring of electric consumption and generation at the customers' premises. They have been introduced with the purpose of improving the electric network reliability and efficiency, and allowing greater control and feedback over the user's own consumption. The integration of such Information and Communication Technologies (ICTs) has opened up new possibilities and services such as accurate consumer billing through dynamic pricing or valuable real-time information for grid operators [1]. However, the interconnectivity and accessibility of such devices gave rise to concerns regarding cybersecurity and privacy.

Especially, the real-time monitoring of the user's electric energy consumption via SM reveals private information such as occupancy, behaviour and wealth. The potential privacy breach has sparked public interest on various media: especially, the potential abuse of such information. The leaked information can go so far to expose the use of individual home

appliances [2], [3] and even the TV program being watched if a sufficient data sampling rate is available (≥ 0.5 Hz) [4]. In short, the power consumption of the TV varies with changing brightness. A person with prior knowledge of the power consumption patterns of certain TV programs or movies can deduce the content being viewed on the TV based on the non-intrusive load monitoring method (NILM) as applied in [4]. Identifying information about health and religious affiliation is also not too far-fetched if, for example, patients are using medical equipments (e.g., heart monitoring) or religious festivities take place (e.g., fasting period with less cooking practices). Similarly to the TV all that is required is an adequate estimate of the power consumption profiles of the individual appliances: in this case the cardiac monitor or the cooking appliances such as a stove, a kettle, and a microwave etc.

This issue creates a conflict of interest between the consumer and the grid utility over the disclosed data. Several solutions and methods have been investigated in achieving a compromise between both factions by guaranteeing safety (encryption) and use of only necessary information (legislations) [1]. However, the aim of this paper does not focus on either option, but instead explores the idea of manipulating the electric consumption profile measured by the SM through

The associate editor coordinating the review of this manuscript and approving it for publication was Shantha Jayasinghe.

energy storage systems (ESSs). In fact, the ESS is utilized to alter the power profile in such a way that the least amount of information about the user can be deduced: i.e. a constant power profile. In [3] and [5] the idea was studied to use ESS to mask the user’s profile or, more specifically, what mitigation impact an ESS can potentially have on privacy. Please note, that in this study it is assumed that the ESS is isolated, i.e., disconnected from the internet and free from other surveillance. The latter focuses on identifying the minimum required storage capacity and power capabilities of an ESS needed to fulfil the task. However, a real ESS is bound by constraints limiting its output or capacity. For example, battery energy storage systems (BESSs) feature limited power output due to their restrictions of discharging current. Similar restrictions apply to other energy storage technologies as well such as flywheels, where a maximum rotational speed marks the upper limit of safe operation. Furthermore, real ESSs exhibit losses and delayed responses to sudden input changes, which affect the storage’s overall performance and efficiency. Here, this translates to important information leakage. Hence, the results in [5] provide an initial picture of the requirement for an ESS to comply with the demand for privacy. But, further investigation is required to transfer previous conclusions to real ESSs.

Providing privacy via ESSs is the main focus of this study. In this study an experimentally verified circuit model of ESSs is applied to residential power consumption profiles to judge what ESS capacities are appropriate to maintain privacy. A set of four different ESSs (li-ion, lead-acid, electric double-layer capacitor (EDLC), flywheel energy storage (FES)) are compared for their suitability in this particular application. In addition, this paper uses actual measured user data from the REDD data set [6] (date, load power consumption etc.).

The paper follows the structure of first introducing the model approach used to analyse ESSs in Section II-A. Section II-B describes the parameters and assumptions made for the ESS model. Then, a reference point for the ESSs and the measure of privacy level is defined (Section II-C). A brief description of the load profiles is provided for the used REDD data in Section II-D. Next, four different ESSs are investigated and discussed for single users (III-A), followed by a comparison of capacity and cost for different levels of privacy protection (III-B), and finally an analysis for multiple consumers (III-C). A short summary of the findings and concluding remarks are given in the Sections IV and V.

II. ENERGY STORAGE FOR PRIVACY

A. ENERGY STORAGE MODEL

In [5] ESSs have been investigated to protect the user’s privacy by masking the user load profile as a constant flat power profile. The premise of the aforementioned study is based on the postulate that a constant profile leaks the minimum amount of information. Hence, the ESS’s task is to store and absorb power in accordance to the user’s behaviour to obtain the desired flat profile. In other words the momentaneous

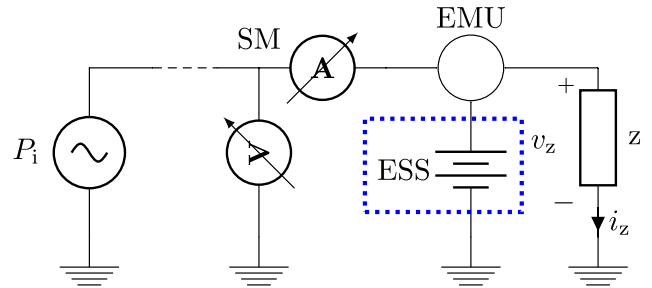


FIGURE 1. Schematic of the electric power supply from the utility (left), denoted as P_i , to the consumer z . The smart meter SM measures the power consumption from the utility to the user. The Energy management unit (EMU) monitors and controls the power in-/outflow between load and ESS.

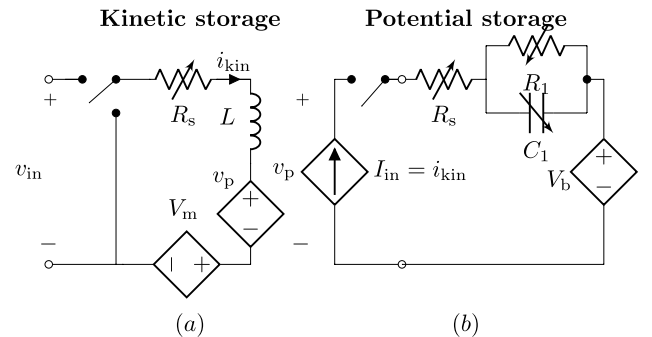


FIGURE 2. Equivalent circuit models for (a) kinetic and (b) potential storages.

power to be handled by the ESS is the power difference P_Δ between the instantaneous power consumption of the user P_z and the desired (and reported by the SM) power $P_i = k$ (see Fig. 1).

$$P_\Delta(t) = P_i(t) - P_z(t) = k - P_z(t) \quad (1)$$

A real ESS may only uphold P_Δ to a limited degree since efficiency, self-discharge and delayed response affect the ESS’s overall performance. Thus, this paper applies a more realistic modelling of ESS to privacy protection schemes. The model used in this context has been adopted from [7] (see Fig. 2). The lumped model encompasses the dynamic behaviour these ESSs display in form of the electrical equivalent components resistance, capacitance, inductance as well as dependent sources. Depending on the type of ESS different parts of the model apply. The potential storage part in Fig. 2 (b) represents the li-ion, lead-acid battery or EDLC. Here, the EDLC is treated as a pure capacitor with the voltage source V_b omitted, and for the batteries two series RC-branch instead of one are used here. More components can be added for better dynamic response behaviour. The flywheel is sufficiently modelled by the kinetic storage part only in Fig. 2 (a). Depending on the nature of storage technology some components vary with the storage’s state. For example V_b changes with the state-of-charge (SoC) of the battery or R_s with the rotational speed of a flywheel. The model is verified in [8], and a more detailed description of the components can be found in [7].

TABLE 1. ESS circuit model parameters and constraints.

ESS type	ESS parameters						ESS constraints						
	R_s [Ω , Nm · s]	L [H, kgm ²]	$R_{1,2}$ [Ω]	$C_{1,2}$ [F]	V_b [V]	V_m [mV]	SoE ₀ [%]	SoE _{min} [%]	SoE _{max} [%]	I_{min} [A]	I_{max} [A]	V_{min} [V, rad/s]	V_{max} [V, rad/s]
Li-ion	0.113	-	0.041 0.019	1027 58880	3.7	-	50	20	100	-1.75	1.75	3.1	4.2
Lead-acid	0.018	-	0.063 0.072	558 32586	6	-	50	20	100	-6	6	5.2	6.6
EDLC	0.014	-	227.4	50	-	-	50	20	100	-1	1	0.25	2.5
FES	1.041e-06	0.871	-	-	-	85.39	50	20	100	-13.75	13.75	280.9	628.31

Note, in this study ageing effects of the ESSs have been neglected partly due to the fact that the studied time frame is short (24 hr) where ageing is deemed negligible. However, for longer time periods (>months) degradation is crucial for a realistic representation of the ESSs, and time dependent components have to be adopted (e.g., $R_s(t)$).

B. ENERGY STORAGE PARAMETERS AND ASSUMPTIONS

Four different storage technologies, namely a li-ion battery [9], a lead-acid battery [10], a EDLC [11] and a FES driven by a permanent magnet synchronous machine (PMSM) [12] have been analysed.

Table 1 summarizes the storage parameters and assumptions made for the models. Note, the table lists only the initial values during the start of simulation. Some parameters such as series resistance R_s or V_b can change over the course, dependent on the condition of the ESS during operation (e.g., $R_s(\text{SOC})$, $R_1(\text{SOC})$, $R_2(\text{SOC})$, $C_1(\text{SOC})$, $C_2(\text{SOC})$ and $V_b(\text{SOC})$ for the li-ion and lead-acid batteries). The data used for the li-ion and lead-acid battery has been established from data sheets [9], [10] and through experimental testing [8]. EDLCs are also electrochemical devices similar to batteries which can also display non-linear characteristics [13], [14]. In this study, however, the EDLC is simplified as a pure capacitor (i.e., constant parameters) which is an acceptable approximation seen in [8] and pointed out in [15]. The FES is a flywheel system enclosed in a vacuum chamber and stabilized by magnetic bearings. The dominant loss factor is attributed to the bearings where V_m and R_s represent a constant and a speed dependent torque loss respectively.

The ESS's operation is limited by the constraints listed on the right side in table 1. Here, we characterize the level of energy reserve of an ESS by the state-of-energy (SoE) instead of the more commonly used term of state-of-charge (SoC) used in batteries. The reason stems from the more intuitive use of this metric for the alternative storage technologies. The SoC expresses the ratio of accumulated electric charge measured in Coulomb (or Ah) to the nominal charge capacity, which is not directly transferable to ESSs of different physical nature such as flywheels or pumped-hydro stations.

All ESSs start with 50 % SoE and cannot be discharged below 20 % state-of-energy (SoE).¹ Note, the assumed initial SoE for the real ESSs differs from the initial SoE (0 %SoE)

¹The minimum and maximum SoE is equal for easier comparison, even though some storage technologies can utilize deeper discharge levels.

of the later described ideal ESS (Section II-C). This reduces the direct comparability between the real and ideal ESS. But, it is a necessary adjustment to represent real ESSs based on the minimum and maximum limitations. Otherwise, an initial empty (SoE = 0 %) or fully charged ESS (SoE = 100 %) would limit its use if further discharge or charge is requested while its SoE lies below SoE_{min} or would rise above SoE_{max}. Choosing either one initial condition for the real ESS leads to a reduction of privacy protection. Hence, for that reasoning we choose 50 % SoE₀ to give leeway for the ESS's operation range. Note though, that this assumption entails that the real ESS needs to be oversized based on the restricted SoE range (SoE_{min}-SoE_{max}) and initial starting point (SoE₀). Furthermore, the BESS's and EDLC's operation is limited by the minimum and maximum allowed voltage and current input. The FES is similarly constrained in the input current to the PMSM and by the allowed rotational speed range (rad/s).

C. IDEAL ENERGY STORAGE AND COVERAGE FACTOR

The main objective is to protect the user's privacy by not leaking valuable information on the user's behaviour based on their electric power consumption. A constant power consumption reported by the SM is postulated to guarantee protection as described earlier in equation (1). However, this has to be achieved with the least effort, i.e., the smallest possible ESS. In this sense, the power k ($P_i(t) = k$) is chosen in such a way to minimize the storage capacity (see (2)). Furthermore, we assume that the energy $W(t)$ in the ideal ESS is empty at the beginning (i.e., $W(0) = 0$) and demand that $W(t) \geq 0 \forall t$ (see (3)). W_{max} denotes the maximum energy stored in the ESS during the course of the studied time period t ($W_{max} = \max(W(t))$). Depending on how k is determined the ESS is charged and discharged differently with different outcome in size. An example can be seen in Fig. 3 where P_{Δ} must be met by the ESS at all times to achieve $P_i = k$. The peak point of $W(t)$ marks the maximum needed energy capacity of the ESS.

$$\arg \min_{k \in [0, \infty]} \{W_{max}\} = \arg \min_{k \in [0, \infty]} \{\max(W(t))\} \tag{2}$$

$$W(t') = \int_0^{t'} P_{\Delta}(t)dt = \int_0^{t'} (k - P_z(t)) \tag{3}$$

The ideal ESS can serve as a reference point for real ESSs. A smaller ESS is not able to provide the necessary capacity to absorb and deliver sufficient energy. An oversized ESS is underutilized, introduces higher self-discharge losses

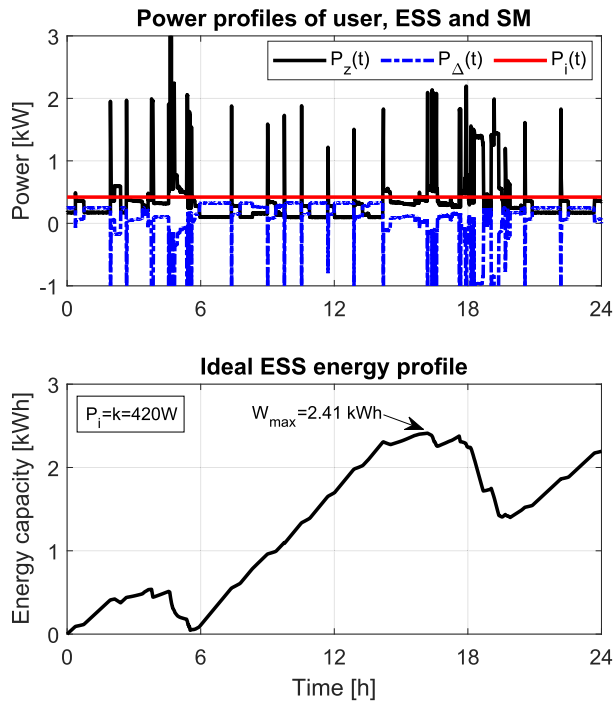


FIGURE 3. Power and energy profile of an ideal ESS ($W_{\max} = 2.41$ kWh) to fulfil privacy requirement ($P_i(t) = k = 420$ W) from the REDD dataset [6]. The SM reports the constant P_i instead of the real consumption.

and investment effort. Since real ESSs feature losses and technical constraints (e.g., minimum or maximum allowed SoE, current or voltage levels etc.) they are bound to deviate from the ideal case. The interesting question to answer is what type and size of different storage technologies is required.

If we understand a breach of privacy by not keeping $P_i(t)$ constant then we can loosely define that the degree of lost privacy is measured by the ESS not satisfying $P_{\Delta}(t)$. In [16] a coverage factor (C_f) was introduced to measure the degree of overlap between the ESS's actual power performance (P_{st}) and a reference power profile. There, C_f is used to optimally size ESSs to just follow the demanded reference curve. This approach is also applicable in this study, where the demanded reference curve is P_{Δ} the ESSs have to satisfy. A C_f of 1 indicates that the ESS is fully able to provide $P_{st}(t) = P_{\Delta}(t) \forall t$ which means 100% privacy protection. On the other hand if C_f is 0 the ESS does not provide any power equivalent to having no ESS and 0% privacy protected. It is noteworthy that the C_f factor does not scale proportionally to the percentage of protected privacy as some leaked power peaks may contain more or less information. For example, the ESS may only partially cover a peak power and revealing a portion of actual user consumption. However, more information will be exposed in case the ESS is fully depleted or charged preventing further operation, and, thus, exposing the original profile.

$$dp(t) = P_{\Delta}(t) - P_{st}(t)$$

$$C_f = 1 - \frac{\int_0^T |dp(t)| dt}{\int_0^T P_{\Delta}(t) dt} \quad (4)$$

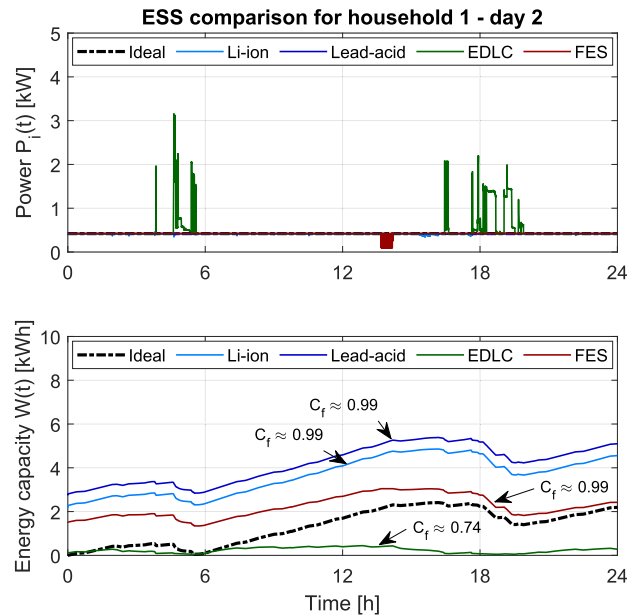


FIGURE 4. Comparison between the ESSs' performance for a single day of household 1. The minimum required capacity of the ESSs to fulfil $P_i = k$ as best as possible for this particular day is the maximum peak of respective $W(t)$.

D. USER LOAD PROFILE FROM REDD DATA

In this study the *Reference Energy Disaggregation data set (REDD)* [6] is used to investigate the privacy focused application of real ESS. The data set measures close to three weeks worth of data on the power usage of six different households. Unfortunately, as it has been pointed out in [5] interruptions in measurements occur throughout the data set, where only a few complete 24 h sets of continuous data are available (i.e., $24 \cdot 60 \cdot 60 = 86400$ consecutive data points). Additionally, interruptions below 60 seconds are neglected by filling the missing data points with a constant power from the previous data point. With these assumptions a total of 27 full 24 h sets divided between the six households are available.

As a side note, the profiles seen for the individual households can vary significantly from each other even within the same household. This coincides with the notion in [17] that examined possible factors contributing to the variation within household energy consumption. There, it is inferred that the behaviour of the occupants is the dominant factor on the variability of consumption which means that the conclusions drawn for one household are only to a limited extent transferable to other households. In our case, the optimal size of the ESS to protect the privacy has to be uniquely defined for each household and cannot necessarily be understood as a general rule of thumb for all residential buildings.

III. OPTIMAL STORAGE CAPACITY

A. REAL CAPACITY REQUIREMENT FOR SINGLE USER PROFILE AT MAXIMUM PRIVACY

In this section the minimum required capacity of the ESSs for the different households is estimated. The example in Fig. 4

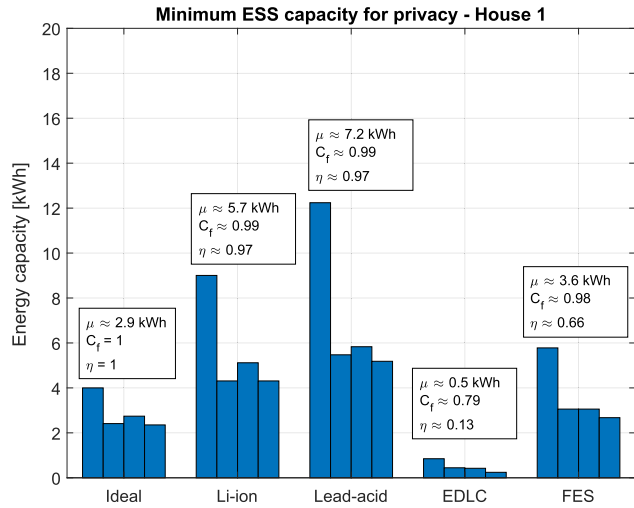


FIGURE 5. ESS comparison household 1 with 4 independent days of data.

shows the comparison between power and energy profiles of the different ESSs for household 1 day 2. The black dashed line represents how an ideally suited ESS operates with the corresponding energy capacity needed. Discrepancies in P_i reveal that not all ESSs are fully able to provide P_Δ , manifesting itself as $C_f \neq 1$. This is especially visible for EDLC (see Fig 4). The desired constant power consumption seen by the utility is therefore not guaranteed. Furthermore, taking a closer look to the energy curves reveals different necessary storage capacities to fulfil this task. The batteries and the FES are considerably oversized (up to 230 % of $W_{max,ideal}$). The necessary flywheel size is slightly above the ideal case (130 % of $W_{max,ideal}$) but lacks in efficiency compared to the batteries. In this particular case, the EDLC's C_f maximizes at 0.74, which results in a storage size of less than one-fifth of the necessary capacity. The EDLC system depletes exponentially dependent on its time constant² hinting to a considerable energy loss of 99 % within 8 hours. Paired with the charge and discharging losses the EDLC system is barely able to uphold energy levels above the minimum SoE, and, thus, low C_f s are obtained even with increasing the capacities. From this it can be concluded that EDLC are unsuited for this application and timespan. The batteries and the FES are technically feasible with li-ion system as the most promising option due to the lower in generally required capacity compared to lead-acid, and higher efficiency than the FES.

Similar results are observed when we take a look at the other households and days. Figure 5-9 show the corresponding storage sizes for the different households where each bar represents one day of the respective house. It becomes apparent that even within one household electricity consumption can vary substantially, where different storage sizes are required to satisfy privacy issues. It is unwise to customize ESS for a single day, but this highlights the high variability in the user's consumption patterns (visible peaks in household

² $\tau = (R_1 C_1)/2 \approx 1.58$ h when considering the relation $W = 0.5 C_1 V^2$

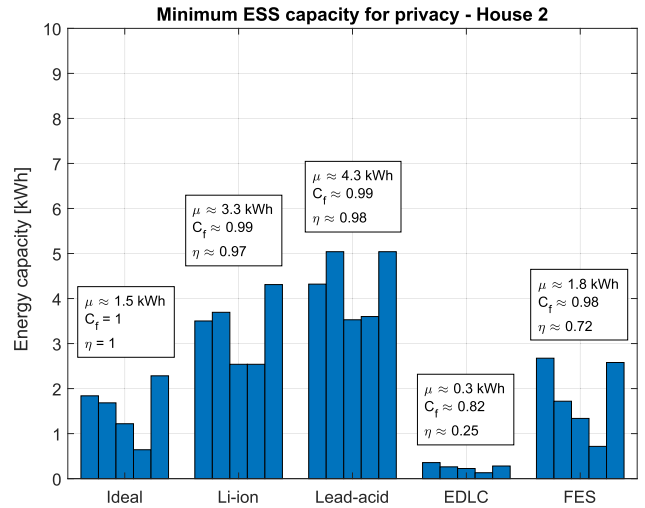


FIGURE 6. ESS comparison household 2 with 5 independent days of data.

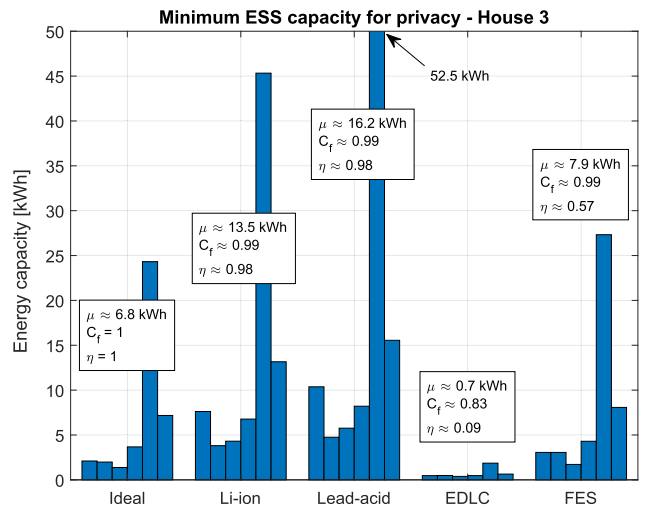


FIGURE 7. ESS comparison household 3 with 6 independent days of data.

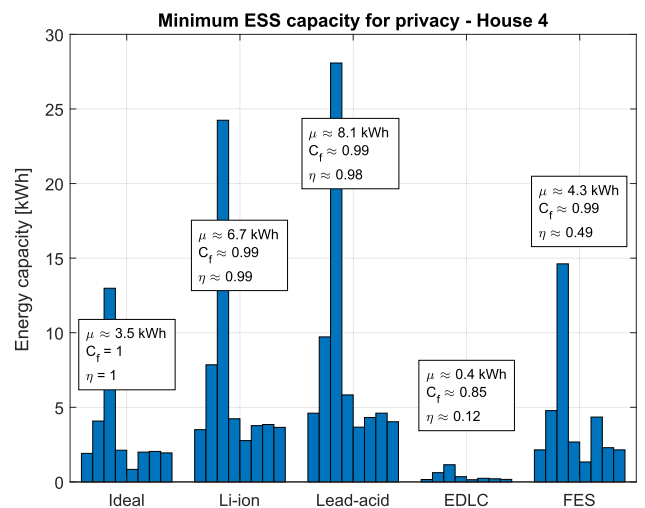


FIGURE 8. ESS comparison household 4 with 8 independent days of data.

1, 3, 4 and 6). Overall, the results seen in Fig. 5-9 and summarized in Table 2 coincide well where li-ion battery systems are 190-220 %, lead-acid battery systems 230-290 % and FES

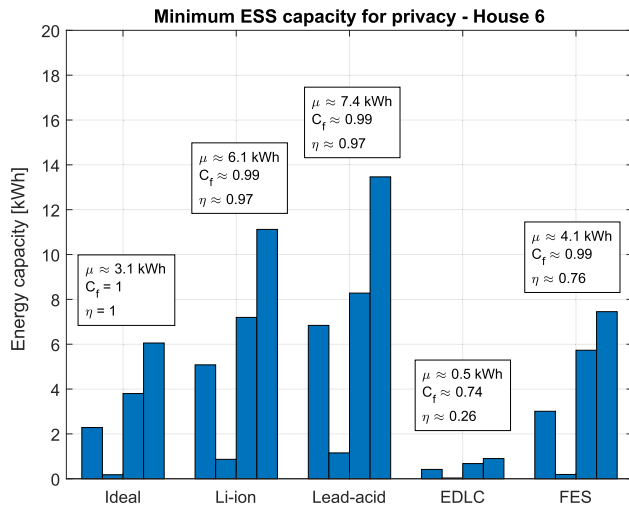


FIGURE 9. ESS comparison household 6 with 4 independent days of data.

TABLE 2. Average capacity requirement for single household.

	W_{\max} [Wh]	C_f [-]	η [-]	% larger/smaller than ideal energy [%]
Ideal	3705	1	1	0
Li-ion	7350	0.99	0.98	100.6
Lead-acid	8962	0.99	0.97	148.7
EDLC	466.6	0.81	0.15	-85.7
FES	4513	0.99	0.62	23.5

115-140 % the size of the ideal storage. The EDLC are only 10-20 % of the size of $W_{\max,ideal}$ due to the fact that larger EDLC sizes do not improve C_f . The variance in percentage is explained by the required power capability in the application. Some profiles exhibit high short term power spikes (up to 10 kW in seconds/minutes intervals) unfavourable to battery systems due to their limited power capabilities. As compensation the BESS size has to be further increased, as dictated by the theory of Ragone plots [18], which leads to redundant capacity just to fulfil power demands. The opposite is true for EDLCs which, in contrary to BESS, feature high power in exchange for low energy capacity per unit.

The results show that the necessary (mean) storage capacities to preserve privacy lie within the margin of existing products on the market. For example, the Tesla Powerwall (5 kW/ 13.5 kWh) [19], the RESU10H (5 kW/ 9.8 kWh) from LG Chem [20] or the Varta element 12 (4 kW/ 13 kWh) from Varta [21] are few examples of viable market available lithium-ion based products. On the other hand EDLC and FES have so far not experienced any residential use, but have potential use in grid focused applications and services such as voltage control, power quality, and smoothing of intermittent power generation of renewable energy sources [22], [23].

B. ENERGY STORAGE SIZE AND COSTS VS PRIVACY

Another crucial aspect to consider is the potential costs for investing in a system for privacy purposes alone, especially

TABLE 3. Main cost items of energy storage systems from [24], [26]. *The $C_{OM,v}$ and C_{RC} for EDLC are not available and assumed 0 €/kWh and 229 €/kW (equal to C_{TCC}) respectively.

	Capital		O&M		Replacement
	C_{PCS} [€/kW]	C_{SV} [€/kWh]	$C_{OM,f}$ [€/kW]	$C_{OM,v}$ [€/kWh]	C_{RC} [€/kW]
Li-Ion	463	795	6.9	2100	369
Lead-acid	378	618	3.4	370	172
FES	287	2815	5.2	2000	151
	C_{TCC} [€/kW]		$C_{OM,f}$ [€/kW]	$C_{OM,v}$ [€/kWh]	C_{RC} [€/kW]
EDLC	229		4.4	0*	229*

answering the question what storage sizes and total costs are expected for different levels of privacy. For example, in exchange for a part of the user's privacy a smaller sized ESS can be a compromise between privacy and necessary investment.

The total costs C_{TC} for an ESS are estimated based on capital, operation and maintenance (O&M) and replacement costs (see (5)). The capital costs divide into two parts: The procurement of the storage vessel (C_{SV} [€/kWh]) and the power conversion system (C_{PCS} [€/kW]). The O&M costs comprise of a fixed ($C_{OM,f}$ [€/kW]) and variable cost factor ($C_{OM,v}$ [€/kWh]). A one time replacement cost (C_{RC} [€/kW]) is also included although this study investigates only a 24 hours time period.³ The individual costs are calculated based on the rated capacity (W_{st}) and rated power (P_{st}) of the ESS at specific C_f values. Table 3 lists the cost assumptions given in [24]. Information on the EDLC are only available for the total capital costs C_{TCC} and the fixed O&M costs.

$$C_{TC} = W_{st} * (C_{SV} + C_{OM,v}) + P_{st} * (C_{PCS} + C_{OM,f} + C_{RC}) \quad (5)$$

Figure 10 illustrates how the ESS sizes and corresponding total costs increase in average with higher requested privacy. The size is detailed as a ratio between the actual compared to the ideal ESS size (W_{st}/W_{ideal}). The BESS are in average more than two times (Li-ion 2.24, lead-acid 2.71) the ideally required size when considering 100 % privacy. Reducing the requirement slightly significantly decreases the storage sizes, where the highest reductions are achieved at the top 10 % C_f (around 80-100 % capacity savings for batteries). The FES has an advantage over the BESS due to its lower necessary storage size even at near 100 % C_f (≈ 130 % of W_{ideal}). However, we keep in mind that the FES is in general less efficient ($\eta \approx 62$ %) than the BESSs. The EDLC rarely reaches C_f values over 80 %. Higher C_f values are only achieved in cases where the ESS is dominantly charged over the time period. On first impression, this seems positive in regard to the small storage size. But, with a low efficiency ($\eta \approx 15$ %) this equates to wasting rather than storing energy even though useful if only concerning the privacy preservation [25]. In this sense the EDLC only works as load without being able to

³Long-time investigations (> several years) may require several replacements.

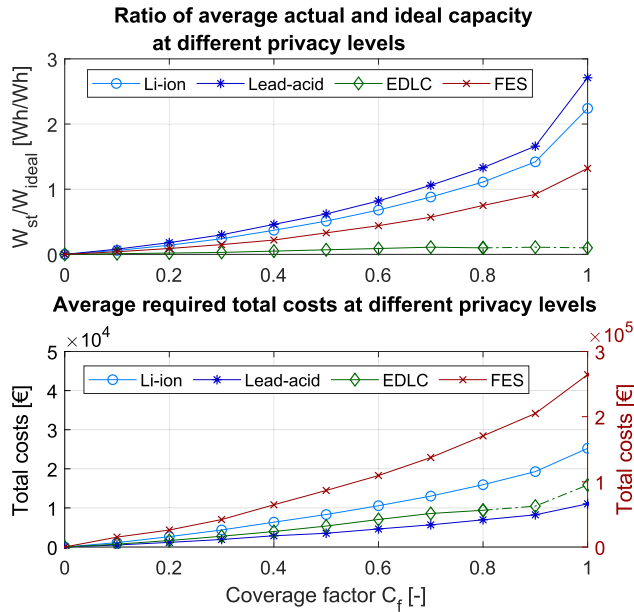


FIGURE 10. Top: Required average storage capacities to fulfil different levels of privacy. Bottom: Total cost estimation for various ESS at different levels of privacy. (left axis: li-ion, lead-acid, EDLC; right axis: FES). Note, high levels of C_f for EDLC are only obtainable under specific conditions (dominantly charging).

return the energy which has already been lost through charging and self-discharge. Ultimately, a small storage capacity is sufficient since only a fraction of the input energy is retained.

Now, taking a closer look at the required costs for different C_f the result is reversed where FES, even though close in size to the reference, features the highest total costs in average (≈ 260000 €) (Fig. 10). This is ten times higher compared to the other ESS alternatives, where li-ion amounts to roughly 25000 €, followed by EDLC (≈ 16000 €), and lead-acid as the cheapest option (≈ 11000 €). The FES is significantly oversized in terms of power capabilities (5.5 kW/unit) due to the fact that the residential application is dominantly energy rather than power focused, which ultimately stacks up the costs for C_{PCS} and C_{SV} . The high specific power of FESs (400-1500 W/kg) compared to BESSs (75-300 W/kg) favours their usage in short term high power applications (up to few hours) such as power quality and voltage regulation control in the power grid [22]. In applications with long discharge times over several hours the advantages of FESs diminish due to significant self-discharge losses similar to the EDLC. Hence, FESs commonly find application in conjunction with other ESS [22], e.g. batteries, to compensate each other's shortcomings if both high power and high energy capacity is demanded.

The cost calculations favour the lead-acid over li-ion battery due the overall low costs for all cost items (Table 3). This is unsurprising with regard to the short time frame, where major differences in performance remain negligible. However, a long-term analysis, and also including

ageing processes over several years will reveal differences due to the distinct lifetimes of the technologies. In general, the expected lifetime of lead-acid batteries is commonly 200-500 cycles dependent on its operation regime compared to 1000+ cycles for li-ion batteries [22], [27]. In niche applications with short term high power demands, i.e. short discharge durations with immediate recuperation, FESs can surpass BESSs in terms of expected lifetime (20000+ cycles [22]). Therefore, this cost calculation does not deliver a full economic evaluation, but an initial picture instead. As previously the EDLC is deemed unsuited in performance and in economy with occurring costs higher than lead-acid.

Finally, the estimated costs for a singular household are in range of market available products. Considering only the capital costs of li-ion batteries the necessary storage size and cost is overestimated to roughly 1100 €/kWh⁴ compared to the available products from Tesla (Tesla Powerwall 650 €/kWh [19]) or LG Chem (RESU10H 540 €/kWh [20]). Hence, mitigating privacy concerns through a single storage module is possible and more so if lower privacy levels are acceptable.

C. REAL CAPACITY REQUIREMENT FOR MULTI-USERS

Alternatively, multiple users can share an ESS to collectively protect their privacy to the outside observer. In this sense, the SM reports the accumulation of profiles similar to that of an apartment complex. The approach remains the same but only the combined load consumptions of all users have to be balanced.

$$P_{\Delta}(t) = k_M - \sum_{j=1}^N P_{z,j}(t) \tag{6}$$

Unfortunately, the data available only provides single user profiles. Therefore, in order to simulate multi-user applications this study artificially generates multiple user profiles by combining the five available household power profiles from the REDD data. The different profiles are summed up, analogously to a situation where these households share a SM in pairs, triplet, quadruple etc.

From Fig. 11 we can observe that the required storage capacity and total cost decrease with increasing numbers of users sharing one ESS as also noted in [5]. The greatest savings in cost are achieved by just sharing the ESS with a second user but converges to a minimum level of around 30-50 % of the initial size and costs (li-ion: 600 Wh/user, 2000 €/user; lead-acid: 850 Wh/user, 1000 €/user; EDLC: 110 Wh/user, 3200 €/user; FES: 670 Wh/user, 38000 €/user). Note, these numbers are heavily dependent on the user's consumption patterns and the ESS device tested. Nonetheless, substantial savings can be expected for groups even in small numbers.

$${}^4c_{TCC} = W_{st} * c_{SV} + P_{st} * c_{PCS}$$

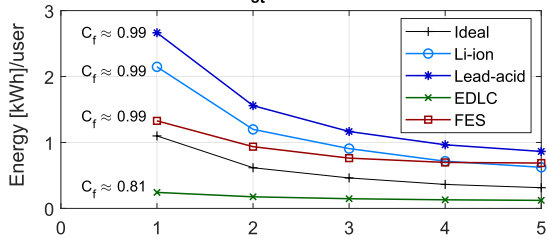
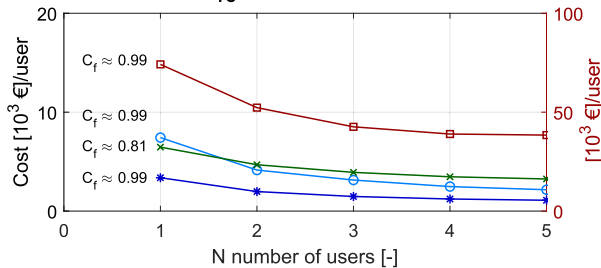
Average energy capacity (W_{st}/N) as a function of number of usersTotal cost per user (C_{TC}/N) as a function of number of users

FIGURE 11. Top: Average shared ESS capacity per user with increasing numbers of users. Bottom: Total costs per user for different storage technologies. (left axis: li-ion, lead-acid, EDLC; right axis: FES).

IV. DISCUSSION

The results from the previous sections have shown that privacy issues due to real-time monitoring of SM can be mitigated by reasonable ESS capacity sizes and costs. Market available products can be utilized to prevent leakage of private information, which can be affordable for individual users but more so for grouped users. However, the public acceptance remains to be discussed since no financial merit is gained from this investment. The results presented have to be interpreted with care. It has to be pointed out that user consumption patterns can vary heavily (e.g., seasonal changes in consumption), even within the same household, that can make appropriate sizing difficult if high levels of privacy ought to be maintained.

Furthermore, what has not been addressed in this study is what constant power $P_i = k$ is suitable for a long time investigation. Here, k is chosen in such a way that yields the minimum of ESS capacity. However, this can lead to an increase of the overall electric power consumption, and thus higher cost, for the user if a constant high power has to be maintained, especially when the ESS is mainly absorbing additional energy.

Other aspects to consider for future investigations are the influence of demand-side management schemes and electric power tariffs on the ESS's required capacity. Adding further functions to the ESS creates additional value if, for example, privacy and minimization of electric power purchase are joined objectives.

Finally, the cost calculation only presents an initial picture, but is incomplete since ageing effects of ESSs are not included in the model. Significant differences become more visible in a long-term study over several years, where the

lifetimes of ESSs have greater impact on maintenance and replacement costs.

V. CONCLUSION

The privacy breach through real-time monitoring of user power profiles is a valid concern and has sparked discussion about effective protection schemes. One option is to alter the consumption profiles to outside viewers by the use of ESSs. A comparison of different energy storage technologies reveals their effectiveness in this particular application and also minimum required capacity to fulfil the role. The BESS are the most suitable options in terms of cost even though considerable oversizing is necessary (up to 2-3x ideal ESS, in average 10-15 kWh). We conclude that the use of commercially available ESSs to protect privacy is possible and viable.

REFERENCES

- [1] M. R. Asghar, G. Dán, D. Miorandi, and I. Chlamtac, "Smart meter data privacy: A survey," *IEEE Commun. Surveys Tuts.*, vol. 19, no. 4, pp. 2820–2835, Jun. 2017. doi: [10.1109/COMST.2017.2720195](https://doi.org/10.1109/COMST.2017.2720195).
- [2] G. Wood and M. Newborough, "Dynamic energy-consumption indicators for domestic appliances: Environment, behaviour and design," *Energy Buildings*, vol. 35, no. 8, pp. 821–841, Sep. 2003. doi: [10.1016/S0378-7788\(02\)00241-4](https://doi.org/10.1016/S0378-7788(02)00241-4).
- [3] G. Kalogridis and S. Z. Denic, "Data mining and privacy of personal behaviour types in smart grid," in *Proc. IEEE 11th Int. Conf. Data Mining Workshops*, Vancouver, BC, Canada, Dec. 2011, pp. 636–642. doi: [10.1109/ICDMW.2011.58](https://doi.org/10.1109/ICDMW.2011.58).
- [4] U. Greveler, P. Glösekötter, B. Justus, and D. Loehr, "Multimedia content identification through smart meter power usage profiles," presented at the CPDP Comput., Privacy Data Protection, 2012. [Online]. Available: <http://citeseerx.ist.psu.edu/viewdoc/summary?doi=10.1.1.727.4674>
- [5] D. Månsson, "Sizing energy storage systems used to improve privacy from smart meter readings for users in Sweden," in *Proc. IEEE PES Innov. Smart Grid Technol. Conf. Eur. (ISGT-Eur.)*, Sarajevo, Bosnia-Herzegovina, Oct. 2018, pp. 1–6. doi: [10.1109/ISGTEurope.2018.8571456](https://doi.org/10.1109/ISGTEurope.2018.8571456).
- [6] J. Z. Kolter and M. J. Johnson, "REDD: A public data set for energy disaggregation research," presented at the SUSTKDD, 2011. [Online]. Available: <http://redd.csail.mit.edu/>
- [7] C.-T. Pham and D. Månsson, "On the physical system modelling of energy storages as equivalent circuits with parameter description for variable load demand (part I)," *J. Energy Storage*, vol. 13, pp. 73–84, Oct. 2017. doi: [10.1016/j.est.2017.05.015](https://doi.org/10.1016/j.est.2017.05.015).
- [8] C.-T. Pham and D. Månsson, "Experimental validation of a general energy storage modelling approach (part III)," *J. Energy Storage*, vol. 20, pp. 542–550, Dec. 2018. doi: [10.1016/j.est.2018.09.023](https://doi.org/10.1016/j.est.2018.09.023).
- [9] *Panasonic Lithium Ion UR18650F Datasheet Panasonic*. Accessed: Aug. 2019. [Online]. Available: <https://www.alldatasheet.com/datasheet-pdf/pdf/598214/PANASONICBATTERY/UR18650F.html>
- [10] *Panasonic Valve-Regulated Lead Acid Batteries: Individual Data Sheet LC-P0612P Panasonic*. Accessed: Aug. 2019. [Online]. Available: https://b2b-api.panasonic.eu/file_stream/pids/fileversion/3546
- [11] *Panasonic Electric Double Layer Capacitors (Gold Capacitor) Panasonic*. Accessed: Aug. 2019. [Online]. Available: <https://industrial.panasonic.com/cdbs/www-data/pdf/RDH0000/ABC0000C95.pdfRL>
- [12] F. Díaz-González, A. Sumper, O. Gomis-Bellmunt, and R. Villafila-Robles, "Modeling and validation of a flywheel energy storage lab-setup," in *Proc. 3rd IEEE PES Innov. Smart Grid Technol. Eur. (ISGT Eur.)*, Berlin, Germany, Oct. 2012, pp. 1–6. doi: [10.1109/ISGTEurope.2012.6465640](https://doi.org/10.1109/ISGTEurope.2012.6465640).
- [13] B. E. Conway, "Similarities and differences between supercapacitors and batteries for storing electrical energy," in *Electrochemical Supercapacitors*, 1st ed. New York, NY, USA: Springer, 1999, ch. 2, pp. 11–31.
- [14] J. Kang, J. Wen, S. H. Jayaram, A. Yu, and X. Wang, "Development of an equivalent circuit model for electrochemical double layer capacitors (EDLCs) with distinct electrolytes," *Electrochimica Acta*, vol. 115, pp. 587–598, Jan. 2014. doi: [10.1016/j.electacta.2013.11.002](https://doi.org/10.1016/j.electacta.2013.11.002).

- [15] H. Yang and Y. Zhang, "Characterization of supercapacitor models for analyzing supercapacitors connected to constant power elements," *J. Power Sources*, vol. 312, pp. 165–171, Apr. 2016. doi: [10.1016/j.jpowsour.2016.02.045](https://doi.org/10.1016/j.jpowsour.2016.02.045).
- [16] C.-T. Pham and D. Månsson, "Optimal energy storage sizing using equivalent circuit Modelling for prosumer applications (part II)," *J. Energy Storage*, vol. 18, pp. 1–15, Aug. 2018. doi: [10.1016/j.est.2018.04.015](https://doi.org/10.1016/j.est.2018.04.015).
- [17] J. Morley and M. Hazas, "The significance of difference: Understanding variation in household energy consumption," in *Proc. Summer Study-Energy Efficiency 1st, Found. Low-Carbon Soc. (ECEEE)*, Lancaster, U.K., 2011, pp. 2037–2046. [Online]. Available: https://www.comp.lancs.ac.uk/~hazas/Morley11_SignificanceofDifference-ECEEE.pdf
- [18] T. Christen and M. W. Carlen, "Theory of Ragone plots," *J. Power Sources*, vol. 91, no. 2, pp. 210–216, Dec. 2000. doi: [10.1016/S0378-7753\(00\)00474-2](https://doi.org/10.1016/S0378-7753(00)00474-2).
- [19] *Powerwall Datasheet Tesla*. Accessed: Aug. 2019. [Online]. Available: https://www.tesla.com/sites/default/files/pdfs/powerwall/Powerwall%20AC_Datasheet_en_northamerica.pdf
- [20] *RESU Datasheet LG Chem*. Accessed: Aug. 2019. [Online]. Available: https://www.memodo.de/media/pdf/c8/0d/3c/memodo_speicher_lgresu_new_02c2f41a1cd44862263dd992c0c905a5.pdf
- [21] *VARTA Element VARTA*. Accessed: Aug. 2019. [Online]. Available: https://www.varta-storage.com/wp-content/uploads/VARTA_element_datasheet_aus_V05.pdf
- [22] X. Luo, J. Wang, M. Dooner, and J. Clarke, "Overview of current development in electrical energy storage technologies and the application potential in power system operation," *Appl. Energy*, vol. 137, pp. 511–536, Jan. 2015. doi: [10.1016/j.apenergy.2014.09.081](https://doi.org/10.1016/j.apenergy.2014.09.081).
- [23] F. Díaz-González, A. Sumper, O. Gomis-Bellmunt, and F. D. Bianchi, "Energy management of flywheel-based energy storage device for wind power smoothing," *Appl. Energy*, vol. 110, pp. 207–219, Oct. 2013. doi: [10.1016/j.apenergy.2013.04.029](https://doi.org/10.1016/j.apenergy.2013.04.029).
- [24] B. Zakeri and S. Syri, "Electrical energy storage systems: A comparative life cycle cost analysis," *Renew. Sustain. Energy Rev.*, vol. 42, pp. 569–596, Feb. 2015. doi: [10.1016/j.rser.2014.10.011](https://doi.org/10.1016/j.rser.2014.10.011).
- [25] O. Tan, D. Gunduz, and H. V. Poor, "Increasing smart meter privacy through energy harvesting and storage devices," *IEEE J. Sel. Areas Commun.*, vol. 31, no. 7, pp. 1331–1341, Jul. 2013. doi: [10.1109/JSAC.2013.130715](https://doi.org/10.1109/JSAC.2013.130715).
- [26] S. M. Schoenung and W. V. Hassenzahl, "Long-vs. short-term energy storage technologies analysis—A life-cycle cost study—A study for the DOE energy storage systems program," Sandia Nat. Lab., Albuquerque, NM, USA, Tech. Rep. SAND2003-2783, Aug. 2003.
- [27] D. Linden and T. B. Reddy, "An introduction to secondary batteries," in *Linden's Handbook of Batteries*, 4th ed. New York, NY, USA: McGraw-Hill, 2011, ch. 15, p. 15.3.

• • •

ORIGINAL RESEARCH PAPER

Effects of smart meter privacy protection management on the lifetime performance of 18,650 lithium-ion batteries

Cong-Toan Pham  | Daniel Månsson 

School of Electrical Engineering and Computer Science, KTH Royal Institute of Technology, Stockholm, Sweden

Correspondence

Daniel Månsson, School of Electrical Engineering and Computer Science, KTH Royal Institute of Technology, Teknikringen 31, Stockholm, Sweden. Email: manssond@kth.se

Funding information

Energimyndigheten, Grant/Award Number: 43019-1

Abstract

Concerns over privacy leaks through real-time monitoring in smart meters (SMs) raise questions about how to effectively protect the user power consumption data. As one potential solution, energy storage systems have been suggested to physically manipulate SM readings to hide the true load pattern. Lithium-ion batteries (LiBs) are commonly utilised in the residential area in various applications such as solar and home batteries. Its use in a privacy-focussed operation has shown potential with reasonable system sizes in the range of commercially available products. However, batteries are subjected to ageing and the deterioration of performance over the course of time, which can limit the feasibility in such application. Hence, this work aims to investigate the ageing influence on LiBs' performance to deduce the life expectancy and how well privacy is protected over time. The study includes ageing tests with a specifically designed cycle life test procedure for the privacy protection scheme to extract relevant model parameters for the equivalent circuit battery model.

KEYWORDS

data privacy, energy storage, power, system cyber-security and privacy, smart meters

1 | INTRODUCTION

The progress towards the smart grid requires a major reform of the traditional power grid with the information and communication technology (ICT) as one of the key areas in this transition. Smart meters (SMs) are a subset of this area and are vital components for the effective management of the power grid. They enable real-time monitoring of generation and consumption data and, furthermore, partial control over smart appliances in response to demand-side management schemes [1]. The higher frequency and accuracy of the data are especially valuable to grid operators and customers alike. Smart meters open up new opportunities and services such as accurate consumer billing (dynamic pricing according to hourly or power tariffs), improved network efficiency and reliability of electric power distribution or third party services (e.g. outsourcing energy management) [1].

The deployment of SMs is in progress for the majority of European countries [2]. Apart from the economic and legal

challenges causing a delayed roll-out in individual countries, concerns over the privacy infringements from SMs have gained both public and scientific interest [1, 3]. The higher resolution of SM data can also mean an invasion into customers' privacy as their behavioural pattern is reflected in their consumption data. In Ref. [1], the potential threats on all levels of the smart metering infrastructure are highlighted, ranging from the customer domain up to the user of the data (e.g. SM tampering, lack of regulation and management protocols etc.). Depending on the sampling resolution information about occupancy, wealth and behaviour can be derived from the aggregated power consumption of the appliances. Through pattern recognition methods, individual appliances can be traced back based on the knowledge of their power consumption patterns: summarised under the method known as non-intrusive load monitoring [4, 5].

To tackle this issue, the authors in Ref. [1] suggest some measurements to protect the data from exploits and leaks through a legal framework, consent to access, cryptography

This is an open access article under the terms of the Creative Commons Attribution-NonCommercial License, which permits use, distribution and reproduction in any medium, provided the original work is properly cited and is not used for commercial purposes.

© 2021 The Authors. *IET Smart Grid* published by John Wiley & Sons Ltd on behalf of The Institution of Engineering and Technology.

and fortification of SMs against tampering. However, the SM itself has been pinpointed as the most exposed and vulnerable component if the data is accessed just before the customer's domain. As countermeasures, two main approaches are employed: data processing at the SM in the form of obfuscation [6, 7], aggregation [8] and anonymisation, and modification of the actual load through clever load management [9] and relying on energy storage systems (ESSs) [9–13]. However, as Ref. [1] pointed out, data distortion at the SM alone does not prevent third parties from installing their own sensors in the victim's vicinity and getting access to the unencrypted original data. This assumes a worst-case scenario and leaves only the last option in manipulating the reported demand itself.

1.1 | Energy storage for privacy

Energy storage systems have long been discussed in conjunction with the smart grid and also for residential customers. But the application of ESSs in context of privacy protection has gained interest fairly recently. A few studies such as Ref. [10] investigated the information leakage in a residential building supported by a renewable energy source (RES) and an ESS. They maximised the privacy protection by minimising the average mutual information shared between the recorded SM data and the actual demand profile. The study concluded that both a large capacity of the ESS or a high availability RES benefit the privacy. In Ref. [9] the investigation expanded to test combinations of a battery with a thermal energy storage and electric vehicle (EV) to optimise their usage to minimise privacy leakage and purchase costs of electric power. The system states are modelled as a Markov decision process, given the stochastic nature of varying demand and availability of the EV. As a result, Ref. [9] infers that a reasonable trade-off between battery size (up to 10 kWh) and costs can be achieved under the assumption that a constant power reading at the SM ensures minimal privacy breach. Both previously mentioned studies investigated the ESS under the premise of a lossless device. However, Ref. [12] states that losses in the storage device and the converter limit the capability of the ESS to aid in the privacy protection scheme, especially, if the controller misjudges the true state of the battery. There, a simplified electric circuit model (ECM) for the battery is used and controlled by an energy management unit (EMU) modelled as a partially observable Markov decision process. Similar to Refs. [9, 10] a metric to measure privacy breach in the form of the adversary's accuracy of detecting the correct event is introduced. The metric further shows dependencies on the initial state of the battery providing optimal protection when the battery is granted sufficient operation freedom in charge and discharge direction. Other investigations such as Refs. [11, 14] have focussed on the perspective of the ESS itself, answering questions about the minimal required capacity to achieve certain privacy levels or what storage technology best fits this purpose. The study in Ref. [11] examined the levels of privacy achieved for a single user up to aggregated users at different storage capacities. The results show that a 10 kWh system is

sufficient to cover for most cases of residential users in Sweden. For aggregated users, the same level of protection can be obtained with smaller capacities and lower investment costs per user. This has been further confirmed in a follow-up study in Ref. [14], where more accurately modelled ESSs such as lithium-ion batteries (LiBs), flywheels and capacitors are contrasted in their performance. The study models the ESSs as an ECM, which moderately reflects the energy storages' dynamics and losses. As a result, batteries have been highlighted as the most feasible option with only slight differences in energy losses. Market available products are adequate options for use in privacy-focussed applications.

Unfortunately, the results in Ref. [14] only present an incomplete picture, especially for the batteries, due to the omission of ageing effects. The continuous stress invokes degradation within the batteries and causes significant performance loss over time. This impacts the feasibility of the batteries over longer usage but has so far not been studied in the context of privacy-focussed applications. Unlike the previously mentioned studies, the main focus of this study is to investigate the effects of the privacy protection scheme on the battery performance over time, providing a more realistic indication of their usefulness in such applications. To fill this knowledge gap, it delivers a comprehensive performance analysis based on experimental ageing tests to this novel use case. The degree of degradation is very much path dependent, that is, in what magnitude and duration it is operated. A stress analysis in Ref. [15] traced the ageing process of commercial 18,650 LiBs at various discharge rates and cut-off voltages and revealed higher capacity and power fade with increasing stress. This correlation is explained by numerous ageing mechanisms such as accelerated lithium plating, solid electrolyte interface (SEI) growth and corrosion effects occurring within the cell [16, 17]. Therefore, to correctly predict the battery life time in privacy-controlled operation, the batteries have to be tested under similar conditions. It is worth mentioning that, to the authors' best knowledge, no real data on EMU with privacy protection management schemes in battery systems is currently available. To compensate for the lack of data, a data set reflecting a privacy-protection management scheme as closely as possible to a realistic scenario is derived based on actual measured power load consumption data from the Reference Energy Disaggregation Data (*REDD*) [18]. Hence, the quality of the data potentially impacts and dilutes the quality of the results. Nonetheless, with no other available data, the approach applied here still provides an initial outlook to the potential use of LiBs.

In the automotive industry, standardized tests with accelerated ageing are common procedures to explore the technical limitations of various products [19–22]. The concept behind these tests coincides with our main goal to investigate the technical feasibility of LiB and how quickly they will degrade under varying stress levels due to the privacy data protection scheme. Hence, in this work, we adopt a cycle life test (CLT) procedure based on realistic profiles for ageing, extract relevant information about capacity fade and model parameters, and extrapolate the life expectancy and performance of LiBs

through simulation. Here, we assume an ideal privacy controller with the premise that a constant load reveals the least information to an adversary. The approach is deterministic, where each state is known, unlike the stochastic approach in other studies [1, 9, 12].

1.2 | Organisation of the paper

The rest of the work is organised as follows: Section 2 introduces the model used to represent the battery's dynamics and age dependency. Section 3 describes the data set used as the basis for the ageing test procedures. In Section 4, the development of the individual test procedures for capacity, model parameter estimation and ageing is described. A short summary of the experiment setup and overall testing routine follows in Section 5. The results are discussed in Section 6, further distinguishing between the experimental results (Section 6.1) for ageing modelling and the simulated results (Section 6.2) for the lifetime and performance analysis. Finally, the findings and some concluding remarks are summarised in Section 7.

2 | BATTERY MODEL

2.1 | Equivalent circuit model

In this work, we employ an ECM for modelling the LiB, which sufficiently reproduces the major battery dynamics as well as energy capacity and power capability degradation. Detailed physical modelling of the cell indeed enhances understanding of the electrochemical degradation processes. However, information about cell design and interior properties is rarely available in normal cases. Furthermore, parameter estimation procedures for ECMs are widely established in academia and in industry [19–21], which can be easily obtained through simple charging/discharging regimes. Hence, we employ a Dual-Polarization (DP) model consisting of a dependent voltage source v_{ocv} , an internal resistance R_s , and two RC branches. The DP model provides an acceptable trade-off between accuracy and complexity, which reflects the dominant polarization effects adequately. The related equations are listed in Table 1 from (I-1) to (I-27) in discrete form, where $x[k]$ is the k^{th} sample of the sequence ($x[k] = x(k\Delta t)$ for $k \in \mathbb{N}$).

According to the DP model, the terminal battery voltage v_{cell} consists of the open circuit voltage (OCV) v_{ocv} and the overpotential contributions (I-1). Overpotential is a collective term for voltage dynamics during a transient state of the battery, further categorised into the ohmic overpotential v_{ohm} (I-2), the activation overpotential v_{ao} (I-3) and the concentration overpotential v_{co} (I-4) [23, 24].

The OCV establishes the cell potential at steady state, which heavily depends on the state of charge (SoC) of the battery. The OCV is synonymous to the electrode potential

described by the Nernst equation relating the activities of the substances [24, 25]. The concentration of the active substances changes over the course of operation, thus affecting the resulting potential. In the simulation, the OCV is tracked as the variable $v_{ocv}[k]$, which changes with SoC.

The ohmic overpotential v_{ohm} measures the voltage of the accumulated resistances of current collectors, electrode, SEI layer, separator and electrolyte ionic conductivity summarised in one component R_s . With ageing, this resistance is expected to increase due to the growth of the SEI layer and other corrosion occurrences [16, 17].

Polarization effects occur due to limitations of charge transfer at the electrode and mass transfer of reactants to the electrode. These are denoted as activation and concentration overpotentials [23, 24, 26], causing a delayed voltage rise in the measured voltage. Both electrochemical processes can be simplified as a pair of resistive and capacitive components with the time constant as the measure of inertia [26, 27]. Figure 1 depicts the DP model with each component associated with the corresponding potential contributions.

The battery cell's status is characterised by the SoC (I-5) and the state of health (SoH) (I-8). The $SoC[k]$ and $SoH[k]$ reflect the current charge level and the cell's degradation at the time instant k , respectively. At 100% SoH, the battery is at its prime condition with full capacity $q_{cell,BoL}$, also denoted as the beginning of life (BoL). At its end of life (EoL), the SoH reduces to 0, which is commonly defined as a capacity degradation to 80% (or by 20% relative capacity loss, $\Delta q_{cell,EoL}$) of $q_{cell,BoL}$.

2.2 | Ageing and SoC dependency

The ageing effects are taken into account through the variable components. However, how these parameters change over time can only be seen through regular testing over the course of the operation. Hence, a major portion of this study focusses on establishing the test procedures, later described in Section 4, to measure the model parameters. The calendar age is measured in the cumulative time passed. The cyclic age is measured in the number of equivalent full cycles performed by tracking the energy throughput ([I-9] in Table 1).

2.2.1 | Open circuit voltage

Apart from the SoC dependency, the battery's age additionally affects the OCVs' curvature. The capacity fade due to the loss of lithium inventory and other active materials causes a seemingly 'shrinking' effect on the OCV profile. Hence, to capture the non-linear age dependency, we record the OCV-SoC profile at different times (measured as accumulated equivalent full cycles n_{cyc}). This forms a data set (look-up table with x -data points of SoC_{data} and y -data points of $n_{cyc,data}$) of $v_{ocv,data}$ to which we apply the bilinear interpolation method to approximate v_{ocv} at each SoC and cycle (I-10)–(I-13).

TABLE 1 Battery cell model equations and parameters for simulation

DP model	Unit	Description
(I-1) $v_{\text{cell}}[k]$	$= v_{\text{ocv}}[k] + v_{\text{ohm}}[k] + v_{\text{ao}}[k] + v_{\text{co}}[k]$	[V] Cell voltage
(I-2) $v_{\text{ohm}}[k]$	$= R_s[k]I[k]$	[V] Ohmic overpotential
(I-3) $v_{\text{ao}}[k]$	$= \frac{\Delta t}{C_{\text{ao}}[k]} \frac{1}{1 + \frac{\Delta t}{\tau_{\text{ao}}[k]}} I[k] + \frac{v_{\text{ao}}[k-1]}{1 + \frac{\Delta t}{\tau_{\text{ao}}[k]}}$	[V] Activation overpotential
(I-4) $v_{\text{co}}[k]$	$= \frac{\Delta t}{C_{\text{co}}[k]} \frac{1}{1 + \frac{\Delta t}{\tau_{\text{co}}[k]}} I[k] + \frac{v_{\text{co}}[k-1]}{1 + \frac{\Delta t}{\tau_{\text{co}}[k]}}$	[V] Concentration overpotential
Cell status		
(I-5) $\text{SoC}[k]$	$= \text{SoC}[k-1] + \frac{I[k]\Delta t}{q_{\text{cell}}[k]}$	[-] State of charge
(I-6) $c_{\text{cell}}[k]$	$= \frac{q_{\text{cell}}[k]}{q_{\text{cell,BoL}}} = 1 - \left(\Lambda_{\text{q}}^{\text{cal}}[k] + \Lambda_{\text{q}}^{\text{cyc}}[k] \right)$	[-] Rel. total cell capacity
(I-7) $q_{\text{cell}}[k]$	$= q_{\text{cell,BoL}} c_{\text{cell}}[k]$	[-] Total cell capacity
(I-8) $\text{SoH}[k]$	$= 1 - \frac{1 - c_{\text{cell}}[k]}{\Delta q_{\text{col}}}$	[-] State of health
(I-9) $n_{\text{cyc}}[k]$	$= n_{\text{cyc}}[k-1] + \frac{ I[k]\Delta t }{2q_{\text{cell}}[k]}$	[-] Accumulated equivalent full cycles
OCV $x = \text{SoC}_{\text{data}} = (0 \dots 1)$, $y = n_{\text{cyc,data}} = (0 \dots n_{\text{cyc,max}})$		
(I-10) \mathbf{b}	$= \begin{bmatrix} v_{\text{ocv,data}}(x_i, y_j) \\ v_{\text{ocv,data}}(x_{i+1}, y_j) \\ v_{\text{ocv,data}}(x_i, y_{j+1}) \\ v_{\text{ocv,data}}(x_{i+1}, y_{j+1}) \end{bmatrix} \begin{cases} x_i \leq \text{SoC}[k] < x_{i+1} \\ y_j \leq n_{\text{cyc}}[k] < y_{j+1} \end{cases}$	[V]
(I-11) \mathbf{A}	$= \begin{bmatrix} 1 & x_i & y_j & x_i y_j \\ 1 & x_{i+1} & y_j & x_{i+1} y_j \\ 1 & x_i & y_{j+1} & x_i y_{j+1} \\ 1 & x_{i+1} & y_{j+1} & x_{i+1} y_{j+1} \end{bmatrix}$	
(I-12) \mathbf{a}	$= [a_0 \ a_1 \ a_2 \ a_3]^T = \mathbf{A}^{-1} \cdot \mathbf{b}$	[V]
(I-13) $v_{\text{ocv}}[k]$	$= a_0 + a_1 \text{SoC}[k] + a_2 n_{\text{cyc}}[k] + a_3 \text{SoC}[k] n_{\text{cyc}}[k]$	[V] Open circuit voltage
Capacity–Calendar and cycle ageing ($v_{\text{st},l} \leq v_{\text{cell}} \leq v_{\text{st},l+1}$)		
(I-14) $\Lambda_{\text{q}}^{\text{cal}}[k]$	$= \Lambda_{\text{q}}^{\text{cal}}[k-1] + \Delta \Lambda_{\text{q}}^{\text{cal}}[k]$	[-] Accumulated relative calendar capacity loss
(I-15) $\Delta \Lambda_{\text{q}}^{\text{cal}}[k]$	$= k_{v,w}(v_{\text{cell}}[k], \alpha_1) (t_{\text{q}}^{\text{eq}}[k-1] + \frac{\Delta t}{86400})^{0.5} - \Lambda_{\text{q}}^{\text{cal}}[k-1]$	[-] Incremental rel. calendar capacity loss
(I-16) $t_{\text{q}}^{\text{eq}}[k-1]$	$= \left(\frac{\Lambda_{\text{q}}^{\text{cal}}[k-1]}{k_{v,w}(v_{\text{cell}}, \alpha_1)} \right)^2$	[days] Eq. time span for given capacity loss
(I-17) $\Lambda_{\text{q}}^{\text{cyc}}[k]$	$= \beta_1 (n_{\text{cyc}}[k])^{\beta_0}$	[-] Accumulated rel. cycle capacity loss
Ohmic resistance–Calendar and cycle ageing		
(I-18) $R_s[k]$	$= R_{s0}[k] (1 + \Lambda_s^{\text{cal}}[k] + \Lambda_s^{\text{cyc}}[k])$	[Ω] Ohmic resistance
(I-19) $R_{s0}[k]$	$= b_0 \text{SoC}^2[k] + b_1 \text{SoC}[k] + b_2$	[Ω] SoC dependent ohmic resistance at BoL
(I-20) $\Lambda_s^{\text{cal}}[k]$	$= \Lambda_s^{\text{cal}}[k-1] + k_v(\gamma_1) \Delta t$	[-] Accumulated rel. calendar resistance increase
(I-21) $\Lambda_s^{\text{cyc}}[k]$	$= \delta_1 (n_{\text{cyc}}[k])$	[-] Accumulated rel. cycle resistance increase
Activation and concentration polarization–SoC dependency		
(I-22) $R_{\text{ao}}[k]$	$= c_{\text{ao},0} \text{SoC}[k] + c_{\text{ao},1}$	[Ω] ao SoC dependent resistance function
(I-23) $R_{\text{co}}[k]$	$= c_{\text{co},0} \text{SoC}[k] + c_{\text{co},1}$	[Ω] co SoC dependent resistance function
(I-24) $\tau_{\text{ao}}[k]$	$= d_{\text{ao},0} \text{SoC}[k] + d_{\text{ao},1}$	[s] ao time constant
(I-25) $\tau_{\text{co}}[k]$	$= d_{\text{co},0} \text{SoC}[k] + d_{\text{co},1}$	[s] co time constant
(I-26) $C_{\text{ao}}[k]$	$= \frac{\tau_{\text{ao}}[k]}{R_{\text{ao}}[k]}$	[F] ao equivalent capacitance
(I-27) $C_{\text{co}}[k]$	$= \frac{\tau_{\text{co}}[k]}{R_{\text{co}}[k]}$	[F] co equivalent capacitance
Parameters		
Δt		[s] Fixed sample time step

TABLE 1 (Continued)

DP model	Unit	Description
$q_{\text{cell,BoL}}$	[As]	Cell total charge capacity at BoL
$\Delta q_{\text{cell,EoL}}$	[-]	Relative capacity loss at EoL (here: 0.2)
α_1, γ_1	[-]	Fitted interp. calendar age parameters (see Equations 1 and 2)
$\beta_0, \beta_1, \delta_0, \delta_1$	[-]	Cycle age fitted parameters
$v_{\text{ocv,data}}$	[V]	OCV data points
SoC_{data}	[-]	SoC data points from the OCV profiles
$n_{\text{cyc,data}}$	[-]	Cycle ageing data points from the OCV profiles
a_0, a_1, a_2, a_3	[-]	Bilinear interp. parameters of OCV profiles
$b_0, b_1, b_2, c_0, c_1, d_0, d_1$	[-]	Fitting parameters for SoC dependency
v_{st}	[V]	Storage voltage during calendar ageing
$F = 9.648 \cdot 10^4$	[As/mol]	Faraday constant
$R_g = 8.314$	$\frac{\text{kgm}^2}{\text{s}^2\text{molK}}$	Gas constant

Abbreviations: BoL, beginning of life; DP, Dual-Polarization; EoL, end of life; OCV, open circuit voltage; SoC, state of charge; SoH, state of health.

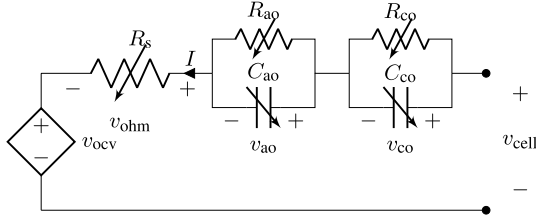


FIGURE 1 Dual-Polarization equivalent circuit model

2.2.2 | Cell capacity

We define the relative cell capacity c_{cell} as a fraction of its initial capacity $q_{\text{cell,BoL}}$ (I-6). Alternatively, c_{cell} is calculated from the relative capacity losses of calendar and cycle ageing. Here, we assume both types of ageing contributions as independent processes¹ and that the sum is the total relative capacity loss.

Calendar ageing describes the cell's deterioration in an idle situation without external load stress. A plethora of studies has proven a significant dependency of the calendar lifetime on the storage condition, mainly charge and temperature level [28–31]. The calendar test is usually conducted at fixed conditions, that is, various temperature and SoC levels. Calendar lifetime prediction models are based on the test observations and often show a root dependency over time [30, 31]. The following general expression summarises the fitting function applied to the observed evolution of the parameters. F and R_g represent the Faraday constant and the gas constant.

$$\Lambda = t^{\zeta_0} k_v k_T \quad (1)$$

$$k_v = e^{\zeta_1 \frac{F}{R_g} \left(\frac{v_{\text{st}}}{T_c} - \frac{v_{\text{ref}}}{T_{\text{ref}}} \right)} \quad (2)$$

$$k_T = e^{\zeta_2 \frac{1}{R_g} \left(\frac{1}{T_c} - \frac{1}{T_{\text{ref}}} \right)} \quad (3)$$

The factors k_v and k_T model the dependency on SoC (expressed as voltage during storage v_{st}) and cell temperature (T_c) to follow the Arrhenius equation [30, 31]. $\zeta_0, \zeta_1, \zeta_2$ are fitting parameters of the measured data. Depending on the assumptions made, not all fitting parameter are required if, as in our case, the temperature is closely kept at the reference ($T_c = T_{\text{ref}} = 298.15\text{K}$) throughout the test, whereby k_T equals 1. To avoid confusion, the fitting parameters are denoted as lower case Greek letters for the different circuit parameters (α : calendar cell capacity, β : cycle cell capacity, γ : calendar ohmic resistance, δ : cycle ohmic resistance). In this study, 10 LiBs are tested for calendar ageing at specified SoCs, where we estimate the fitting parameters through least-squares curve fitting. The relative capacity loss to calendar ageing is derived from Equations (1) and (2) at the stored voltage $v_{\text{st},l}$ with the omission of k_T . The index l enumerates the data for five SoC points (20%, 35%, 50%, 80%, 100%) at which the cells are stored; for example, $v_{\text{st},2}$ refers to the cell data stored at 35% SoC for calendar ageing. To cover cell voltages outside the measured stored voltages, an interpolated function Λ^{cal} is calculated from the adjacent fitted functions using a weight factor w .

$$\Lambda_l^{\text{cal}} = t^{\zeta_{0,l}} e^{\zeta_{1,l} \frac{F}{R_g} \left(\frac{v_{\text{st},l} - v_{\text{ref}}}{T_{\text{ref}}} \right)} \quad (4)$$

$$\Lambda^{\text{cal}} = w k_v(v_{\text{st},l}) t^{\zeta_{0,l}} + w' k_v(v_{\text{st},l+1}) t^{\zeta_{0,l+1}} \quad (5)$$

If the fitting functions use equal exponents, that is, $\zeta_0 = \zeta_{0,20\%} = \dots = \zeta_{0,100\%}$, Equation (5) simplifies to

¹This assumption is not necessarily proven, but is a conservative approximation by associating all losses in the cycle testing to cycle ageing.

Equation (6). For the fitting function of the cell capacity, ζ_0 is set to 0.5. The combination of k_v at different v_{st} is summarised in the factor $k_{v,w}$.

$$\Lambda^{\text{cal}} = \left[\overbrace{wk_v(v_{st,l}) + w'k_v(v_{st,l+1})}^{k_{v,w} t^{\zeta_0}} \right] \quad (6)$$

$$w = \frac{v_{st,l} - v_{\text{cell}}}{v_{st,l} - v_{st,l+1}} = 1 - w' \quad (7)$$

So far, the estimated functions are only valid under the set conditions and are not directly transferable in a dynamic operation. In dynamic operation, the cell voltage continuously changes, which either accelerates or decelerates the ageing progress as demonstrated in Ref. [30]. Following the approach in Ref. [31], we define a differential capacity loss $\Delta\Lambda_q^{\text{cal}}[k]$ for each progressing time step Δt as in (I-16). Note, in this work, Δt is uniform at 1s. Hence, the total relative capacity loss $\Lambda_q^{\text{cal}}[k]$ is the sum of all incremental capacity losses up to this point (I-16). To estimate $\Delta\Lambda_q^{\text{cal}}[k]$, we introduce an equivalent relative capacity loss $\Lambda_q^{\text{eq}}[k]$, which expresses a theoretical loss progression at the current voltage level up to time k (see Equation 9). $t_q^{\text{eq}}[k-1]$ is the theoretical time, which would lead to the current relative capacity loss $\Lambda_q^{\text{cal}}[k-1]$ under the current voltage level $v_{\text{cell}}[k-1]$ (Equation 10 and [I-16]).

$$\Delta\Lambda_q^{\text{cal}}[k] = \Lambda_q^{\text{eq}}[k] - \Lambda_q^{\text{cal}}[k-1] \quad (8)$$

$$\Lambda_q^{\text{eq}}[k] = k_{v,w}(v_{\text{cell}}[k-1], \alpha_1)(t_q^{\text{eq}}[k-1] + \Delta t)^{0.5} \quad (9)$$

$$t_q^{\text{eq}}[k-1] = k \left(\frac{\Lambda_q^{\text{cal}}[k-1]}{k_{v,w}(v_{\text{cell}}[k-1], \alpha_1)} \right)^2 \quad (10)$$

Cyclic ageing concerns the capacity degradation due to operation stresses. It is accelerated by higher current rates and operated SoC range [15]. Unlike Ref. [15], we apply a cycle procedure specifically tailored to the privacy-focussed application. By doing so, we obtain a clearer estimate of the cell's ageing as a direct consequence of the privacy application. It is a dynamic cycling test with changing current stress to reflect the actual application as realistically as possible (Section 4). However, we analyse the cyclic ageing only at 0%–100% SoC range. This is a conservative standpoint that overestimates cycle ageing contributions for operations with lower SoC swings (e.g. 10%–90% SoC range). According to Refs. [15, 31], a root function sufficiently models the relative capacity decay (I-17). With one SoC range test, one fitting function is sufficient.

2.2.3 | Ohmic, charge transfer, mass transfer overpotentials

The ohmic resistance R_s changes with the SoC and is accounted for by a fitted second order polynomial expression

(I-18) and (I-19). R_{s0} is the ohmic resistance at BoL and serves as the reference point for the ageing progress. Within our data, the SoC dependency did not show significant changes over time. Furthermore, R_{s0} is adjusted with the calendar and cycle ageing contributions (Λ_s^{cal} , Λ_s^{cy}) similar to the cell capacity ageing. According to Ref. [30], the calendar age is modelled as a linear growth ($\zeta_0 = 1$) over time. No significant SoC dependency of the calendar ageing has been observed in our data, that is, $k_{v,w} = k_v$. Hence, Λ_s^{cal} is summarised in one function as in (I-20). The cycle ageing contribution is estimated by a fitted linear function (I-21).

Charge and mass transfer parameter changes are modelled similarly to the ohmic resistance. However, from the data collected, the cell's dynamics described by R_{a0} , R_{c0} , τ_{a0} and τ_{c0} only feature SoC dependency but do not display significant ageing trends.

2.3 | System model

So far, the model has described a single battery cell. To accomplish greater power and capacity requirements, cells are stacked in N series and M parallel components. By reverse, to obtain the input power through each cell the total storage system power P_{ess} is scaled down by the product of the series and parallel connected cells². Furthermore, the power input $P_{\text{ess}}[k]$ is converted into a current input $I[k]$ that fits our model equations in Table 1. Table 4 lists the equations for the system model.

The basis for this conversion is derived from (Table 1, I-1) by multiplying $I[k]$. By extension, replacing the variables with the respective equations from (I-2) to (I-4) results in a quadratic function whose solution serves as the input current for the model equations (II-2). Further, system constraints are introduced to restrict the operational limits, for example maximum and minimum voltage levels. The first limitation is described by (II-5), which expresses the maximum obtainable power from the battery cell, that is, a near empty cell might not provide the requested power to the load. The second level of constraints concerns the voltage limits with the purpose of safety (II-6 & II-7). Here, we define both $v_{\text{min}} \approx 3.0$ V and $v_{\text{max}} \approx 4.2$ V according to the later determined measured OCV profiles. The third limitation (II-8 & II-9) is given by the data sheet on the recommended maximum allowed currents for charge or discharge ($I_{\text{ch,max}}$, $I_{\text{dc,min}}$). I_{max} and I_{min} are then chosen depending on the smaller value between $I_{v_{\text{max}}}$ and $I_{\text{ch,max}}$ and the greater value between $I_{v_{\text{min}}}$ and $I_{\text{dc,min}}$, respectively. These limitations must be upheld as a realistic representation of a safe system. Temperature constraints are not implemented due to our assumption of a constant temperature throughout operation. This is a valid assumption for Swedish residential buildings as ambient temperatures have shown little variation with mean values around $22 \pm 2^\circ\text{C}$ [32]. Nevertheless, to ensure constant ambient condition, the LiBs are

²We assume that the cells age equally at each point in time.

operated at 25°C within a climate chamber. Contact temperature measurements further confirmed fairly constant temperature operation.

3 | REDD DATA SET

In Ref. [11] it has been hypothesised that a constant power in-/outlet leaks the least amount of information. Based on this assumption and, also, by limiting the number of possible scenarios to realistic amounts, the ESS must cover the power difference between the load consumption (P_{load}) and the desired constant power ($P_{\text{SM}} = p_{\text{constant}}$) reported by the SM. In this scenario, the power grid supplies both the load and ESS unidirectionally (Figure 2).

$$P_{\text{ess}} = P_{\text{SM}} - P_{\text{load}} = p_{\text{constant}} - P_{\text{load}} \quad p_{\text{constant}} \in \{0, \infty\} \quad (11)$$

$$W_{\text{ess}} = \int_0^{\infty} P_{\text{ess}} dt \quad (12)$$

Note, depending on how p_{constant} is adjusted, the P_{ess} changes. Increasing p_{constant} results in higher power import and more frequent and unnecessary charge of the ESS. Thus, the ESS has to be oversized to accommodate the additional input from the grid. Conversely, lowering the p_{constant} also yields unfavourable results as the ESS will be dominantly discharged. Hence, a large initial capacity is required to compensate for frequent discharge over the day. Furthermore, if the ESS is either fully charged or depleted by the end of the day, the capacity of the ESS to deal with the following day is limited. In face of this, p_{constant} is determined in such a way as to minimise the total energy capacity W_{ess} of the ESS and balance the charge and discharge ratio as shown in the energy capacity profile in Figure 3b. Slight focus has been put to discharge for the creation of the CLT profile. Additionally, we assume that the same load profile P_{load} (Figure 3a) is used every day as a good approximation of an average behaviour over time.

This study uses the *REDD* [18] set as the base for the residential consumption data. The data includes three weeks' worth of data including the power consumption of six different households. Unfortunately, sampling interruptions occur at several places within the measured time frame leaving us with

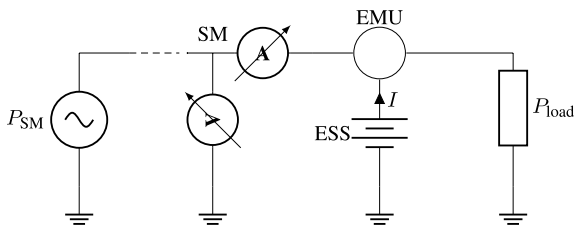


FIGURE 2 Adapted schematic [14] of the electric power supply from the utility, which is equal to the smart meter (SM)-drawn power P_{SM} . The energy management unit (EMU) monitors and controls the power in-/output between the load and energy storage system (ESS)

only 27 continuous 24 h sets of data (86,400 consecutive data points). The *REDD* data reveal a high diversity of power and energy consumption among the households. Load patterns are also inconsistent, which follow the notion made in Refs. [33, 34] where consumer behaviour even in similar environmental conditions varies heavily. This variation relates to the individual occupants (wealth, age, lifestyle etc.) rather than the environment alone. However, despite these differences in the profiles, we observe a common stress pattern for the ESS after finding fitting combinations of p_{constant} and W_{ess} among all 27 load profiles. Although the values for p_{constant} and W_{ess} vary, the frequency of power levels of P_{ess} is similarly distributed between all load profiles. In other words, the power peaks may occur at different times during the day, but the total amount of required power demands (e.g. 0.2 kW or 3 kW) remains the same overall. Throughout the day, 90% of the ESS operation revolves around 0.3 kW in average ($\sigma^2 = 0.15$ kW), that is, 21 hours of low ESS operation. The ESS operates between 1 and 2 kW around 2% (≈ 30 min) of the total time. Only in a fraction of the time (1% ≈ 15 min) the demand increases above 2 kW. Hence, we convert one of the available 24 h data sets (household 1) to obtain the CLT profile for the LiB tests. The corresponding power distribution for household 1 is presented in Figure 4. As comparison, a solar battery operates, that is, managing the difference of generation and load demand, in a wider spectrum with high power ratings and longer durations.

4 | TEST PROCEDURE FOR AGEING TESTING

The test procedure involves three main parts: Capacity measurement using a capacity test, performance tests using a hybrid pulse power characterisation (HPPC) test to estimate model parameters and ageing using a CLT procedure. The capacity and HPPC tests are commonly applied throughout the literature [15, 27, 35]. However, more focus has to be put here on the development of CLTs since these are currently standardized for electric traction and not for our privacy-focussed application. The operation conditions and requirements vary and should be considered in the development of the CLT. The test should be representative of the actual scenario, maintaining the key features of the particular application. The features in the privacy-focussed application are based on the following key parameters: the minimum and maximum power ($P_{\text{min}}, P_{\text{max}}$)³, the total cycled energy capacity (E_{tot}), the (SoC) range ($\text{SoC}_{\text{min}}, \text{SoC}_{\text{max}}$).

The authors of Ref. [19] highlight the different approaches to battery testing of EVs by the U.S., EU and Japan, mainly pointing out the derivation of test profiles and the definition of key parameters. Apart from the differences, the procedures in Refs. [20–22] are in part applicable to our own investigation. In the context of this study, we will take specific interest in the capacity test, the HPPC test and the CLT for performance and life tests.

³Negative power: discharge. Positive power: charge.

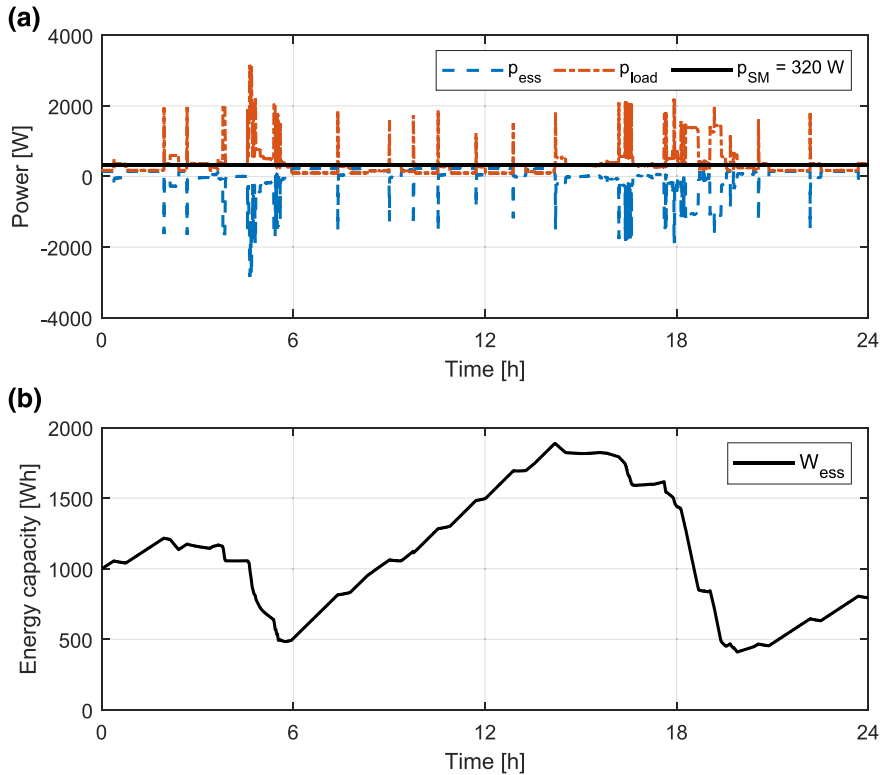


FIGURE 3 (a) Reference Energy Disaggregation Data consumption pattern and necessary energy storage system (ESS) power profile of household 1; (b) Example of an ESS with 50% initial capacity ($W_{\text{ess}} = 2000$ Wh) (adapted from [14]). SM, smart meter

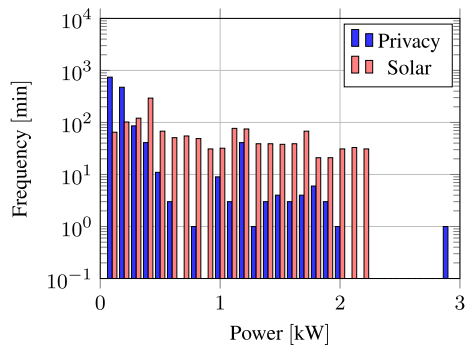


FIGURE 4 Frequency of demanded power over one 24 h period (household 1 from Reference Energy Disaggregation Data set). Comparison between privacy-focussed and solar battery application

4.1 | Capacity test and open circuit voltage

To measure available capacities at different operations, the battery is discharged and charged at various C-rates [20, 35]. In the presence of polarization losses, the amount of extractable energy is limited and decreases with increasing C-rate. The procedure dictates a constant current (CC) discharge and charge at the specified C-rate from full charge to depletion (Figure 5), which is set by the recommended maximum and minimum voltage levels provided by the manufacturer. Here, we test the LiB LG INR 18,650 B4 [36] with the relevant cell specifications summarised in Table 2 at 1C and C/8 CC discharge and CC-constant voltage (CV) charge at 25°C. During charge, the procedure changes from CC to CV when the voltage passes a threshold value and

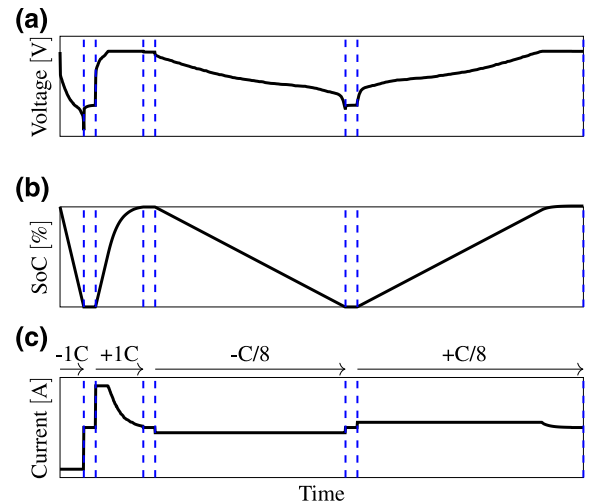


FIGURE 5 Schematic of the capacity test at 1C and C/8. (a) Resulting battery voltage profile; (b) Estimated state of charge profile through Coulomb counting; (c) Dynamic current profile. SoC, state of charge

stops when the measured currents drops below 50 mA. The total capacity is estimated by the mean of the C/8 charge and discharge capacities, which are measured through the Coulomb counting, that is, integral of the current into the battery over time.

Additionally, the C/8 profile provides a good approximation of the OCV curve. Low current rates reduce the polarization influence and help in tracking the potential changes over the charge levels. From the C/8 charge and discharge profile, the mean OCV is estimated as the mean of both curves.

4.2 | Hybrid pulse power characterisation test

The HPPC's main purpose is to map the power capabilities of the tested battery at different SoC levels and charge/discharge rates. In Ref. [20], this procedure is recommended to measure various equivalent resistances and power values. However, in our context, we extend the characterisation also to the battery model parameters including the transient behaviour modelled as the two levelled RC branches. Figure 6 illustrates the HPPC routine. The HPPC procedure is segmented into two parts consisting of a discharge phase to selected SoC levels (90%, 70%, 50%, 35% and 20%), followed by the dynamic power discharge and charge pulses. The model parameter characterisation ($R_s, R_{ao}, R_{co}, C_{ao}, C_{co}$) is based on the relaxation period of the battery (2) and (3) and validated through the pulse procedure (3)–(7). The SoC conditioning is accomplished through Coulomb counting based on the current battery capacity. The SoC levels are adjusted to the current capacity from the capacity test. For example, if the measured capacity amounts to 2500 mAh, the LiB will be discharged to 2250, 1750, 1250, 875 and 500 mAh, respectively. At each SoC level, the battery is first discharged for a short pulse at its highest rated output based on the manufacturer's recommendation ($I_{dc,max}$ for 20 s), then reduced to 75% at longer duration ($0.75I_{dc,max}$ for 120 s), followed by a resting phase of 40 s and finally regenerated with the maximum charge current ($I_{ch,max}$ for 20 s). The locations (1)–(7) mark the points of change in the procedure with special interest in the points (2)–(3) for determining the model parameters.

All relevant parameters are derived from the measured battery voltage v_{cell} . The ohmic overpotential v_{ohm} is the instantaneous voltage difference caused by R_s , which is calculated by Equation (13). To determine R_s , we measure at the positions (2) and (3) for the ohmic resistance (Figure 7). Here, charge and discharge resistances are approximated by R_s .

TABLE 2 Cell specifications for LG INR 18,650 B4

Pos. electrode	LiNiMnCoO ₂
Nominal capacity (0.2 C)	2600 mAh
Nominal voltage	3.6 V
Nominal energy	9.36 Wh
Maximum continuous current	
Charge	2.5 A
Discharge	4.4 A
Maximum voltage	4.2 V
Minimum voltage	2.75 V
Temperature range	
Charge	0–45°C
Discharge	0–60°C

$$R_s = \frac{v_{cell}[k+1] - v_{cell}[k]}{I[k+1] - I[k]} \quad [\Omega] \quad (13)$$

The parameters $R_{ao}, R_{co}, C_{ao}, C_{co}$ are estimated by least-squares curve fitting of the resulting battery voltage. Since we retrieve v_{ocv} from the capacity test and v_{ohm} by determining R_s , the remaining parameters can be fitted from the remaining voltage ($v_{ao} + v_{co}$) after subtracting v_{ocv} and v_{ohm} from v_{cell} . For the objective function, we apply the time constants and the initial potentials $\tau_{ao}, \tau_{co}, v_{0,ao}, v_{0,co}$ as optimization parameters. The estimated voltage $v[k]$ is derived from the battery model for the two capacitive branches. Between (2) and (3), the battery relaxes from its discharge with no current input where the following model is fitted to $v_{ao} + v_{co}$. The initial potentials $v_{0,ao}, v_{0,co}$ of the RC branches are estimated in conjunction with the corresponding time constants τ_{ao}, τ_{co} . R_{ao} and R_{co} can be found through the current input I_{1-2} from period (1) to (2) in Figure 6, given that the initial potentials are zero after sufficient resting time. Δt_{1-2} and Δt_{2-3} measure the time between (1) to (2) and (2) to (3) Figure 6.

$$\hat{v}[k] = v_{0,ao} e^{-\frac{\Delta t_{2-3}}{\tau_{ao}}} + v_{0,co} e^{-\frac{\Delta t_{2-3}}{\tau_{co}}} \quad (14)$$

$$\arg \min_{v_{0,ao}, v_{0,co}, \tau_{ao}, \tau_{co} \in (-\infty, \infty)} \sum_{k=1}^n (v_{ao}[k] + v_{co}[k] - \hat{v}[k])^2 \quad (15)$$

$$R_{ao} = \frac{v_{0,ao}}{i_{1-2} (1 - e^{-\frac{\Delta t_{1-2}}{\tau_{ao}}})}; \quad C_{ao} = \frac{\tau_{ao}}{R_{ao}} \quad (16)$$

$$R_{co} = \frac{v_{0,co}}{i_{1-2} (1 - e^{-\frac{\Delta t_{1-2}}{\tau_{co}}})}; \quad C_{co} = \frac{\tau_{co}}{R_{co}} \quad (17)$$

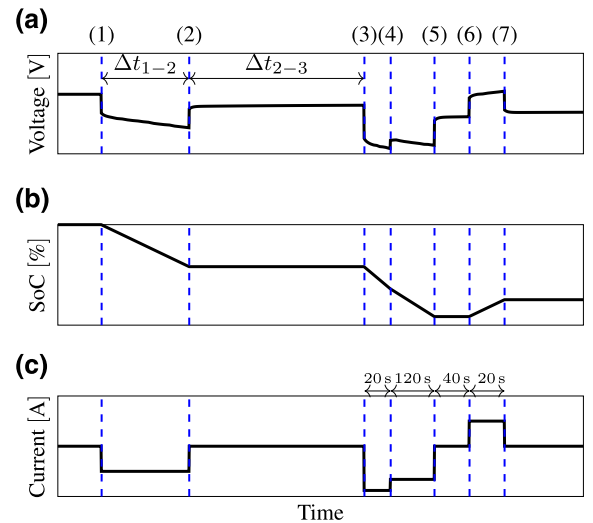


FIGURE 6 Schematic of the hybrid pulse power characterisation profile. (a) Resulting battery voltage profile; (b) Estimated state of charge profile through Coulomb counting; (c) Dynamic current profile. SoC, state of charge

4.3 | Cycle life test procedure

The degradation of battery performance is sensitive to operation and environmental factors such as maximum charge/discharge rates, SoC range, the overall energy throughput, and temperature etc. Hence, these parameters have to be known and set according to the application in question to limit the amount of necessary tests. The EU and U.S. define a pre-set CLT profile with intervals at specific power levels [20, 21], which only differs in when and what duration these peaks occur within the profile. The profiles are mostly static and remain opaque in how the chosen profile relates to the driving sequence to be tested. A more generic way is proposed by the authors in Ref. [22], which aims to develop a CLT profile based on the original load profile. This allows for a more realistic approach to test battery cells for our desired application, whose results have more comprehensible implications on the ability to provide privacy.

The method, also adopted in this work here, follows three steps: (1) sorting the power profile in increasing order (i.e. discharge to charge), (2) compressing the sorted profile to test suitable cycle durations and optional (3) simplification of the profile. The advantages of this concept are that it retains the

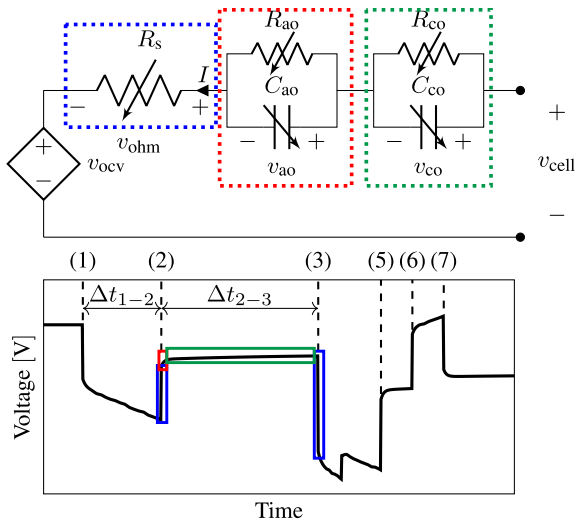


FIGURE 7 Schematic of the polarization contributions of ohmic, activation and concentration overpotentials in the voltage profile. The short-term time constant is associated with the activation polarization, whereas the long-term time constant with the concentration polarization

original information of the maximum power and energy throughput, simply portioned into smaller time windows for accelerated testing. Additionally, the universality also allows the development of CLT profiles for any application including ours. Hence, we adjust our own test procedure according to Ref. [22]. Figure 8 visualises the step-by-step procedure.

1. *Scale down to single cell profile*: To run ageing tests on a single cell, the profile is scaled down by the nominal energy capacity of the tested battery (9.36 Wh). The scaled down version of the power profile then serves as the initial profile for the CLT. One cell then deals with the maximum discharge/charge power of $P_{\min} = -13.3$ W, $P_{\max} = 1.1$ W, and cycles roughly $E_{\text{tot}} = 22$ Wh in 24 hours.
2. *Sorting profile*: In the second step, the given profile is sorted in increasing order, concatenating all discharge and charge in separate sections. A final minor adjustment is made by reversing the charge section, starting from the highest power in decreasing order. The reasoning behind this is to match the discharge profile from the highest power and end with a resting phase.
3. *Compressing profile*: The idea behind compression is to portion the data into a more timely manageable routine [22]. The compressed version still contains the key parameters of the maximum power P_{\min} , P_{\max} and cycles equal amount of energy if repeated over the same time period. The window for one test cycle, a compressed version of the original 24 h cycle (Figure 8), is set to 1800 s.
4. *Simplifying profile*: To maintain the same information content the profile is minimally simplified (0.1 W discretisation steps). To accommodate the SoC range in the test, the LiB is cycled with the final CLT profile starting at the maximum SoC until it reaches the lowest set SoC. Here, we set the SoC range between 0% and 100% according to the manufacturer's voltage limits (2.75–4.2 V).

5 | EXPERIMENT SETUP AND SCHEDULE

5.1 | Experiment setup

An experimental setup is designed to apply the testing procedures to the LiBs, which is divided into two main parts: the

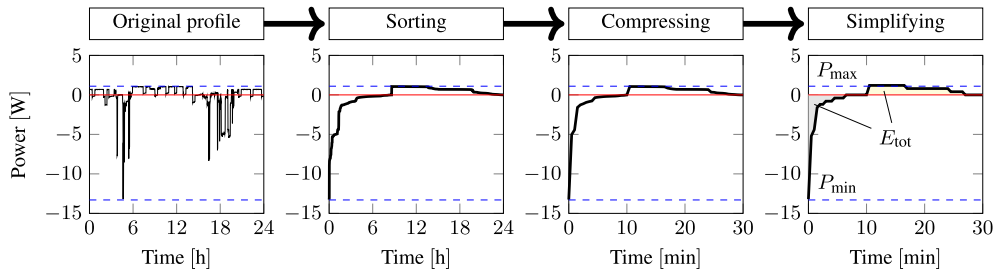


FIGURE 8 Schematic of the CLT profile procedure from left to right. (1) The original power profile for the battery is sorted in increasing order. The charge section is sorted reversely in decreasing order. (2) The sorted profile is compressed from 24 h in a 30 min routine. (3) Optional simplification of the profile

power circuitry and the control/data acquisition (DAQ). The power circuitry is the physical setup to charge and discharge the LiB in the desired manner by using a DC power supply as the charging source and a low resistive load for discharging purposes (Figure 9). A simple buck-converter topology with Metal Oxide Semiconductor Field-Effect Transistors (MOSFETs) is employed to regulate current and voltage input to the LiBs. The control of the setup is accomplished by the Arduino microcontroller (Mega 2560) with its main purpose of controlling the MOSFETs' pulse-width modulation input and measuring current, voltage and cell temperature for data acquisition and safety. The current measurement is achieved by an INA 260 power sensor unit [37, 38] with 16 bit ADC resolution over -15 – $+15$ A range ($dA = 1.25$ mA). The voltage is measured through an ADS1015 breakout [39, 40] (12 bit resolution); here set to a voltage range ± 6.144 V with $dV = 3$ mV. Three negative temperature coefficient thermistors [41] are mounted on the MOSFETs and the battery cell's surface to monitor the temperature development. The data is processed in the Arduino script and simultaneously transferred through serial connection with a Python script on the host computer for DAQ. The microcontroller adjusts the power input to the LiB according to the reference value (P_{ref}) continuously sent by the Python script. At the same time, the data is stored after the routine ends. Two out of three setups test the two cycled LiBs, and one is designated for the calendar ageing batteries. To maintain constant temperature throughout testing, a climate chamber (Firlabo Eurotherm 2208e) is used.

5.2 | Cycling and calendar ageing

With the previously established testing procedures, two sets of LiBs are analysed. One set of two LiBs (Cyc1, Cyc2) are

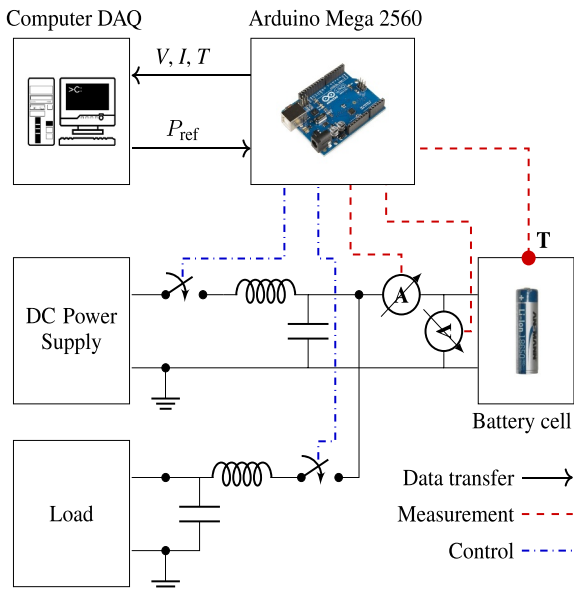


FIGURE 9 Schematic of the experimental setup

continuously cycled through the CLT procedure and occasionally halted (every 30 days in average) for performance testing (capacity and HPPC): 1. Capacity \rightarrow 2. HPPC test \rightarrow 3. CLT \rightarrow 4. Repeat 1.

Another set of 10 LiBs (Cal1-10) are assigned for calendar ageing, which are stored at constant 25°C at five different charge levels, two each for 100%, 80%, 50%, 35%, 20% SoC, for example, Cal1&2 at 100%, Cal3&4 at 80% etc. These batteries undergo the capacity and HPPC test every 6 weeks in average: 1. Capacity \rightarrow 2. HPPC test \rightarrow 3. Storage \rightarrow 4. Repeat 1.

6 | RESULTS AND DISCUSSION

6.1 | Experimental results

6.1.1 | Capacity degradation

The capacity loss over calendar and cycle ageing is summarised in Figure 10. The top plot shows the accumulated capacity loss Λ_q^{cal} due to calendar ageing at different stored SoCs. The results reflect similar impact of the storage condition on the capacity loss as seen in other studies [29, 30, 42, 43]. The capacity fade has been correlated with the SEI growth rate as its increase mainly stems from the lithium inventory [43]. The increasing SEI layer further hampers the diffusion rate of lithium ions, which causes a gradual decrease of the capacity loss, thus counteracting the ageing process. The influence of SoC on the capacity fade is well documented (e.g. in [30]) and known to accelerate ageing with increasing SoC storage condition. The

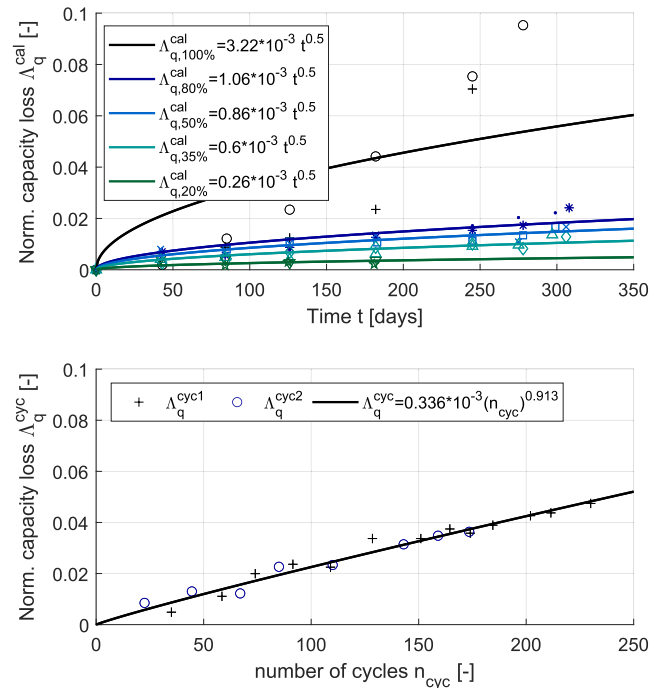


FIGURE 10 Calendar ageing experimental results and fitted curves of the normalized capacity loss ($C/8$ capacity) at 25°C (Calendar & cycle ageing)

same result is observed in Figure 10 with the given estimated fitting functions for each SoC level. Deviations from the root fitting function can be observed from the 100% storage condition. The first two measurement points were mistakenly measured at a slightly lower voltage point below the intended 4.2 V and readjusted to the appropriate voltage, which explains the more rapid increase in the later stages. Further, after 250 storage days, both Cal1&2 neared their EoL with rapidly increasing capacity loss ($\Lambda_q^{\text{cal}} > 0.1$ together with Λ_q^{cyc} are close to $\Delta q_{\text{cell,EoL}}$ of 0.2) until the battery's protection circuit prevented any further use.

The accelerating degradation effect cannot be modelled according to our root-dependent decay model, which causes a high discrepancy. Furthermore, $t = 240$ days onwards, Cal9&10 seemingly recovered from the accumulated ageing effects to its original capacity. This phenomenon is not unheard of as some ageing mechanisms such as lithium plating are in part reversible [44, 45]. One possible explanation may be the formation of reversible lithium plating during the capacity and HPPC sequence. A prerequisite for reversibility is the direct electrical contact of the plating with the electrode, which allows the lithium to intercalate into the electrode over time. However, the capacity loss of Cal9&10 during calendar ageing is relatively small and, also, the recovered portion. This recovery effect has not been observed for the other tested LiBs and the cause for this remains unknown to us. For the curve fitting, these data points are omitted as they skew the previously observed trend.

The capacity loss contribution due to cyclic ageing is given in the lower plot in Figure 10, which shows a similar ageing

trend as calendar ageing. Observe that this fitted capacity loss Λ_q^{cyc} is unique to our cycle test procedure and changes if the operation conditions change.

6.1.2 | Ohmic resistance

The top plot in Figure 11 shows the normalized resistance increase Λ_s^{cal} with respect to the storage days passed. The data confirms an overall increase of resistance for all SoC levels but fails to distinguish significant SoC—age dependencies due to the high variance of the data. This stands in contrast to observations made in Ref. [30]. In Ref. [30], higher rates of increase are observed between 35% and 70% SoC, and the authors hypothesise the inhomogeneous growth of the SEI layer as a cause for variation. However, this theory is yet to be proven and the results have to be interpreted with caution. Additionally, lithium plating increases polarization effects [45], seen as a higher measured R_s . The recovery effect from Cal9&10 reversed the otherwise increasing R_s , which could be attributed to reversible plating as a dominant factor instead of the growth of irreversible SEI. In the simulation, a mean average growth function (Table 3, III-7) is used to estimate R_s calendar age.

TABLE 3 Fitted ageing and SoC model functions

Capacity—Calendar and cycle ageing			
(III-1)	$\Lambda_{q,100\%}^{\text{cal}}$	$= 3.22 \times 10^{-3} t^{0.5}$	[-]
(III-2)	$\Lambda_{q,80\%}^{\text{cal}}$	$= 1.06 \times 10^{-3} t^{0.5}$	[-]
(III-3)	$\Lambda_{q,50\%}^{\text{cal}}$	$= 0.86 \times 10^{-3} t^{0.5}$	[-]
(III-4)	$\Lambda_{q,35\%}^{\text{cal}}$	$= 0.6 \times 10^{-3} t^{0.5}$	[-]
(III-5)	$\Lambda_{q,20\%}^{\text{cal}}$	$= 0.26 \times 10^{-3} t^{0.5}$	[-]
(III-6)	Λ_q^{cyc}	$= 0.336 * 10^{-3} n_{\text{cyc}}^{0.913}$	[-]
Ohmic resistance—Calendar & cycle ageing			
(III-7)	Λ_s^{cal}	$= 0.67 * 10^{-3} t$	[-]
(III-8)	Λ_s^{cyc}	$= 0.87 * 10^{-3} n_{\text{cyc}}$	[-]
(III-9)	$R_{s,0}$	$= 0.05\text{SoC}^2 - 0.066\text{SoC} + 0.167$	[Ω]
Activation and concentration polarization—SoC dependency			
(III-10)	R_{ao}	$= R_{\text{ao},0}$	[Ω]
(III-11)	$R_{\text{ao},0}$	$= 0.004\text{SoC} + 0.017$	[Ω]
(III-12)	R_{co}	$= R_{\text{co},0}$	[Ω]
(III-13)	$R_{\text{co},0}$	$= -0.013\text{SoC} + 0.024$	[Ω]
(III-14)	τ_{ao}	$= \tau_{\text{ao},0}$	[s]
(III-15)	$\tau_{\text{ao},0}$	$= 0.36\text{SoC} + 27.28$	[s]
(III-16)	τ_{co}	$= \tau_{\text{co},0}$	[s]
(III-17)	$\tau_{\text{co},0}$	$= 103.66\text{SoC} + 171.41$	[s]

Abbreviation: SoC, state of charge.

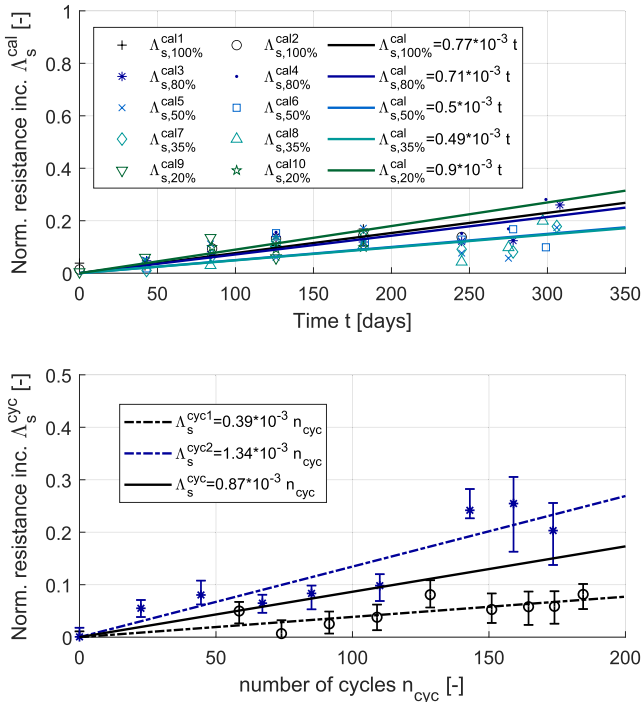


FIGURE 11 Experimental results and fitted curves of the normalized resistance increase (R_s) at 25°C. Top: Calendar ageing. Bottom: Cycle ageing

The lower plot in Figure 11 shows the ageing progress through the cycling procedure. The resistances of both Cyc1 and Cyc2 have been measured at different charge levels to test if the trends coincide. A slight variation between Cyc1 and Cyc2 is observable, but uncertainties in measurements can

influence the slope of the growth rate. For simplification, the mean of both fitting functions Λ_s^{cyc} is taken (I-21).

Finally, the SoC dependency of R_s has also been taken into consideration. The data is plotted in Figure 12b for Cyc1 and Cyc2 at BoL. Close observation reveals that the

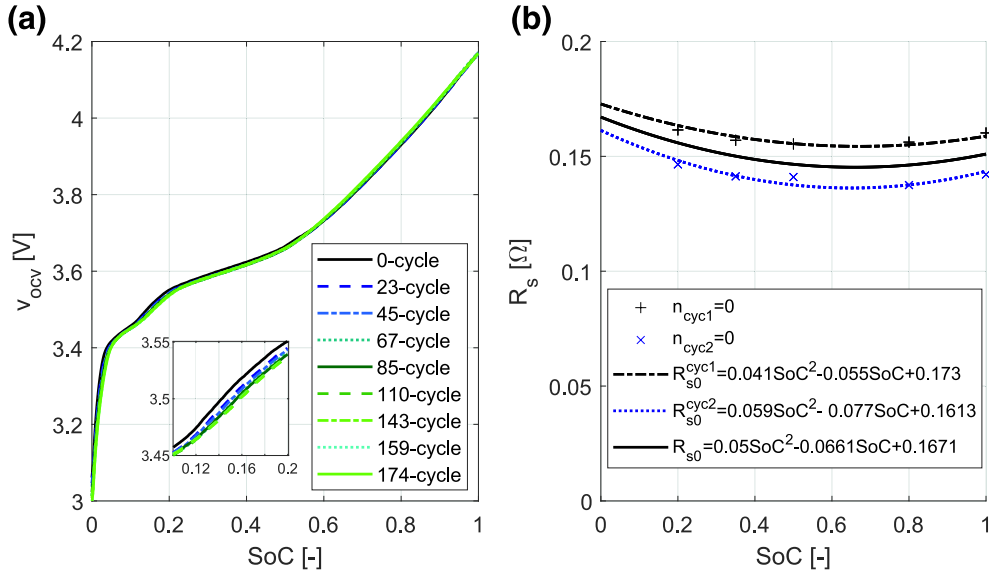


FIGURE 12 (a) Open-circuit voltage profile at different cycle stages (Cyc2); (b) Experimental results and fitted curves of the state of charge (SoC) dependency of R_s at 25°C at beginning of life

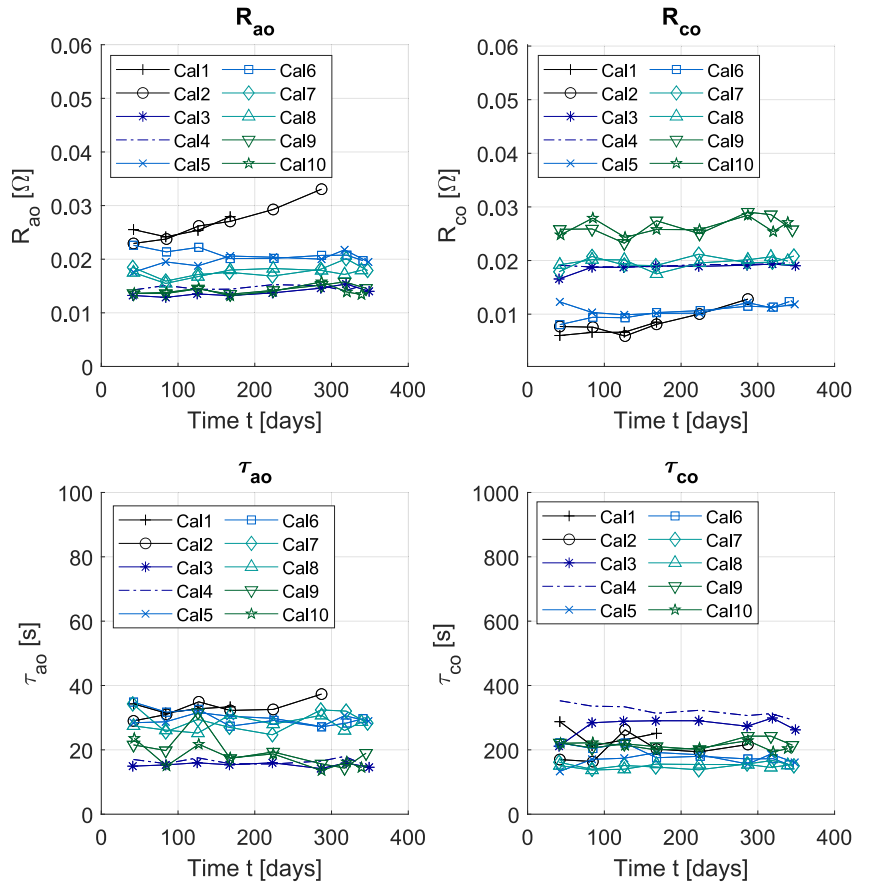


FIGURE 13 Calendar ageing results of R_{ao} , R_{co} , τ_{ao} and τ_{co} at 25°C and different stored charge levels

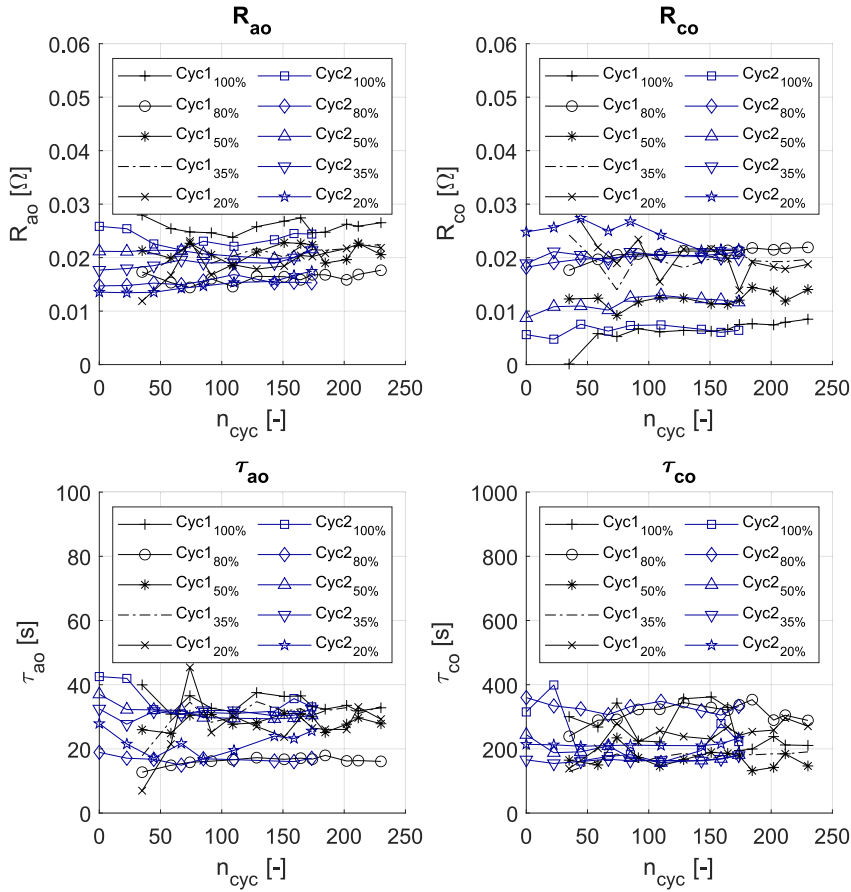


FIGURE 14 Cycle ageing results of R_{ao} , R_{co} , τ_{ao} and τ_{co} at 25°C for different charge levels

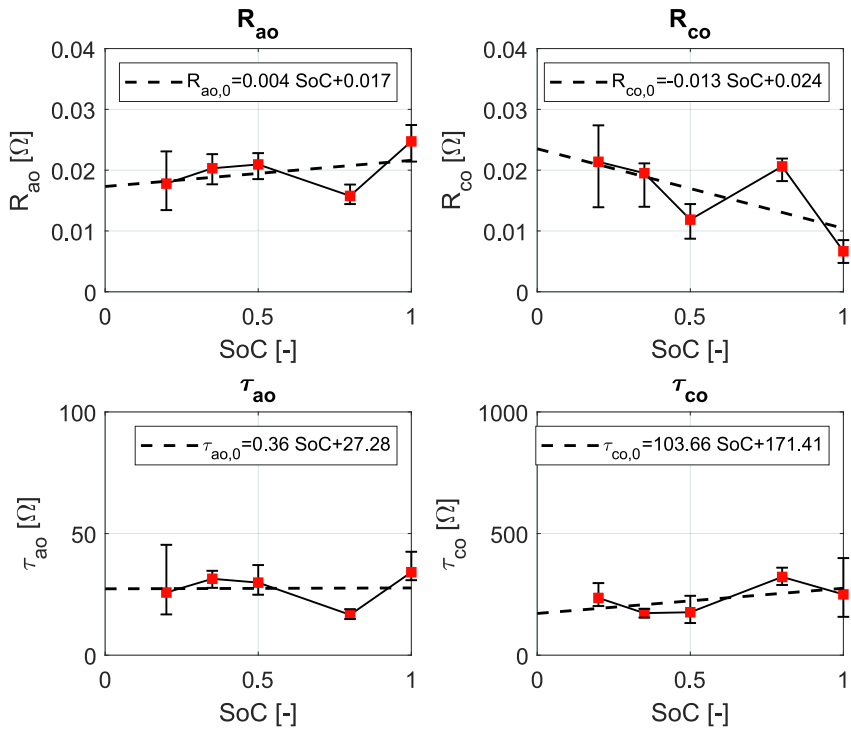


FIGURE 15 Experimental results and fitted curves of the state of charge (SoC) dependency of R_{ao} , R_{co} , τ_{ao} and τ_{co} at 25°C (Cyc1 & Cyc2)

highest values persist at the lowest ($\approx 20\%$) and highest point ($\approx 100\%$) of SoC with the dip in the centre. It is assumed that the R_s -SoC relation at all stages in the ageing process remains the same as no significant deviations have been observed in our data. A second order polynomial function is chosen to fit the measured data points (I-19).

6.1.3 | Open circuit voltage profile

The OCV profile in Figure 12a shows that the changes in curvature are minuscule. Only a zoom reveals differences, which result in minor adjustments to the cycle dependency of equation (I-13).

6.1.4 | Charge and mass transfer polarization

The estimated parameters for the activation and concentration polarization resistances and time constants for the calendar ageing are presented in Figure 13. The data suggests no evident trend for a significant change of both parameters over time where value variations are associated with the measurement and fitting uncertainty. The same conclusion can be drawn for the cyclic ageing with no significant trend as in Figure 14. Ageing information about the evolution of the charge transfer and diffusion resistance is scarce, but few studies such as [15, 46] observed an increasing trend opposed to our data. One reason for the discrepancy can be the lower stress level from the CLT procedure, which significantly lowers the ageing progress, whereas both studies cycle the batteries at fixed C-rates over 1C. In this case, the model parameters for R_{ao} , R_{co} , τ_{ao} and τ_{co} are assumed constant over time as if ageing does not affect the dynamic behaviour.

Furthermore, the SoC dependency is plotted in Figure 15 to establish if any correlations and trends are apparent. Out of the four parameters R_{co} shows the strongest relation to SoC with a declining tendency towards higher SoCs. A similar observation was reported in Ref. [46], where overpotential contributions from mass transfer decreases towards higher SoC levels. On the other hand, R_{ao} and the time constants τ_{ao} and τ_{co} weakly demonstrate increasing tendencies. However, the SoC's influence concerning the polarization dynamics themselves has not been directly discussed as far as the authors are concerned. The weak correlation can, therefore, be a special artefact of this study alone. The results of the parameter estimation are summarised in Table 3 and used for the equations listed in Table 1.

6.2 | Simulation results

The previously discussed experimental results are implemented into the simulation model to extrapolate the influence of ageing effects on the battery system's performance for the privacy protection scheme. The first question of interest

concerns the lifetime under the assumption that the ESS is operated in the same manner as depicted in Figure 3, that is, the same load pattern and request for a constant grid input of 320 W every day. Under this ideal condition, the LiB cells last for approximately 800 days before reaching the defined EoL (SoH = 0, $c_{cell} = 0.8$) as shown in Figure 16. The data points are taken at 1, 0.75, 0.5 and 0 SoH. During that time, the ESS cycles roughly 980 cycles. The capacity degradation rate is the highest at the earlier operation points and slows down over time. The results are in line with similar studies for other applications such as a photovoltaic system [47] and a plug-in hybrid EV (PHEV) [48]. The authors in Ref. [47] investigate a LiB system with different energy management strategies, which yield lifetimes between 2 and 6 years. In Ref. [48], a

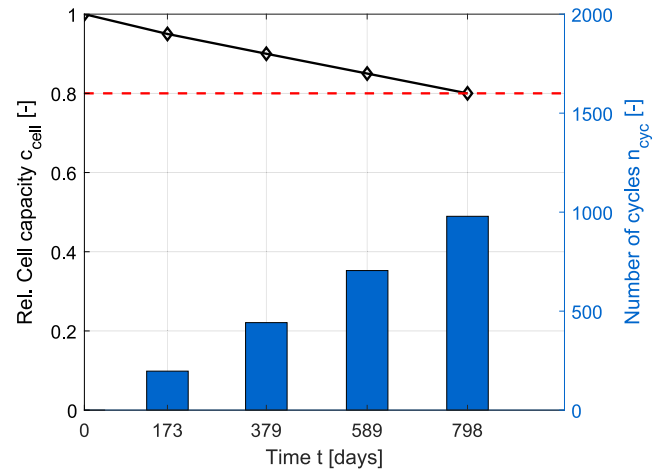


FIGURE 16 Relative cell capacity evolution in privacy operation scheme over time. The red dashed line marks the defined end of life at 0.8 of the beginning of life cell capacity

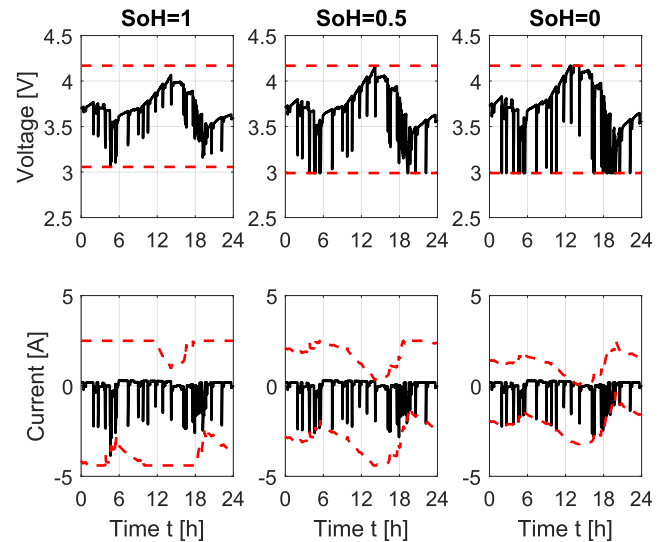


FIGURE 17 Battery cell performance at different stages of state of health (SoH). Red dashed lines indicate the voltage and current constraints

capacity and power fade model for LiB is introduced and validated for PHEV application. Their results show that 10% of the capacity is lost after roughly 830 cycles compared to 440 cycles in our case. Similar results are reported in [49] where $c_{\text{cell}} = 0.8$ is reached in 800 cycles under 1 C CC/CV operation. However, these comparisons should be interpreted with caution as the studies are conducted under different conditions and cannot guarantee full comparability. Nonetheless, the results lie within a reasonable margin of LiB's life expectancy.

Furthermore, the ageing of the R_s is highly relevant to the battery's performance, as can be seen in Figure 17 for various SoHs. As R_s increase over time, the voltage swings in the voltage profiles significantly increase. Due to the system

constraints, the potential operation range, limited by I_{max} and I_{min} , greatly decreases over time, thus reducing the power capabilities of the system as well. In Figure 18 a Ragone plot [50] helps to visualise the capacity and power capability loss at different stages of lifetime. At the extreme points, the available energy is approximately $\lim_{P_{\text{dc}} \rightarrow 0} E_{\text{cell}} = q_{\text{cell}} v_{\text{ocv}}$ and $\lim_{P_{\text{dc}} \rightarrow \frac{-m_2}{4m_1}} E_{\text{cell}} = 0.5q_{\text{cell}} v_{\text{ocv}}$, where P_{dc} is the maximal available discharge power. m_1 and m_2 are described by the expressions in Table 4.

$$E_{\text{cell}}(P_{\text{dc}}, \text{SoH}) = \frac{2m_1 P_{\text{dc}} q_{\text{cell}}(\text{SoH})}{-m_2 + \sqrt{m_2^2 + 4m_1 P_{\text{dc}}}} \quad (18)$$

The plot describes the potentially available energy capacity at different discharge powers. For example, if we discharge the LiB at low powers ($< 10^{-2} \text{W}$), we can effectively extract the full energy capacity. However, with increasing P_{dc} , polarization losses increase, hence reducing the useful energy as seen with the sharp decline at higher power levels. Consequently, the system's efficiency will decline with higher drawn powers. To maintain high efficiencies it is recommended to operate at the flat part of the curve. In our privacy protection scheme, the LiB cell is operated below 8 W at 99% of the total time, resulting in efficiencies higher than 93%. However, with progressing age capacity, power capability and efficiencies fade, leading to $\eta_{\text{cell}} = 88\%$ and $\eta_{\text{cell}} = 85\%$ at 0.5 and 0 SoH. This has significant implications on the ESS's performance in the later stages in its life.

Figure 19 illustrates the hourly amount of energy 'leaked' at different SoH stages as an indicator of lost privacy. Ideally, the contributions from the grid and ESS manage the load in such a way as to keep the SM reading constant at all times, that is, zero

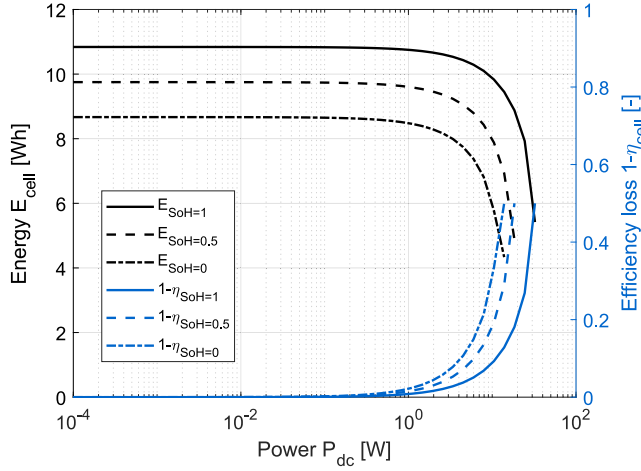


FIGURE 18 Ragone plot of lithium-ion battery cell at different state of health (SoH)

System model ($I_{\text{min}}[k] \leq I[k] \leq I_{\text{max}}[k]$)

$$(II-1) \quad P_{\text{ess}}[k] = k - P_{\text{load}}[k] \quad [\text{W}]$$

$$(II-2) \quad I[k] = -\frac{m_2[k]}{2m_1[k]} + \left(\left(\frac{m_2[k]}{2m_1[k]} \right)^2 + \frac{P_{\text{ess}}[k]}{m_1[k]} \right)^{0.5} \quad [\text{A}]$$

$$(II-3) \quad m_1[k] = R_s[k] + \frac{\Delta v}{C_{\text{ao}}[k]} \frac{1}{1 + \frac{\Delta v}{\tau_{\text{ao}}[k]}} + \frac{\Delta v}{C_{\text{co}}[k]} \frac{1}{1 + \frac{\Delta v}{\tau_{\text{co}}[k]}} \quad [\Omega]$$

$$(II-4) \quad m_2[k] = v_{\text{ocv}}[k] + \frac{v_{\text{ao}}[k] - 1}{1 + \frac{\Delta v}{\tau_{\text{ao}}[k]}} + \frac{v_{\text{co}}[k] - 1}{1 + \frac{\Delta v}{\tau_{\text{co}}[k]}} \quad [\text{V}]$$

System constraints

$$(II-5) \quad P_{\text{ess}}[k] \geq -M \cdot N \cdot \frac{m_2^2[k]}{4m_1[k]} \quad [\text{W}]$$

$$(II-6) \quad I_{v_{\text{max}}}[k] = \frac{v_{\text{max}} - m_2[k]}{m_1[k]} \quad [\text{A}]$$

$$(II-7) \quad I_{v_{\text{min}}}[k] = \frac{v_{\text{min}} - m_2[k]}{m_1[k]} \quad [\text{A}]$$

$$(II-8) \quad I_{\text{max}}[k] = \min(I_{v_{\text{max}}}[k], I_{\text{ch,max}} = 2.5) \quad [\text{A}]$$

$$(II-9) \quad I_{\text{min}}[k] = \max(I_{v_{\text{min}}}[k], I_{\text{dc,min}} = -4.4) \quad [\text{A}]$$

Parameters

$$M \quad \text{Numbers of series components} \quad [-]$$

$$N \quad \text{Number of parallel components} \quad [-]$$

$$v_{\text{max}} \quad \text{Maximum voltage limit} \quad [\text{V}]$$

$$v_{\text{min}} \quad \text{Minimum voltage limit} \quad [\text{V}]$$

TABLE 4 System model and constraints

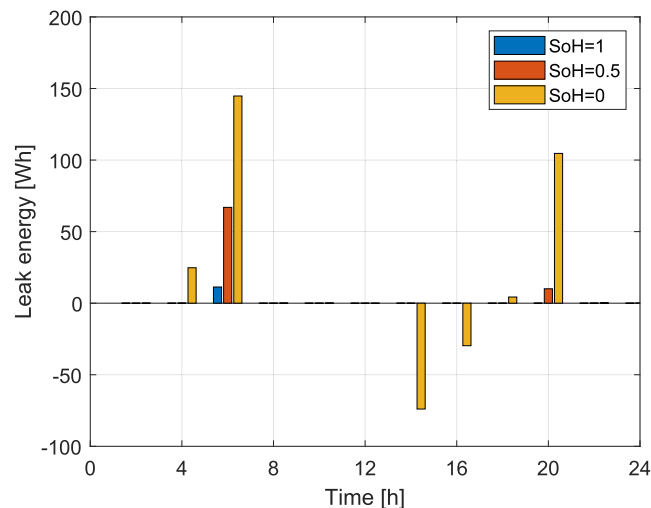


FIGURE 19 Lithium-ion battery system performance at different stages of state of health (SoH)

leak energy. If the battery fails to provide energy, the grid takes over which results in an additional input on top of the constant demand and manifests itself as a positive leak energy. In case of low load demands, the grid recharges the LiB with the exact amount to reach k . If the LiB fails to absorb the grid input due to the lack of available capacity, the SM reading will dip. With progressive ageing, the LiB system gradually loses its capacity, unable to provide the additional energy needed to maintain k , mainly observed at peak times (5–6 h). At 0 SoH, that is, with 20% capacity loss, energy leak is apparent at several peaks at 4, 15 and 20 h, even unable to absorb grid energy. As a consequence, the 2 kWh ESS cannot fully maintain its privacy protection function until the EoL.

To summarise, the energy management scheme for a privacy-focussed operation puts low stress on the LiBs, which allows for operation lengths roughly around 2 years until 0 SoH. However, privacy leak occurs earlier in the operation due to significant losses in the power capability but can be offset by increasing the overall ESS size, which further reduces stress on individual cells and provides more leeway in power capability. Therefore, to guarantee long-term functionality, here, in terms of sustaining a constant SM reading, the influence of ageing on the LiB's performance needs to be taken into consideration in the design stage. However, this analysis only provides initial insights as no real time data of this particular application is currently available. Hence, ideal assumptions such as static load pattern and a fixed constant SM reading are made. Daily and seasonal variations can change the stress on the ESS, leading to either higher or lower life expectancies. Additionally, P_{SM} is conveniently set in such a way as to minimise the required total ESS size, which does not necessarily guarantee the most economic solution as additional power is imported to recharge the ESS. Lastly, the influence of temperature is neglected, which is known to have a significant impact on the ageing progress.

Although temperature variation in residential buildings is low, including temperature dependencies into the model simulates a more realistic scenario.

7 | CONCLUSION

The use of ESS for the protection of private information through power consumption patterns is an unusual application possibility that has garnered research interest in the context of data protection. LiBs have shown widespread applicability including residential areas with solar or home batteries. However, the impact of the privacy protection scheme on the feasibility of LiBs has not been studied so far. To provide the first insights, this work has addressed the ageing influence on the cell performance on how well the function of maintaining privacy is guaranteed and what lifetime can be expected. To accomplish this, an application-specific CLT procedure is established to age the LiB cells under a fairly realistic load pattern. The results reveal an expected lifetime of about 2 years with constant use, which is in line with the life expectancies of similar applications. Note that these results are derived from tests of a single 18,650 cell type with 0%–100% SoC range. Other cell types and/or smaller SoC operation windows may yield more favourable results with higher life expectancies. However, information leakage occurs at earlier stages during operation as the cells experience gradual energy capacity and power capability loss. In conclusion, the application of LiBs for the privacy protection of SM readings is feasible but the ageing impact on the battery performance has to be taken under consideration in the design stage of the ESS through redundancy implementations or regular maintenance.

CONFLICT OF INTEREST

None.

PATIENT CONSENT STATEMENT

Not applicable, no patients were involved in this study.

PERMISSION TO REPRODUCE MATERIAL FROM OTHER SOURCES

No material is reproduced for this study.

CLINICAL TRIAL REGISTRATION


Not applicable, not a clinical trial.

DATA AVAILABILITY STATEMENT

The data that support the findings of this study are openly available in 'The Reference Energy Disaggregation Data Set' at <http://redd.csail.mit.edu/>.

ORCID

Cong-Toan Pham  <https://orcid.org/0000-0002-3070-9059>

Daniel Månsson  <https://orcid.org/0000-0003-4740-1832>

REFERENCES

- Asghar, M.R., et al.: Smart meter data privacy: a survey. *IEEE Commun. Surv. Tutor.* 19(4), 2820–2835 (2017)
- Alaton, C., Tounquet, F.: Benchmarking Smart Metering Deployment in the EU-28—Final Report, pp. 35–69. European Commission (2020)
- Cuijpers, C., Koops, B.J.: Smart metering and privacy in Europe: lessons from the Dutch case. In: Gutwirth, S., et al. (eds.) *European Data Protection: Coming of Age*, pp. 269–293. Springer, Dordrecht (2013)
- Aladesanmi, E.J., Folly, K.A.: Overview of non-intrusive load monitoring and identification techniques. *IFAC-PapersOnLine.* 48(30), 415–420 (2015)
- Zoha, A., et al.: Non-intrusive load monitoring approaches for disaggregated energy sensing: a survey. *Sensors.* 12, 16838–16866 (2012)
- Bohli, J., Sorge, C., Ugus, O.: A privacy model for smart metering. In: 2010 IEEE International Conference on Communications Workshops, pp. 1–5. Capetown (2010)
- Backes, M., Meiser, S.: Differentially private smart metering with battery recharging. In: Garcia-Alfaro, J., et al. (eds.) *Data Privacy Management and Autonomous Spontaneous Security*, pp. 194–212. Springer, Berlin (2014)
- Li, F., Luo, B., Liu, P.: Secure and privacy-preserving information aggregation for smart grids. *Int. J. Secur. Network.* 6, 28–39 (2011)
- Sun, Y., Lampe, L., Wong, V.W.S.: Smart meter privacy: exploiting the potential of household energy storage units. *IEEE Internet Things J.* 5, 69–78 (2018)
- Giaconi, G., Gúndúz, D., Poor, H.V.: Smart meter privacy with renewable energy and an energy storage device. *IEEE Trans. Inf. Forensics Secur.* 13, 129–142 (2018)
- Månsson, D.: Sizing energy storage systems used to improve privacy from smart meter readings for users in Sweden. In: 2018 IEEE PES Innovative Smart Grid Technologies Conference Europe (ISGT-Europe), pp. 1–6. Sarajevo (2018)
- Avula, R.R., Oechtering, T.J., Månsson, D.: Privacy-preserving smart meter control strategy including energy storage losses. In: 2018 IEEE PES Innovative Smart Grid Technologies Conference Europe (ISGT-Europe), pp. 1–6. Sarajevo (2018)
- Yang, L., et al.: Optimal privacy-preserving energy management for smart meters. In: *IEEE Infocom 2014—IEEE Conference on Computer Communications*, pp. 513–521. Toronto (2014)
- Pham, C.-T., Månsson, D.: A study on realistic energy storage systems for the privacy of smart meter readings of residential users. *IEEE Access.* 7, 150262–150270 (2019)
- Gao, Y., et al.: Lithium-ion battery aging mechanisms and life model under different charging stresses. *J. Power Sources.* 356, 103–114 (2017)
- Schlasza, C., et al.: Review on the aging mechanisms in Li-ion batteries for electric vehicles based on the FMEA method. In: 2014 IEEE Transportation Electrification Conference and Expo (ITEC), pp. 1–6. Dearborn (2014)
- Vetter, J., et al.: Ageing mechanisms in lithium-ion batteries. *J. Power Sources.* 4(2), 335–346 (2005)
- Kolter, J.Z., Johnson, M.J.: REDD: A public data set for energy disaggregation research. In: *Proceedings of the SustKDD Workshop on Data Mining Applications in Sustainability*. Boston (2011)
- Conte, M., et al.: Ageing testing procedures on lithium batteries in an international collaboration context. *World Electr. Veh. J.* 4(2), 335–346 (2010)
- International Organization of Standardization: *Electrically Propelled Road Vehicles Test Specification for Lithium-ion Traction Battery Packs and Systems Part 4: Performance Testing*. Geneva (2018)
- Idaho National Lab: *Battery Test Manual for Electric Vehicles*. Idaho (2015)
- Morita, K., Akai, M., Hirose, H.: Development of cycle life test profiles of lithium-ion batteries for plug-in hybrid electric vehicles. In: *EVS24 International Battery, Hybrid and Fuel Cell Electric Vehicle Symposium*, pp. 1–7. Stavanger (2009)
- Varini, M., Campana, P.E., Lindbergh, G.: Semi-empirical, electrochemistry-based model for Li-ion battery performance prediction over lifetime. *J. Energy Storage.* 25, 100819 (2019)
- Wang, W., et al.: Chapter 1—electrochemical cells for medium- and large-scale energy storage: fundamentals. In: Menictas, C., Skyllas-Kazacos, M., Lim, T.M. (eds.) *Advances in Batteries for Medium and Large-Scale Energy Storage* (Woodhead Publishing Series in Energy), pp. 3–28 (2015)
- Bard, A.J., Faulkner, L.R.: *Electrochemical Methods: Fundamentals and Applications*, 2nd ed. John Wiley & Sons, New Jersey (2001)
- Cittanti, D., et al.: Modeling Li-ion batteries for automotive application: a trade-off between accuracy and complexity. In: *International Conference of Electrical and Electronic Technologies for Automotive*, pp. 1–8. Torino (2017)
- He, H., et al.: Comparison study on the battery models used for the energy management of batteries in electric vehicles. *Energy Convers. Manag.* 64, 113–121 (2012)
- Ecker, M., et al.: Development of a lifetime prediction model for lithium-ion batteries based on extended accelerated aging test data. *J. Power Sources.* 215, 248–257 (2012)
- Sarasketa-Zabala, E., et al.: Calendar ageing analysis of a LiFePO₄/graphite cell with dynamic model validations: towards realistic lifetime predictions. *J. Power Sources.* 272, 45–57 (2014)
- Naumann, M., et al.: Analysis and modeling of calendar aging of a commercial LiFePO₄/graphite cell. *J. Energy Storage.* 17, 153–169 (2018)
- Magnor, D.T.: *Global Optimization of Grid-connected PV Battery Systems Under Special Consideration of Battery Aging*. PhD thesis, RWTH Aachen University (2017)
- Dahlblom, M., Nordquist, B., Jensen, L.: Variations in indoor temperature in residential apartments of different size and building category. In: *NSB 2014: 10th Nordic Symposium on Building Physics*, pp. 830–837. Lund (2014)
- Stemers, K., Yun, G.Y.: Household energy consumption: a study of the role of occupants. *Build. Res. Inf.* 37(5–6), 625–637 (2009)
- Morley, J., Hazas, M.: The significance of difference: understanding variation in household energy consumption. In: *eceee Summer Study Proceedings*, Presqu'île de Giens (2011)
- Ecker, M., et al.: Calendar and cycle life study of Li(NiMnCo)O₂-based 18650 lithium-ion batteries. *J. Power Sources.* 248, 839–851 (2014)
- Ansmann, L.G.: INR 18650 B4 2600mAh. https://www.elfa.se/Web/Downloads/_t/ds/1307-0000_eng_tds.pdf (2017). Accessed 21 Oct 2020
- Bryan, S.: Adafruit ina260 current + voltage + power sensor breakout. <https://learn.adafruit.com/adafruit-ina260-current-voltage-power-sensor-breakout> (2019). Accessed 21 Oct 2020
- Texas Instrument.: INA260 Precision Digital Current and Power Monitor With Low-Drift, Precision Integrated Shunt. <https://www.ti.com/lit/ds/symlink/ina260.pdf> (2016). Accessed 21 Oct 2020
- Bill, E.: Adafruit 4-Channel ADC Breakouts. <https://learn.adafruit.com/adafruit-4-channel-adc-breakouts>. Accessed 21 Oct 2020
- Texas Instrument.: ADS101x ultra-small, low-power, i2c-compatible, 3.3-kSPS, 12-bit ADCs with internal reference, oscillator, and programmable comparator. <https://www.ti.com/lit/ds/symlink/ads1015.pdf> (2018). Accessed 21 Oct 2020
- TDK.: NTC thermistors for temperature measurement. https://www.elfa.se/Web/Downloads/_t/ds/B57560G-B57560G1_eng_tds.pdf (2019). Accessed 2 Sept 2019
- Grolleau, S., et al.: Calendar aging of commercial graphite/LiFePO₄ cell predicting capacity fade under time dependent storage conditions. *J. Power Sources.* 255, 450–458 (2014)
- Wang, J., et al.: Degradation of lithium ion batteries employing graphite negatives and nickel-cobalt-manganese oxide + spinel manganese oxide positives: part 1, aging mechanisms and life estimation. *J. Power Sources.* 269, 937–948 (2014)
- Epding, B., et al.: Investigation of significant capacity recovery effects due to long rest periods during high current cyclic aging tests in automotive lithium ion cells and their influence on lifetime. *J. Energy Storage.* 22, 249–256 (2019)
- Zhang, J., Xu, W., Henderson, W.: *Lithium Metal Anodes and Rechargeable Lithium Metal Batteries*, pp. 25–29. Springer, Cham (2017)

46. Ovejas, V., Cuadras, A.: State of charge dependency of the overvoltage generated in commercial Li-ion cells. *J. Power Sources*. 418, 176–185 (2019)
47. Beltran, H., et al.: Lithium ion batteries ageing analysis when used in a PV power plant. In: *IEEE International Symposium on Industrial Electronics*, Hangzhou (2012)
48. Cordoba-Arenas, A., et al.: Capacity and power fade cycle-life model for plug-in hybrid electric vehicle lithium-ion battery cells containing blended spinel and layered-oxide positive electrodes. *J. Power Sources*. 278, 473–483 (2015)
49. Yang, F., et al.: Prognostics of Li(NiMnCo)O₂-based lithium-ion batteries using a novel battery degradation model. *Microelectron. Reliab.* 70, 70–78 (2017)
50. Christen, T., Carlen, M.W.: Theory of Ragone plots. *J. Power Sources*. 91(2), 210–216 (2000)

How to cite this article: Pham, C.-T., Månsson, D.: Effects of smart meter privacy protection management on the lifetime performance of 18,650 lithium-ion batteries. *IET Smart Grid*. 1–19 (2021). <https://doi.org/10.1049/stg2.12055>